Liquid-Mediated Solid-State Metathesis Reactions

Daniel Morrison

A thesis submitted to the University of London
in partial fulfilment of the requirements
for the degree of Doctor of Philosophy in Chemistry.

University College, University of London
London, United Kingdom

September, 2001

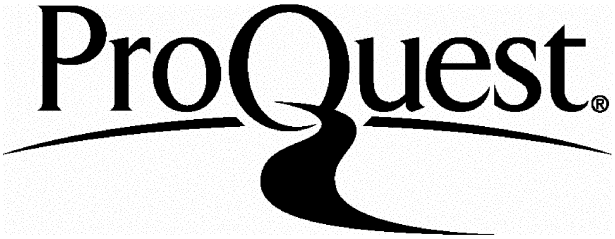

I. Abstract:

A variety of metathetical reactions have been carried out in a liquid medium to explore the variety and depth of such reactions. A comparison with the similar solid-state reactions gives a clear indication of the differences and similarities between the two alternate routes. The fact that these reactions go to completion at all is interesting in that the conditions employed are very mild and do not employ any "forcing" means to induce reaction.

Main group and transition metal sulphide, selenide and telluride and transition metal phosphide, arsenide and antimonide binary and ternary compounds were synthesised and characterised. An in-depth investigation into the synthesis and characterisation of the chalcopyrite $CuInE_2$ (E = S, Se, Te) family of ternary compounds has also been carried out with a specific focus on liquid variation, reaction duration and temperature and annealing treatment. Solid-state metathesis synthesis of $CuInE_2$ was also carried out for comparison purposes.

The main conclusions drawn from the use of the liquid-mediated metathesis methodology are that the reactions, for the most part, go to completion and produce single-phase products. Reactions require a much lower temperature and take much longer to go to completion as compared with the solid-state metathesis method. The majority of the products are X-ray amorphous before being subjected to annealing, and crystallinity can be induced under relatively mild conditions and with good control of crystallinity level. Product particle size is significantly reduced both before and after annealing.

I suppose that when the bees crowd round the flowers it is for the sake of honey that they do so, never thinking that it is the dust which they are carrying from flower to flower which is to render possible a more splendid array of flowers, and a busier crowd of bees, in the years to come. We cannot, therefore, do better than improving the shining hour in helping forward the cross-fertilisation of the sciences.

Lecture given at Cambridge, May 14, 1878
while directing a demonstration of the telephone

James Clerk Maxwell
Distinguished Professor of
Experimental Physics
Cambridge University

II. Table of Contents:

III. List of Figures:

IV. List of Tables:

V. List of Abbreviations:

XRD	Powder X-ray Diffraction
SEM	Scanning Electron Microscopy, Scanning Electron Micrograph
EDAX	Energy-Dispersive Analysis by X-rays
IR	Infrared
SSM	Solid-State Metathesis
SHS	Self-propagating High-temperature Synthesis
LMM	Liquid-Mediated Metathesis

VI. Acknowledgements:

I would most of all like to thank my supervisor Dr. Ivan Parkin for all his supervision and discussions. I would also like to thank Dr. Claire Carmalt for her support, useful discussion and advice. I would like to thank Kevin Reeves of the Institute of Archaeology for his helpfulness, patience and perseverance in putting up with me and my questions. I would like to thank the Committee of Vice-Chancellors and Presidents for an Overseas Research Studentship.

I would also like to thank all those who I have worked with in the last three years. I would like to thank them all for making both the work and after-work environments pleasurable and relaxed. I would lastly like to thank my wife, Janet Bertsch, who made it all worthwhile and kept me going through both the good times and the slow times.

1. *Introduction:*

1.1 Preamble:

The synthesis of solid compounds from the elements or other solid precursor compounds has been carried out since before recorded history, as witnessed by the finds of ceramic pots and brass and iron implements. Since the starting materials in traditional solid-state syntheses frequently have high melting points and low vapour pressures, overcoming diffusion barriers is an important consideration. Conventional ceramic or metallurgical synthetic techniques therefore require high-temperature ovens and prolonged and complex regimes of heating and cooling cycles, interspersed with manual grinding, to arrive at a final product in the desired state.

In modern times many methods have been devised to overcome these difficulties. Since the reaction rate is directly proportional to the surface contact between particles, high surface area precursors have been employed from ball milling, grinding or precipitation in order to speed up reaction times. Using molten fluxes or high-temperature solvents, such as molten Sn, Bi or halide salts, as media for solid-state reactions has also been used to circumvent the solid-state diffusion barrier. This can be most simply defined as the temperature above which the rate of diffusion of one atom through another atom matrix becomes significant.

An alternate, high-speed synthetic method that has come to prominence is what is known as combustion synthesis. This category includes the Self-propagating High-temperature Synthesis (SHS) method and the metathesis reaction.

1.2 Combustion Synthesis:

The combustion synthesis, or more specifically, the self-propagating high-temperature synthesis (SHS) method was pioneered in Russia in the 1960's. This method uses the highly exothermic redox reaction between a fuel and an oxidiser to form a product of interest. The most studied compounds are refractory materials, that is, borides, carbides, nitrides, silicides, ceramics, intermetallics and oxide materials. More recently, some electronic engineering materials such as superconductors ($3Cu + 2BaO_2 + \frac{1}{2}Y_2O_3 \rightarrow YBa_2Cu_3O_{7-x}$)[1], ferroelectric and magnetic materials ($BaO_2 + 5Fe_2O_3 + 2Fe + O_2 \rightarrow BaFe_{12}O_{19}$)[2] have been synthesised by SHS. To date over 500 different compounds have been synthesised by SHS, and many products are made on a commercial basis in Russia. A general SHS reaction is shown in Eq. 1-1:

$$nA + mB \rightarrow A_nB_m \qquad \text{(Elemental SHS)} \quad \text{Eq. 1-1}$$

where A is a fuel like Ti, Zr, Hf, Ta, B, Be or Si, and B is an oxidizer like B, C, N, O, S, Si or Se. Other SHS reactions can involve compounds as precursors which form a single product, as in Eq. 1-2,

$$BaO_2 + 5Fe_2O_3 + 2Fe + O_2 \rightarrow BaFe_{12}O_{19} \qquad \text{Eq. 1-2}$$

or can involve multiple precursors and multiple products to form composites, as in Eq. 1-3:

$$TiO_2 + B_2O_3 + 5Mg \rightarrow TiB_2 + 5MgO \qquad \text{Eq. 1-3}$$

The precursor materials are usually pressed into a pellet which is then ignited to produce the reaction. The reaction mixture requires ignition at a temperature of greater

than ~1500°C. This can be accomplished by laser irradiation, resistance coil heating, electrical arcs or chemical oven means. After reaction initiation, the reaction proceeds *via* a reaction wave which travels through the reaction pellet in a self-propagating manner reaching temperatures from 1500 to 4900 K. This wave usually passes through the reaction mixture within a few seconds. A value called the adiabatic temperature (T_{ad}), which is a measure of the reaction exothermicity, is also a measure used to predict whether a particular reaction will be self-propagating or not. It has been determined that if the T_{ad} is greater than ~1800 K the reaction will be self-propagating. Other important factors that are important in SHS reactions are particle size and shape of the reactants, ignition method, stoichiometric ratio, green mixture density, that is, the density of the pellet before ignition.

Various methods have been employed to lower this ignition temperature. Mechanical alloying, that is, utilising ball milling to impact the reacting particles, thus increasing surface area, is one such method. Field activated combustion synthesis uses an applied voltage to activate certain reactions. The field direction can also affect the synthesis wave velocity.

SHS is advantageous over conventional routes in that it is very simple, very fast, energetically efficient in that it only requires initiation, after which it is self-sustaining, and it yields products of high-purity. An interesting factor of SHS is that the green mixture can be pressed into any shape and then ignited and the product will maintain the shape of the green mixture. Being a high-temperature method, the products are invariably the thermodynamically stable phases. However, given the rapid heating and cooling rates, there is the potential for metastable phases to be formed.

Given this, that the product can be formed *in situ*, and that there is no need for post-reaction purification or removal of by-products, an interesting use of SHS is the synthesis of materials in their final shape or in situations of difficult fabrication. For example, the green mixture can be pressed into a mould the shape of a turbine blade, rather than a simple pellet shape, and can be ignited inside the mould and a ready-formed

product is synthesised.

Another interesting usage of this *in-situ* synthesis is the coating of the insides of steel pipes (for oil pipelines, etc.) by what is called the 'centrifugal thermite reaction'. This uses the well-known thermite reaction ($3Fe_3O_4 + 8Al \rightarrow 9Fe + 4Al_2O_3$) inside a spinning pipe segment which spreads the precursors evenly on the inside of the pipe and is then ignited. This coats the inside of the pipe, due to the density difference of the products, to an inner layer of metal and an outer layer of ceramic, thus having the toughness of the one and the abrasion resistance of the other.

1.3 Metathesis Reactions:

The focus of this thesis is on a set of reactions that have been called metathesis or metathetical reactions. Being a relatively new development in inorganic chemistry, these reactions are not generally known. Therefore, it is essential to give an introductory explanation and some general properties/characteristics of these reactions.

Metathesis reactions are a subset of the combustion synthesis methods described above but rather than using elemental or oxide precursors, they use metal halides and alkali metal main group compounds. A general definition of a metathesis reaction is, a reaction where there is an exchange of chemical "partners" between the reactants involved, with each other, to form the desired product and a co-produced salt. This is shown generally in Eq. 1-4:

$$AB + CD \rightarrow AD + BC \qquad \text{Eq. 1-4}$$

Some specific examples are shown in Eqs. 1-5 to 1-8:

$$TiCl_3 + Na_3P \rightarrow TiP + 3NaCl \qquad \text{Eq. 1-5}$$

$$TiBr_4 + 2Li_2S \rightarrow TiS_2 + 4LiBr \qquad \text{Eq. 1-6}$$

$$TiI_4 + 2CaC_2 \rightarrow TiC + 2CaI_2 + C \qquad \text{Eq. 1-7}$$

$$3TiCl_4 + Al_4C_3 \rightarrow 3TiC + 4AlCl_3 \qquad \text{Eq. 1-8}$$

All metathesis reactions share the following characteristics: the reagents are a transition-metal or main-group metal halide ($TiCl_3$, $FeCl_3$, $InCl_3$, $SnCl_2$ etc.) and a group 1, 2, 13 or 14 carbide, silicide, chalcogenide or pnictide (Na_2S, Li_3N, CaC_2, Al_4C_3, KSi etc.) Reaction schemes are balanced in relation to the co-produced salt (called salt-balancing). In some cases, as in Eqs. 1-5 & 1-6, this leads to a fully balanced chemical reaction scheme. In other cases, as in Eq. 1-7, one element will not balance and this may or may not have some effect on the product of the reaction.

1.4 Solid-State Metathesis Reactions:

1.4.1 General Introduction:

Metathesis reactions which are performed between two reactants which are solids have become known as solid-state metathesis (SSM) reactions. SSM reactions offer an alternative to long, difficult and costly traditional materials processing techniques. SSM reactions require significantly less, and in some cases, no external energy input to go to completion. This low energy input requirement is due to the built-in chemical energy inherent in the system. The driving force of the reaction is the heat of formation and the heat of crystallisation of the by-product alkali or alkaline earth metal / halide salt. This can account for up to 90% of the reaction energy.

SSM reactions involve the mixing of the two reactants as powders and then placing them in a ceramic boat or glass or quartz ampoule. These reactions, while not requiring a large energy input for the reaction to proceed, do require a source of initiation. Suitable initiation methods include contacting the reaction mixture with a hot filament, heating the reaction mixture in a furnace, grinding the reaction mixture vigorously and stirring the mixture lightly. In some rare cases even mere contact of the reactants with each other is sufficient to initiate the reaction. The level of severity of initiation required is dependent on the nature of the two reactants.

The initial initiation energy is sufficient to start the reaction and from that point the reaction is self-sustaining. The reactions are very exothermic, sometimes explosive. They usually proceeds *via* a bright thermal flash or synthesis wave, lasting from 1 to 3 seconds. The reaction mixture, depending on total amount, has usually cooled to room temperature within 30 seconds (5 mmol reactions).[3] This propagation wave can be seen to travel along the sample mass from the initiation point outwards. The temperature reached by the reaction mixture is dependent on the boiling point of the co-produced salt, usually in the 1000 to 1400°C range. This is because the bulk of the reaction product is the co-produced salt and all excess reaction energy is used to heat, melt and then begin

to vaporise the salt.

Solid-state metathesis reactions are interesting because they are so rapid. Conventional ceramic synthetic methods rely on high temperatures (>1200°C) and long reaction times (often days) in order to reach some appreciable solid-state diffusion rate of the reacting species through the solids[4]. The extraordinary speed of completion of SSM reactions has been attributed to the high internal temperatures reached at the time of reaction, which in course leads to a molten flux of the alkali/alkaline earth salt, which provides a 'liquid' medium in which atoms can diffuse much more rapidly than if they had to diffuse through a solid material.

One advantage of SSM reactions is that, with variations, it is possible to get some control over reaction conditions and particle sizes compared with traditional ceramic syntheses[5]. Other than their rapidity, SSM reactions also offer the advantage that the product synthesised is already crystalline as synthesised. Thus there is no need for subsequent annealing step to induce crystallinity.

The products synthesised are typically of high purity. The purity of the product is directly controlled by the purity of the precursors. In ceramic synthesis techniques that involve long timespans at elevated temperatures, there is often a problem with contamination of the product with the material of the container in which the ceramic is being sintered or synthesised. In SSM reactions, because the timespans are so short, there is no time for the diffusion of the container material into the product.

Another potential issue is incorporation or cross-contamination of the product with chloride residues. In all metathesis reactions the synthesised product is an intimate mixture of the product and the co-produced salt. The purification of the product is simply done by washing the product mixture with methanol, ethanol, water or some other liquid in which the co-produced salt is soluble. It has been seen repeatedly, in most metathesis reactions, that after washing of the reaction product mixture, there is no detectable contamination of the product with chloride.

An interesting effect is noticed when the scale of the solid-state reaction is varied.

Under the standard conditions used for most reactions, the reaction pathway follows a rapid temperature rise followed by a rapid cooling of the reaction mass. When the reaction scale is increased, the subsequent smaller ratio of surface area to volume leads to a greater self-insulation of the reaction mass. This leads to the reaction mixture remaining at a higher temperature for longer. This leads to products of higher phase purity and crystallinity. However it is also observed, in some cases, that, due to the greater temperature difference between the surface and centre, the reaction product was inhomogeneous from region to region.[6] Another effect of increasing the reaction mass was that in ternary sulphide-selenides higher temperatures were obtained, leading to higher sulphur incorporation, due to the inherently different diffusion constants of S and Se.[7]

In SSM reactions it is possible to control the average particle size of the product by judicious use of an inert additive to act as a dilutant. This dilutant is usually the same salt as is produced in the reaction. The addition of various mole equivalents of dilutant to the reaction, given a constant mole amount of reactants, leads to a larger reaction mass over which the same amount of reaction heat has to be distributed. This therefore serves to lower the overall reaction temperature. Thus the formed product receives less heat per mole and less energy goes into crystal growth in the product.

Since SSM reach high temperatures they generally produce thermodynamic phases, but in some cases it is possible get metastable, quenched high-temperature phases, which may be desired or interesting.[3]

1.4.2 Theory:

SSM reactions have been postulated to proceed *via* a set of intermediates which fall into two extreme routes; 1) ionic pathway or 2) elemental pathway, which are shown schematically in Fig. 1- 1. Most SSM reactions will probably fall somewhere between

these two extremes. In both routes the assumption is that salt formation occurs first. In the elemental route, the metal and other reacting species are reduced/oxidised to the elements, which then under the reaction conditions combine to form the product, perhaps undergoing the proper redox process to the appropriate form for the product. In the ionic route, the reacting species retain their charges and combine to form the product directly. There is some scope for redox chemistry in the ionic pathway as well, as shown figuratively by the excess E in Fig. 1- 1. This is in such cases where the charges in the product do not match those of the precursors.

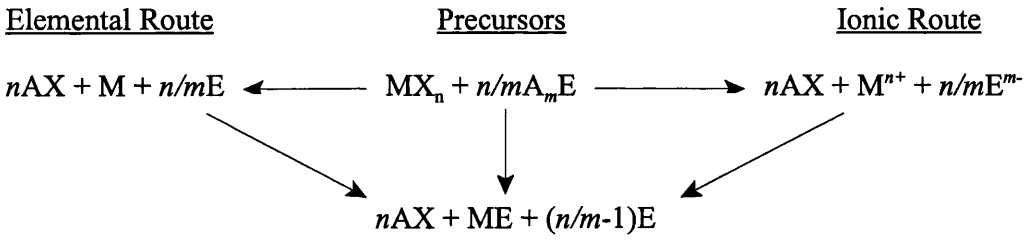

Fig. 1-1 Elemental *vs.* Ionic Pathway

The propagation of an SSM reaction has been treated theoretically in terms of its thermodynamic energies as to whether it will be spontaneous or not. A value called the Theoretical Adiabatic Temperature, T_{ad}, has been calculated from standard thermodynamic data based on two assumptions: 1) SSM reactions are so fast that all energy produced is used to heat the products and 2) the reactions go to completion. This maximum theoretical temperature value is expected to be close to that reached in real systems due to the short time-scale of reaction. This value has been used to predict whether a reaction will propagate or not. While this value has some usefulness in predicting whether a particular reaction will be self-propagating or not, an alternate value has been devised which appears to be more accurate in its predictive value. This is the Theoretical Adiabatic Temperature for the first, intermediate, step of the reaction, that is, for salt formation only and does not consider the heating of the product itself ($T_{ad,s}$). For self-propagation to occur, $T_{ad,s}$ should be higher than the melting point of the salt.

This seems to strongly suggest that a molten medium is necessary for a rapid, unassisted reaction to occur.[3] While there are more subtle factors that affect propagation, this indicator is useful as a relatively accurate predictor of propagation.

These indicators of self-propagation are only an issue for those reactions initiated by a hot filament. Reactions that do not self-propagate may still be caused to react by providing external energy input such as heating the reaction mixture in an ampoule in an oven or providing added energy from a second simultaneous chemical reaction.

1.4.3 Previous Work:

Since the beginning of the 1990s, the scope and implications of solid-state metathesis reactions have been explored in quite some detail. The groups of I. P. Parkin and R. B. Kaner have been the two most prolific in this area. It can be said, with almost no exaggeration, that virtually every binary compound of a main group metal, transition metal or lanthanide element with a main group element in the periodic table has been made.[8] Attempting to summarise all the results would only lead to more confusion than enlightenment. I will endeavor to touch upon all the prominent observations and conclusions that have been discovered through the work of these groups. Reference 8 is an excellent review of solid-state metathesis reactions up to 1996.

Refractory nitrides and carbides form a large portion of the materials formed by SSM. Ceramic nitrides normally require high nitrogen pressures and long times or noxious ammonia gas for nitrogen reaction to occur. Using more reactive nitrogen precursors, such as Li_3N, NaN_3, Mg_2N_3 and Ca_2N_3, allows nitrides to be quite easily synthesised. Early transition metal nitrides of the formula MN (M = Ti, Zr, Hf, V, Nb, Ta, Cr) have all been obtained. Later transition metal nitrides, however, decompose above 1000°C and are thus decomposed by the reaction temperature. Modification of reaction conditions allow some of these compounds to be obtained. The further to the right in the transition metal row one goes the more likely it is that nitrogen-deficient

nitrides are obtained. For chromium, a mixture of CrN and Cr_2N are obtained. Lanthanides readily form LnN phases.

Phosphides, arsenides and antimonides have also been synthesised by SSM. For these reactions Na_3E (E = P, As, Sb) is the pnictide precursor. Phosphides of the formula MP are the predominant product for reactions of metal halides and Na_3P. Reactions of Na_3As form predominantly MAs, but there are a number of cases where varied and mixed phases are observed. Reactions of Na_3Sb sees mainly MSb_2 products but many reactions result in metal antimonide and antimony metal. This trend continues when one uses Na_3Bi which results in only metal and bismuth. This trend shows that as the co-reactant element gets heavier the reaction mechanism favours the elemental recombination pathway but lacks the energy to complete the recombination.

Metal oxide formation from SSM reactions using Li_2O, Na_2O_2 and Na_2O has formed a wide variety of compounds. Most reactions formed metal oxides with the metal unchanged in oxidation state. When Li_2O is used, in a number of cases, there is lithium incorporation into the product leading to the formation of lithium metal oxides.

Sulphides, selenides and tellurides have been synthesised using Na_2E (E = S, Se, Te) as the chalcogenide precursor. For most transition, main group and lanthanide metal halides, single-phase sulphide formation occurs after both filament and oven initiation. Most of these reactions maintain the oxidation state of the metal precursor. Less work has been done on selenides and tellurides but for main group metals the products show the same trend as for sulphides. An interesting observation is in reactions aiming to form ternary metal sulphur-selenides. It was noted that the product did not contain the chalcogenide ratio of the starting materials. The products were enriched in the more volatile sulphur component presumably due to its increased mobility during the brief period of reaction heat.

Relatively less work has been done on metal silicides, borides and aluminides. The metal silicides formed tend to be of mixed phases. In select cases, Mg_3B_2 and MCl_n form single phase metal boride products. Some recent work on forming aluminides has

shown some promising results.[9]

1.4.4 Drawbacks:

SSM reactions have been shown to be versatile, useful reactions that allow the rapid and facile synthesis of a number of compounds. However, like all things, there are always drawbacks and limitations to the reaction methodology. These limitations are derived from the same factors that make the reactions interesting and successful.

One problem encountered has been the result of the very high temperatures reached during the short time of the SSM reaction. For most cases these high-temperatures contribute to the completion of the reaction and the subsequent self-annealing, however in some cases the temperatures reached are sufficient to first form, and then decompose, the desired product. For example in the following reaction the product is formed intermediately but is almost immediately decomposed;

$$2Li_3N + WCl_6 \rightarrow 6LiCl + \tfrac{1}{2}N_2 + \{WN\}^* \rightarrow W_{(met)} + \tfrac{1}{2}N_2 \qquad \text{Eq. 1-9}$$

One method devised for counteracting such an effect is the addition of an inert heat sink or dilutant, as mentioned above, to the reaction mixture in order to attempt to control the violence of the reaction. The inert salt absorbs the reaction energy so that less energy goes into heating the products. This has enabled some formerly inaccessible products to be synthesised.

In SSM reactions the products formed are often the thermodynamic product because the high temperatures reached allow the reaction to go to completion. In other cases the reaction pathway is a very quick rise in temperature followed almost immediately by a very quick cooling to ambient temperatures. This leads to the product synthesised being a quenched-in kinetic or meta-stable phase.

Another result of the rapid heating and subsequent rapid cooling of the reaction

products is that there can be a high defect proportion in the product. Like any quenching procedure the defect concentration at the high temperature is quenched in on cooling rapidly. Likewise there has been observed considerable lattice strain in such quenched products.[10]

Some SSM reactions are vigorous to the point where, as mentioned above, mere contact of the two reagents causes the reaction to initiate. In such reactions it is impossible to intimately mix the precursors before the reaction is started. Such intimate mixing has been shown to have a considerable effect on the purity and homogeneity of the final product. In the spontaneous reactions mentioned above, there is no way of achieving the most pure and homogeneous theoretically possible.

1.5 Liquid-Mediated Metathesis:

Simultaneous to the development of solid-state metathesis reactions, there was some interest in performing metathesis reactions in a non-reacting liquid medium. There doesn't seem to be any clear consensus on a name for this type of reaction, but various names are used such as solution-phase metathesis, solvent-based metathesis and solvothermal synthesis (providing that heat is applied) have all been used in the literature.

For this thesis the term liquid-mediated metathesis (LMM) will be used. Due to the nature of the reactions and reactants it will become clear from the ensuing discussion that it is difficult to give a name to these reactions which is as truthful as possible, since for the majority of reactions it is unclear whether, and if so, to what extent, the liquid acts as a solvent (species actually dissolved) and to what extent it is merely a liquid medium.

1.5.1 General Introduction:

As it has been described above, the solid-state metathesis reaction method employs rather severe reaction conditions. It has been sought to employ milder conditions in order to gain a greater grasp on control of the reaction conditions and thus the reaction products. One such approach is the liquid-mediated metathesis reaction mechanism. The reasoning is as follows:

To perform metathesis reactions in a liquid is seen as comparable to the use of an inert salt additive with the difference that a liquid is seen as a better heat sink. It is also usual to use an amount of liquid which is 100 to 200 mole equivalents of the reactants, whereas inert salt additions are from 2 to 20 mole equivalents. A stirring liquid reaction medium would also be a more efficient dissipator of the exothermic reaction energy than a solid salt in which the heat dispersion would be dependent on the heat diffusion through the static salt.

The liquid in use can also act as a maximum temperature limiter. Due to the high

volume of liquid present, the maximum temperature possible for the reaction (at ambient pressure) is the boiling point of the liquid. While the addition of an inert salt to an SSM reaction does reduce the maximum temperature of a reaction, this still only amounts to a reduction from ~1600K to ~900K for a 20:1 dilution (for $MoCl_5 + Na_2S$) which is still far higher than most liquids' boiling points.

Another role that the liquid can play is as a particle dispersant. In a stirred reaction scheme the reactant particles will be separated by the stirring liquid and will be kept disperse, unlike in SSM reactions where the reactants are tightly packed together. Contact between particles does still occur in the stirring action in the reaction vessel. The liquid can also act to renew the surfaces of the reacting particles to further promote the reaction.

There are numerous reasons to carry out research in this field of liquid-mediated metathesis reactions. One is that there has not been very much work in this area. The majority of papers focus on II-IV and III-V semiconducting materials. While these are important technological materials, the intense focus on these materials means that there is very little known about the potential and limitations of liquid-mediated metathesis reactions in general. One motivation is that it will be possible to attain greater control of the product properties due to the relatively mild reaction conditions.

A second motivation is that if some industrially relevant discovery is made, the ease of scaling up the reaction in the LMM regime would be easier. It was seen in SSM reactions that scaling up the reaction can drastically change the product outcome, which would not occur in LMM reactions, provided the liquid-reactant ratio was maintained.

A third motivation is that in the work carried out to date, it has been observed that reduced particle sizes are obtained. This is beneficial in a variety of different areas of science and technology and will be explained in more detail in the 'Nanoparticulates' section.

1.5.2 Previous Work:

If we consider reactions that are strictly within what we have defined as metathesis reactions, that is a metal halide and an alkali metal main group compound, then there has been very little reported literature on liquid mediated metathesis reactions as compared with the volume of work on SSM reactions.

One of the earliest papers reports the synthesis of a variety of MS_2 compounds (M = Ti, Zr, Hf, V, Mo, Nb and Ta). Chianelli and Dines[11] employed 10 mmol amounts of MCl_4 (MCl_5 for Nb and Ta) in 30 ml amounts of THF or ethyl acetate to which they add 20-40 mmol amounts of Li_2S or Na_2S in 30 ml of the same solvent. The Li_2S or Na_2S / THF or ethyl acetate mixture was a slurry rather than a true solution. This mixture was allowed to stir at room temperature for several hours to one day. The precipitate was collected and washed with the solvent used.

An alternate method was the use of amine or ammonia sulphides or hydrosulphides. These were synthesised *in situ* by combining the organic solvent with the amine or ammonia and bubbling H_2S through the solution. The reactions proceeded as in Eqs. 1-10 and 1-11.

$$MCl_4 + 2A_2S \rightarrow MS_2 + 4ACl, \text{ or} \qquad \text{Eq. 1-10}$$

$$LCl_5 + {}^5/_2A_2S \rightarrow LS_2 + 5ACl + \tfrac{1}{2}S \text{ , where} \qquad \text{Eq. 1-11}$$

M = Ti, Zr, Hf, V, Mo

L = Nb, Ta.

A = Li, Na, NH_4.

The first thing that the authors point out is that the reaction of H_2S with $TiCl_4$, for example, is thermodynamically unfavourable at room temperature. In fact, it is unfavourable at temperatures less that 400°C. Replacing H_2S for Li_2S allows the reaction to proceed at room temperature. The powders obtained were amorphous and it was found difficult to remove all traces of the co-produced LiCl due to the layered structure

of many of these compounds, leading to inclusion compounds. Crystalline TiS_2 could be made by increasing the temperature of the reaction to 65°C. Annealing the amorphous product at 400°C yielded crystalline TiS_2. Lastly, they report that the synthesis of VS_2 is only achievable using such a low-temperature technique as the one reported. VS_2 was previously thought not to exist, but this method allows previously inaccessible areas of phase diagrams to be reached. There is no direct reference to the particle sizes obtained but there are XRD diagrams showing highly broadened peaks, which is commonly taken as a sign of restricted particle size.

One thing that the authors noted in relation to the reagents used is that the nature of the precursors seemed to influence the reaction rate significantly. They observed that when they used highly crystalline Li_2S or Na_2S the reaction rate was significantly reduced when compared with poorly crystalline precursors. To make the reactions using crystalline precursors proceed at any reasonable rate it was necessary to heat the reactions. The highly crystalline precursors would not react with even neat $TiCl_4$ while poorly crystalline precursors would react very violently with pure $TiCl_4$. It was found that commercial Li_2S and Na_2S samples vary widely from batch to batch in their crystallinity, and they were forced to obtain X-ray diffraction patterns for each sample. They attempted to alleviate this by synthesising highly reactive LiHS from *n*-butyllithium and H_2S. This represents an intermediate compound between H_2S and Li_2S or Na_2S.

Kaner *et al.* report the synthesis of CdTe, HgTe and $Hg_{1-x}Cd_xTe$ from a liquid-mediated metathetical reaction.[12] They poured 0.74 mmol CdI_2 in 50 ml of oxygen-free MeOH and 0.74 mmol Na_2Te in 50 ml oxygen-free MeOH simultaneously into a beaker contaning 30 ml of oxygen-free MeOH all inside an argon-filled glovebag. The product precipitates within seconds and is filtered and washed with MeOH. The reactions were performed at room temperature and at 65°C.

The authors reported a wide particle size range distribution, with particles from 1 to 100 nm. They reported that the average size was *ca.* 2 nm but there was a large tail-off in the size histogram showing that there are a significant quantity of particles in the

5 to 20 nm size range. Annealing studies showed that moderate annealing at 100° for greater than 4 hours had a marked effect on crystallite size. The average particle size is shifted to between 5 and 7 nm, while the larger particle sizes are also enchanced, with a significant quantity of particles now reaching 35 nm. Performing the reaction at 65°C shifts particle size to somewhere intermediate between the room-temperature synthesised product and the annealed product. It is reported that performing the synthesis at elevated temperatures does not affect the upper range of particle sizes.

Kher and Wells[13] reported the synthesis of GaAs and GaP by a similar liquid-mediated metathesis procedure. The reaction scheme is shown in Eqs. 1-12 and 1-13

$$3(Na/K) + E \xrightarrow{Toluene} (Na/K)_3E \qquad \text{Eq. 1-12}$$

$$(Na/K)_3E + GaX_3 \xrightarrow{Toluene} GaE + 3(Na/K)X \qquad \text{Eq. 1-13}$$

(When E = As, X = Cl, I; when E = P, X = Cl)

The $(Na/K)_3As$ precursor was produced *in situ* by the reaction of 7.74 mmol As and 17.04 mmol Na/K alloy (36% excess As) in refluxing toluene for 2 days. Without further processing, to the resulting slurry was added 5.98 mmol $GaCl_3$ (5% excess) in 90 ml diglyme with stirring at 0°C. The temperature was slowly raised to reflux and maintained for 2 days. The resulting product was filtered and washed with deionised water to remove the salt and to neutralise any remaining arsenide. The resulting powder was placed in a vacuum sublimer at 350°C to remove excess arsenic. Similar procedures were followed for the use of toluene, 1,4-dioxane and monoglyme as solvents for the $GaCl_3$ component. Similar procedures were also used for the synthesis of GaP.

The average particle size obtained for both GaAs and GaP was found to be approximately 10 nm *after* sublimation. The sublimation process resulted in the annealing of the product and the pre-sublimation particle size was surmised to be approximately less than 3 nm. They also found that there was a portion of the product

which consisted of an amorphous component. It was observed that there were some particles of smaller diameter and some as small as 1 nm were found. There is no mention of the distribution of particle sizes, particularly as to the particle sizes of the larger particles. The annealing process resulted in the marked sharpening of the XRD peaks showing that there is an increase in average particle size.

Doubling the amount of precursors while keeping the amount of liquid constant had the effect of increasing the particle size obtained by approximately a factor of 2. The authors relate this to the effect observed by Kaner *et al.* when varied amounts of salt diluents were added to solid-state metathesis reactions. It was also stated that the halide employed seemed to have some effect on particle size. Substituting GaI_3 for $GaCl_3$ had the effect of reducing the particle size from 10 nm to 6 nm. They also state that the temperature of the reaction seemed to alter the particles sizes of the resulting powders, but they do not say how. The authors observed that the synthesised particles tended to agglomerate into larger clusters.

The biggest effect that the authors noted was the difference in particle size when utilising different solvents to dissolve the GaX_3 precursor. As stated, when using diglyme to dissolve the $GaCl_3$, the particle size was approximately 10 nm. When using monoglyme the average particle size was found to be 17 nm, both toluene and 1,4-dioxane resulted in particle sizes of approximately 36 nm. The authors put forward the theory that this can be related to the degree of chelating ability that the various solvents have. It is proposed that the multidentate ligands are able to cause dissociation of the gallium halide which leads to ionic coordination complexes. The observation that dioxane does not cause any particle size reduction while the multidenate ligands do, shows that merely forming adducts is not sufficient in itself to lead to reduced particle sizes. The effect of substituting toluene for diglyme in the synthesis of GaP, resulted in 21 nm particles compared to 10 nm. This shows that the particle size increase observed when toluene is substituted for diglyme is not readily transferable between reaction systems and that individual reaction schemes do have some influence on the particle size

outcome. The reaction scheme above was also extended to other 13-15 semiconductor materials including GaN and InN,[14] and GaSb, InP, InAs, InSb.[15]

More recently, and concurrently with this project, the group of Y. T. Qian has reported a number of varied liquid-mediated metathesis reactions. I will describe two in detail as examples. One such reaction is the formation of SnS_2 from $SnCl_4$ and Na_2S.[16] Stoichiometric amounts of the reagents were placed in an autoclave. There is no indication as to the absolute amounts used. To this was added 90 ml of toluene and this was allowed to react at 150°C for 8 hours. The resulting powder was washed with absolute ethanol and a yellow powder was collected. It was characterised as SnS_2 with spherical particles of 12 nm diameter. The reaction was described as a solid-liquid reaction since $SnCl_4$ is soluble in toluene. Eq. 1-14 shows that no redox chemistry occurs in this reaction.

$$SnCl_4 + 2Na_2S \rightarrow SnS_2 + 4NaCl \qquad \text{Eq. 1-14}$$

The authors describe that when reaction temperatures were reduced to below 100°C or reaction times were reduced to below 4 hours, the product yield and quality was negatively affected. Substituting THF for toluene had the effect of allowing the reaction to occur at room temperature and yielded an amorphous, yellow product. Performing the reaction in THF but at 150°C for 8 hours did not yield products of similar crystallinity to the product from the reaction in toluene. The solvent effect here was ascribed to the polarity difference between the two liquids.

The same authors also report the synthesis of a number of cobalt sulphides by varying reaction conditions.[17,18] The general reaction involves cobalt chlorides ($CoCl_2$ or $CoCl_2 \cdot 6H_2O$) and Na_2S_3 in toluene at 120-170°C for 4-24 hours. When anhydrous $CoCl_2$ is used only CoS_2 with an average 20 nm particle diameter results after 12 hours at 120°C. When hydrated $CoCl_2$ is used, Co_9S_8 results. The average particle diameter is again 20 nm. Increasing the reaction temperature to higher than 150°C, when using

the hydrated $CoCl_2$, results in a mixed-phase product including Co_9S_8, Co_3S_4 and CoS_2. No explanation is given as to why the water of hydration should have these effects on the products.

They also describe the synthesis of cobalt phosphide[19] and nickel phosphide[20] from the reaction of the metal chlorides and Na_3P in either benzene (Co) or toluene (Ni) in an autoclave at 150°C for 12 hours. They report Ni_2P with an average particle size of 10 nm. In the cobalt reactions they report a mixture of CoP and Co_2P.

They have also synthesised a number of chalcogenides, among them Sb_2S_3[21] (orthorhombic, 150 nm) from $SbCl_3$ and Na_2S_3 in benzene at 150°C for 12 hours, NiS_2[22] (28 nm) from $NiCl_2$ and Na_2S_3 in toluene at 180°C and Bi_2S_3[23] (40 nm by 150 nm rods) from $BiCl_3$ and $Na_2S{\cdot}9H_2O$ in alkaline aqueous solution at 150°C for 12 hours.

A more unusual metathetical reaction reported is that of $CdSO_4$ and Na_2S_3 in benzene at 80-120°C for 12 hours to form hexagonal CdS.[24] The authors also describe that the higher temperatures lead to the preferred formation of hexagonal CdS while increasing the water content of the system leads to cubic CdS formation and reduces overall particle size.

There are also two reported syntheses that do not strictly fit the description of metathetical reactions but I will argue that they do have certain similarities. The authors report the synthesis of ZnSe and CdSe[25] from MCl_2, Na and Se in ethylenediamine at 100°C for 6 hours, and SnSe[26] from $SnCl_2$, Se and Na in ethylenediamine at 130°C for 5 hours. The products of these reactions displayed a rod-like morphology with a *ca.* 30:1 aspect ratio. The authors make a deliberate point of avoiding the need to synthesise and handle precursors such as Na_2Se. I would argue that these reactions could be metathesis reactions in which the Na_2Se precursor is formed *in situ* and then react with the halide in a standard metathetical manner. The authors did not stop the reactions halfway to see if any Na_2Se could be isolated or not. In the authors' defence it should be stated that they have also reported a large number of elemental combination reactions in which, for example, CdS is formed from Cd and S in diethylamine at 180°C.[27] It may be the case

in the above reactions that the metallic Na extracts the halide from the metal halide and the formed element goes on to react with the elemental Se.

One illustrative application of liquid-mediated metathesis reactions is a reaction where the product is not binary but a single element. One such reaction is the synthesis of nanocrystalline Si by the reaction of $SiCl_4$ and KSi in glyme solutions.[28] The authors report that the average particle size is *ca.* 2 nm, but that particles at least as large as 30 nm were observed. Mg_2Si can also be used as a precursor.[29] Germanium nanoparticles were also synthesised by a similar process from $GeCl_4$ and Mg_2Ge. It may be that group 4 is the only group where this type of metathesis is possible.

G. A. Shaw has performed a number of metathetical reactions in liquid ammonia at room temperature.[30,31]

1.5.3 Final Word:

An important, yet complicated, factor of using a liquid medium for performing metathesis reactions is the issue of reactant dissolution. In most reported cases of liquid-mediated metathesis reactions one reactant (usually the halide) is wholly soluble in the liquid being used. This is mostly due to the widespread use of strongly coordinating and often multidentate liquids which often add to the solubility of halides, either by leading to dissociation or the formation of complexes. It will become apparent in the subsequent chapters, that in most of the reactions discussed in this thesis, the reagents are insoluble or only partially soluble in the liquids used. This is an important issue for theoretical and comparison purposes, and also leads to the specific title of this thesis.

1.6 Solid-Liquid Metathesis:

One third category should be mentioned for the sake of completeness. Reactions have been carried out in which one of the reagents is a solid and the other reagent itself, (not the medium, as in LMM) is a liquid. This is the case in reactions which employ liquid metal chlorides ($TiCl_4$, VCl_4 etc.). In this case the initiation of the reaction is spontaneous upon contact of the solid and liquid precursors. This has been attributed to the lack of solid-state diffusion barrier because of the liquid metal chloride.

The violence of the reactions using neat metal chloride liquids is the fiercest of the metathesis reactions studied. They proceed *via* a bright flash, instantly upon contact, and the material is spattered through the reaction vessel.

The synthesis of Ti_xV_yN, VO_2 and TiO_2 by this route from VCl_4 or $TiCl_4$ and Li_3N or Li_2O was successfully carried out.[32] As well, TiP, VP, TiAs and VAs have been synthesised by this route from VCl_4 or $TiCl_4$ and Na_3P or Na_3As.[33] In contrast, TiSb, VSb, TiBi and VBi were not accessible by this route, giving the elements rather than the binary compounds.

Interestingly, Y. T. Qian and coworkers report that $SnCl_4$ does not react spontaneously with Na_2S.[16] However it is unclear whether this is with neat $SnCl_4$ or whether it was diluted with toluene first.

1.7 Other Metathesis-like Reactions:

There are many reactions that fit into a category that consists of reaction that are metathesis-like but do not employ either metal halides or solid or liquid components. The example of $CdSO_4$ with Na_2S_3 has already been mentioned above. There are many other reactions that display exchange between reactants.

Many chemical vapour deposition (CVD) reactions depend on gas-phase exchange between metal halide or organometallic components. Eqs. 1-15 to 1-17 show some CVD reactions which rely on gas-phase metathesis reactions.

$$SnCl_4 + 2H_2S \rightarrow SnS_2 + 4HCl \quad [34] \qquad \text{Eq. 1-15}$$

$$GaCl_3 + AsH_3 \rightarrow GaAs + 3HCl \quad [35] \qquad \text{Eq. 1-16}$$

$$(CH_3)_3Ga + AsH_3 \rightarrow GaAs + 3CH_4 \quad [36] \qquad \text{Eq. 1-17}$$

Similarly, high-temperature ammonolysis of metal oxides to form metal nitrides shows an example of a solid-gas metathesis reaction (Eq. 1-18).

$$MO_{3y/2} + yNH_3 \rightarrow MN_y + 3y/2H_2O \qquad \text{Eq. 1-18}$$

Sol-gel reactions forming silica glasses also show some exchange character (Eq. 1-19). Subsequent loss of water leads to SiO_2.

$$Si(OR)_4 + 4H_2O \rightarrow Si(OH)_4 + 4ROH \qquad \text{Eq. 1-19}$$

Substantial research has been carried out on metathetical reactions that do not employ the traditional Na_2E (E = S, Se, Te) or Na_3E' (E′ = P, As, Sb). In their place organometallic silyl-based precursors are used. These precursors are $E(SiMe_3)_2$ (E = S) and $E'(SiMe_3)_3$ (E′ = P, As, Sb). Reactions are performed in a manner similar to that of

the LMM reactions described above, that is, in a refluxing organic solvent with a group 3 halide (e.g. $GaCl_3$).[15,37,38]

Gas-liquid metathesis reactions are experienced by most undergraduates in their first-year cation indentification laboratory exercise (Eq. 1-20).

$$PbCl_{2(aq)} + H_2S_{(g)} \rightarrow PbS_{(s)} + 2HCl_{(aq.)} \qquad \text{Eq. 1-20}$$

1.8 Nanoparticulates:

The interest in performing metathesis reactions in cooler conditions has as one of its major motivations the control of particle sizes, particularly in reducing particle sizes. Particles in the regime where they have dimensions of less than one micrometer have been generally called nanoparticles. In practice, the word 'nanoparticle' only refers to particles of less than 100 nm in all dimensions. There are many situations and applications where small particles are seen as desirable or useful. Another definition is any particle which has a significant percentage (greater than 1%) of their atoms associated with surfaces.

There are many fascinating phenomena that occur when the size of a particle is reduced below a certain size, depending on the particular phenomenon. In general, spatial confinement can affect any property when the size of the particle becomes comparable to or smaller than the critical length scale for the mechanism that is responsible for the property.

Electronic properties are one area that is affected. One effect is called quantum confinement in semiconductor particles. This is the case when the size of the particle becomes comparable to the de Broglie wavelength of the electron-hole pair excitonic states which are responsible for absorption. This leads to a "blue shift" of the optical absorption and is, in effect, a size-dependent band gap in semiconductors.[39] Another electronic effect is quantized conductance in metal and semiconductor wires of nanometer thickness. As the size of the conductor is reduced to very small width scales the conductance of such a wire goes down stepwise rather than linearly as is normal at macroscopic scales.[40]

Mechanical properties of particles or arrays of particles are also affected. One such phenomenon is the size-dependent melting point of nanoscale metal and semiconductor particles. For example, gold particles maintain the bulk melting point of 1336K until about 3 nm when it drops dramatically to about half its value for 2.5 nm

diameter particles.[41] A similar drop in melting point is seen in CdS particles. This phenomenon has been explained as the result of the surface area becoming a significant proportion of the whole and thus the surface tension of the particle has a greater effect on the particle as a whole.[42]

Some other mechanical effects are the strengthening of normally soft metals as their grain sizes fall below about 50 nm. At this size, dislocations become difficult to activate under conventional applied stresses.[43] Ceramics which are normally very brittle can be made more ductile, by synthesising them from particles of about 15 nm. This is due to the increased ease of grain-boundary sliding as a deformation mechanism. Due to the small grain sizes, the cracks that formed in this sliding are more easily healed due to the short diffusion distances.[44] Of course such a reduction in grain size for an advantage in one property, leads to degradation in other properties (for example, creep strength in this case).

Small particle sizes are also desireable for the moderate-temperature sintering of both ceramics and powder metallurgy compacts. Again this is due to the shorter diffusion distances.

1.9 Introduction Conclusions:

Exchange reactions have been shown to be a versatile synthetic route to a large variety of inorganic materials. They utilise the chemical energy built in to the reagents to drive the reaction. The transition from SHS to SSM to LMM shows a path leading from very high-temperature routes to intermediate and low temperatures. This has been driven by the desire for greater control of products, the synthesis of low-temperature phases and the lessening of the ferocity of the reactions for safety and scale-up reasons.

Previous syntheses of materials by liquid-mediated metathetical routes have focused heavily on II-VI and III-V semiconductor materials. Little work has been reported on the LMM synthesis of other materials and the wide variety of work done by SSM has yet to be matched by liquid-mediated equivalents. The main aim of this project has been to expand the scope of knowledge on liquid-mediated metathesis reactions and to compare and contrast the results with previously known solid-state reactions.

2. *Metal Chalcogenides:*

2.1 Introduction:

Metal chalcogenide compounds have a wide variety of commercial applications, in both high-technology and commodity fields. A selection of lanthanide and metal lanthanide chalcogenides have uses as infra-red lenses[45], catalysts[46], colour phosphours in television sets[47] and neodynium sulphide lasers.[48]

2.1.1 Thin Films:

The electronics industry is currently dominated by the use of silicon-based semiconductors, with an approximately 95% market share. However, in optoelectronic applications (*eg.* photonic communiation and computing), silicon-based semiconductors are problematic because of their weak photoemission efficiency due to their indirect bandgap.[49] Therefore, there has been increasing interest in alternative technologies employing chalcogenide-based binary and ternary compounds. The group 12-16 family of semiconductors is more suitable for these applications due to their direct transition. Their wide bandgap makes them potentially important for emission and detection in the visible and near-UV region of the spectrum.[50]

Due to limitations of current processing and manufacturing techniques in the production of suitably refined and pure thin films of 12-16 materials, they have been confined to relatively simple uses. Among these are optical coatings, gratings, photoconductors and a range of optical windows.[51] Zinc and cadmium sulphides and selenides are used in the production of light emitting diodes due to their semiconductor and luminescent properties.[52] Recent progress in the formation of high purity and high homogeneity thin films by metalorganic chemical vapour deposition (MOCVD) techniques may allow further device applications to become viable. ZnS and ZnSe show

promise as fast switching devices and as laser diode devices in the blue-green region with potential application in optical high density data storage materials.[53] ZnS-based thin film electroluminescent displays are also available commercially by MOCVD methods. Cadmium chalcogenides find use as solid-state solar cells and photo detectors,[51,54] field-effect transistors and transducers.[55]

Indium and gallium chalcogenides of the form M_2E_3 (M = In, Ga; E = S, Se, Te), are also direct transition, wide band gap semiconductors, similar to the 12-16 materials described above. The indium compounds adopt a defect spinel structure and the gallium compounds adopt a zinc blende structure. The alternative ME structures have narrower band gaps similar to those of 13-15 materials further discussed in Chapter 3.

Tin sulphides adopt a variety of distinct semiconducting phases. These include trigonal SnS_2, rhombic Sn_2S_3, tetragonal Sn_3S_4 and orthorhombic SnS. These compounds show a wide range of electronic properties. Tin (IV) sulphide has an optical band gap of 2.07 eV and has n-type conductivity, while tin (II) sulphide displays p-type conductivity and has a band gap of 1.08 eV, similar to that of silicon. The mechanism of charge transport in SnS is based on acceptor levels created by tin vacancies normally present in the lattice. An excess of tin can thus change the conductivity from p-type to n-type. Thin films of SnS are employed as or have potential as photovoltaic materials,[56] solar control coatings and heat mirrors.[57]

2.1.2 Bulk Materials:

High-technology uses of chalcogenide materials is overwhelmingly dominated by their formation into thin films. The uses of bulk chalcogenide materials are, for the most part, associated with less advanced, but no less important, industries.

One such industrial use is zinc, cadmium and mercury chalcogenides as high-temperature pigments. A full range of colours from bright yellow to deep red can be achieved by judicious selection of binary and ternary solid solution mixtures of these

compounds. For example CdS is bright yellow colour. Incorporating increasing amounts of zinc into CdS to form a [(Cd,Zn)S] ternary compound allows a range of yellows to be obtained. Similarly cadmium sulphoselenides [Cd(S,Se)] and cadmium mercury sulphides [(Cd,Hg)S] form a range of colours from orange to deep red.[58]

A similar range of Cd_xHg_yTe ($x + y = 1$) compounds has been used as a method for calibrating and standardising certain spectroscopic equipment. This is due to their regular band gap variations with variable cadmium content. These inorganic compounds are especially useful as pigments in high-temperature applications or ceramics where high temperatures are used in processing. They are also used as pigments for artists. Commercial pigments are often mixtures of compounds including the coloured component, dilutants and dispersal media. The colour variation is often achieved not only with the help of composition variation of the coloured material but also in particle size variation.[58]

Other industrial uses of these chalcogenides include roles as catalysts, lubricants and battery cathode materials. Tin, titanium, zirconium and hafnium di-sulphides all adopt a wurtzite structure consisting of hexagonal close-packed layers of sulphur atoms with the octahedral holes of alternate layers being occupied by metal atoms. This results in a structure in which the inter-layer bonding is relatively weak. Tantalum and molybdenum sulphide also have such a layered structure. This weak inter-layer bonding allows the layers to slide relatively easily against each other. This makes them ideal candidates as high-temperature lubricants in situations where normal hydrocarbon-based lubricants are broken down by the operating temperature. The layer structure of the metal sulphides remain stable at high temperatures.[52] These layer-structured compounds also find use in theoretical studies of charge-wave coupling on two-dimensional surfaces as studied by scanning tunneling microscopy (STM).[59] Another use of such layered compounds is as cathode materials for high-temperature batteries. S^{2-} ions travel through the relatively open layer structure and react in a controlled manner at the cathode interface.

The catalytic uses of various chalcogenides include that of MoS_2 in the petrochemical industry, various layered sulphides in hydrodesulphurisation and cadmium and zinc sulphides as potential catalysts for photodecomposition of water.

This chapter deals with the synthesis and characterisation of a selection of metal chalcogenides. A number of variations in synthetic conditions and post-synthesis treatment has been considered and explored.

2.2 *Results - Synthesis and Characterisation:*

2.2.1 *First Row Transition Metals - Titanium, Vanadium, Iron, Cobalt & Nickel:*

The reaction of transition metal halides with sodium chalcogenides was performed using the liquid-mediated methatetical route, as shown in Eqs. 2-1 to 2-5:

$TiI_4 + 2Na_2S$	$\rightarrow$	$TiS_2 + 4NaI$	Eq. 2-1
$2VBr_3 + 3Na_2S$	$\rightarrow$	$V_2S_3 + 6NaCl$	Eq. 2-2
$2FeCl_3 + 3Na_2S$	$\rightarrow$	$Fe_2S_3 + 6NaCl$	Eq. 2-3
$CoCl_2 + Na_2S$	$\rightarrow$	$CoS + 2NaCl$	Eq. 2-4
$NiCl_2 + Na_2E$	$\rightarrow$	$NiE + 2NaCl$ (E = S, Se)	Eq. 2-5

The reaction of metal halides with sodium chalcogenides in refluxing toluene for 48 h resulted in the formation of X-ray amorphous black or dark grey powders. The powders were washed with ethanol and water and analysis of the water washing showed them to contain sodium halide. Annealing the washed powders resulted in varying results. The reactions involving iron, nickel and cobalt produced crystalline products after annealing at 500°C for 60 h.

2.2.1.1 XRD Data:

XRD data showed that iron sulphide was found in a slightly iron-deficient form of formula $Fe_{0.89}S$ rather than the intended Fe_2S_3 structure, cobalt sulphide was again found in a slightly metal-deficient form of formula $Co_{0.90}S$ and nickel sulphide was found to crystallise into a slightly metal-deficient $Ni_{0.98}S$ structure (Fig. 2-1). Nickel selenide was found to crystallise into a $NiSe_2$ (penroseite) structure (Fig. 2-2). Some product and XRD data is shown in Table 1.

Table 1 Product and XRD data* for transition metal chalcogenides

Phase: by XRD[a]	**Colour**	**Unit Cell Params. Lit. Values/Å[60]**	**Unit Cell Params. Observed/Å [a]**
$Fe_{0.89}S$	Black	$a = 3.43$ $c = 3.79$	$a = 3.43$ $c = 3.79$
$Co_{0.90}S$	Black	$a = 3.38$ $b = 5.15$	$a = 3.38$ $b = 5.15$
$Ni_{0.98}S$	Black	$a = 3.42$	$a = 3.42$
$NiSe_2$	Black	Characterised using JCPDS file no. 11-0552	

[a] after annealing at 500°C for 24 h. * Unit cell dimensions *a, b, c* in Å (±0.01Å).

2.2.1.2 EDAX Data:

EDAX analysis before annealing showed that cobalt sulphide consisted of a 1:1 atomic ratio. After annealing the ratio observed matched that of the product observed by XRD. Nickel sulphide, before annealing showed a nickel-rich composition by EDAX corresponding to a 2:1 Ni:S atomic ratio. A search of the literature revealed that there is no known compound which has a Ni_2S structure, although there are various Ni_3S_2 structures. After annealing there was still found to be an overall excess of nickel but that it was segregated into nickel-rich areas. One explanation could be that it is an intimate mixture of nickel metal and NiS and that before annealing EDAX can not distinguish areas of differing concentration because of the intimate scale of the mixing. After annealing there has been enough agglomeration for EDAX to distinguish regions of high nickel content, but the annealing was insufficient to cause the nickel to crystallise and thus it did not appear on the XRD spectrum.

The reaction to form nickel selenide took a different pathway. The XRD pattern showed only $NiSe_2$ after annealing but the EDAX data shows that there are approximately equal amounts of NiSe and $NiSe_2$ present, both before and after annealing. This indicates that the NiSe compound remained X-ray amorphous after annealing and that higher temperatures or longer annealing times would have to be employed to induce crystallinity.

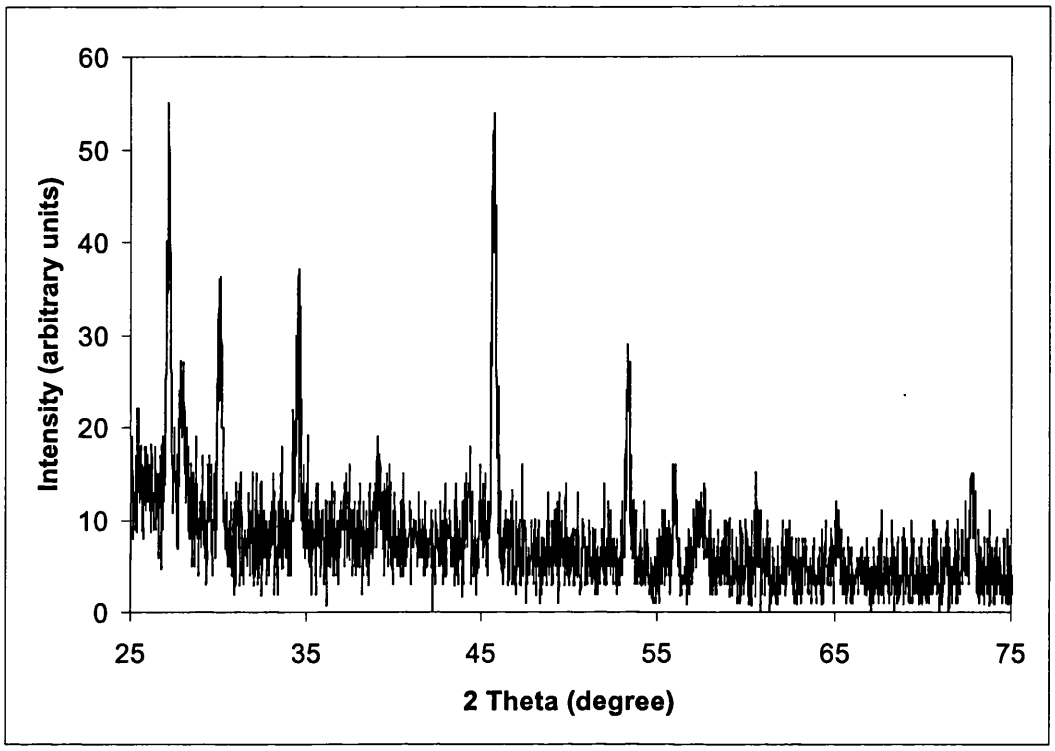

Fig. 2-1 XRD pattern of $NiS_{0.98}$, annealed.

EDAX of the annealed iron sulphide showed an overall atomic ratio of 3:1 Fe:S. This conflicts with the evidence supplied by the XRD pattern which showed a 1:1 iron sulphide structure. Spot EDAX analysis did not reveal any iron-rich areas, meaning that the iron excess was uniformly distributed throughout the sample. This may be due to some partial oxidation of the iron sulphide, liberating H_2S, and thus there would appear to be an excess of iron with respect to sulphur (oxygen is not detectable by the EDAX system used).

The reactions involving the early transition metals titanium and vanadium resulted initially in dark grey powders but they were seen to slowly transform over a period of a few hours to a few days from a dark colour into a lighter colour; white in the case of titanium and a pale green in case of vanadium. Analysis of the powders by EDAX after this change showed them to contain only the metal element and no sulphur. Annealing these powders gave TiO_2 (anatase) by XRD for the titanium case and no pattern was obtainable in the vanadium case. Powders analysed before the transition was completed

gave results consistent with the formation of sulphides. EDAX data for the vanadium sulphide showed it to consist of a 1:1 vanadium to sulphur ratio, rather than the intended V_2S_3 structure. The VS structure was confirmed by Raman microscopy which also discovered significant amounts of V_2O_5. This indicates that the oxidation reaction of the synthesised powders occurs as soon as the product is exposed to air and/or moisture and that the reaction proceeds at a not unappreciable rate.

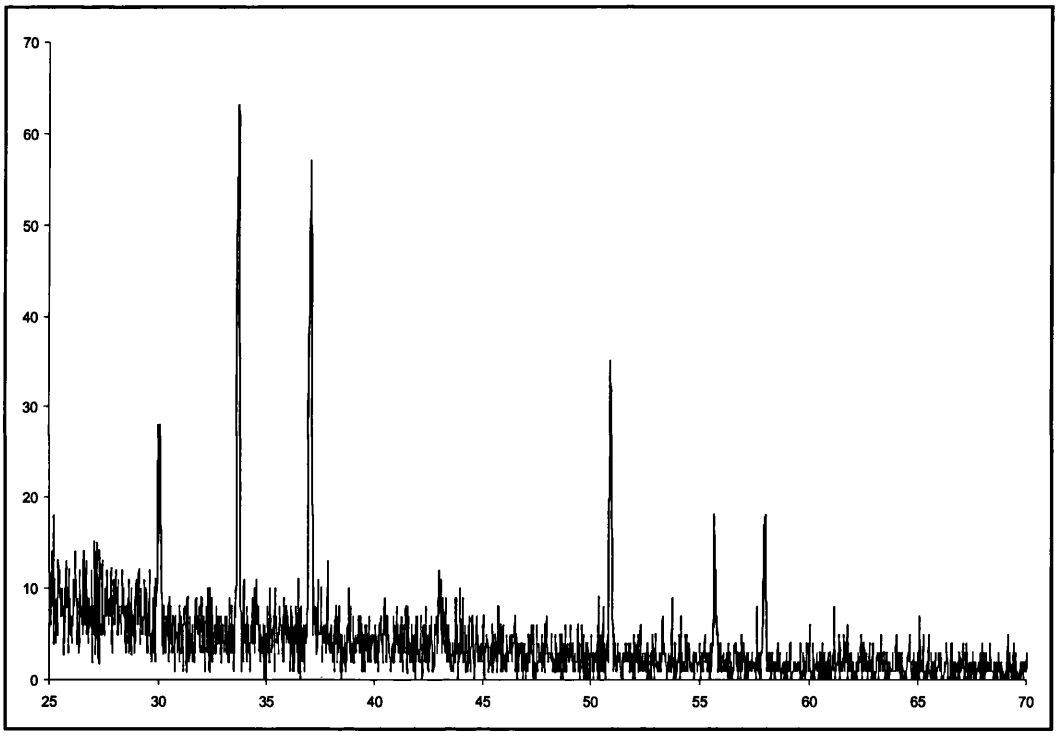

Fig. 2-2 XRD pattern of $NiSe_2$, annealed.

2.2.1.3 Particle Morphology & Sizes:

All the transition metal sulphides synthesised showed remarkably similar agglomerate size and morphology. All the samples except VS showed spherical agglomerates of less than 1 μm diameter, with a small number of agglomerates in the 5-10 μm size range. Examination of the surfaces of these spherical agglomerates showed them to have small surface features on the order of *ca.* 50-100 nm. This is an estimate

due to this being quite close to the resolution limit of the SEM equipment, however it does give an order of magnitude indication of individual crystallite size. Application of the Scherrer equation (See Ch. 2.3.5 for details) gives average crystallite sizes of approximately 20-30 nm, after annealing. The vanadium sample showed slightly larger agglomerates with an average diameter of approximately 3 μm.

2.2.2 Group 11 - Copper & Silver:

The reaction of silver and copper halides with sodium chalcogenides was performed using the liquid-mediated methatetical route. The reaction schemes are shown in Eqs. 2-6 to 2-8:

$$2CuBr + Na_2E \rightarrow Cu_2E + 2NaBr \ (E = S,Se) \qquad \text{Eq. 2-6}$$

$$CuCl_2 + Na_2E \rightarrow CuE + 2NaCl \ (E = S,Se) \qquad \text{Eq. 2-7}$$

$$2AgF + Na_2E \rightarrow Ag_2E + 2NaF \ (E = S,Se) \qquad \text{Eq. 2-8}$$

The reaction of metal halides with sodium chalcogenides in refluxing toluene for 48 h resulted in these cases in the formation of crystalline black or dark grey powders in approximately 90% yield. The powders were washed with ethanol and water and analysis of the water washing showed them to contain sodium halide. Annealing the washed powders resulted in further crystallisation of the products. Similar to the transition metal reactions, the precursors were found not to dissolve in the toluene liquid.

XRD data showed the formation of Ag_2S (acanthite) (Fig. 2-4) and Ag_2Se (naumanite) (Fig. 2-3) before annealing. EDAX data confirms the 2:1 atomic ratio of the elements. The reaction of AgF with Na_2S was repeated but utilising a shorter reaction time of 8 hours. XRD analysis of the product from this short reaction also showed the formation of Ag_2S (acanthite) which was indistinguisheable from that of the 48 h reaction. This showed that the reaction was completed in substantially shorter time than

the time allowed for the reaction to go to completion.

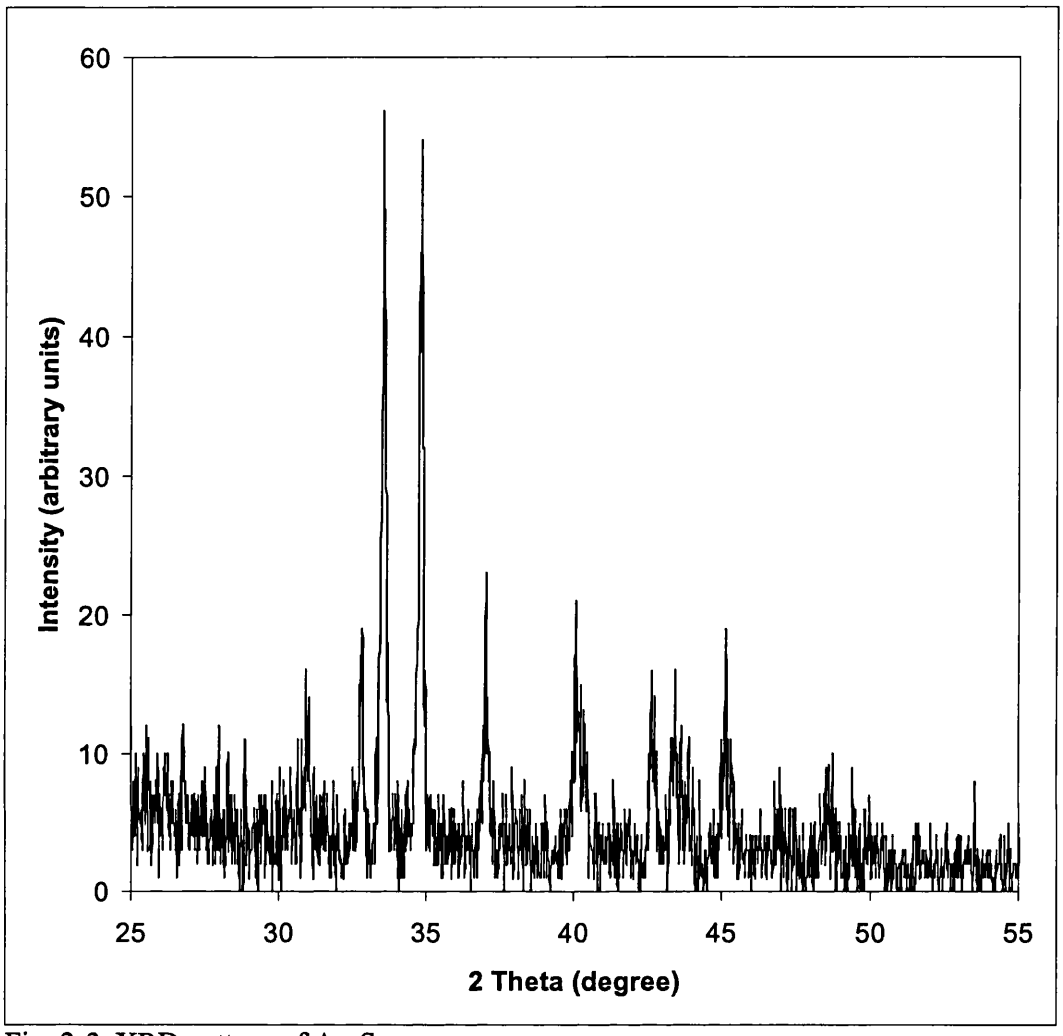

Fig. 2-3 XRD pattern of Ag_2Se.

The reaction of $CuCl_2$ with Na_2E resulted in the formation of crystalline CuS (covelite) and CuSe (klockmannite) before annealing. Annealing at 500°C results in the transformation to a Cu_7S_4 (anilite) structure by XRD. Annealing at a milder temperature of 300°C shows no such conversion, maintaining the CuS (covelite) structure. Some XRD and product data is presented in Table 2.

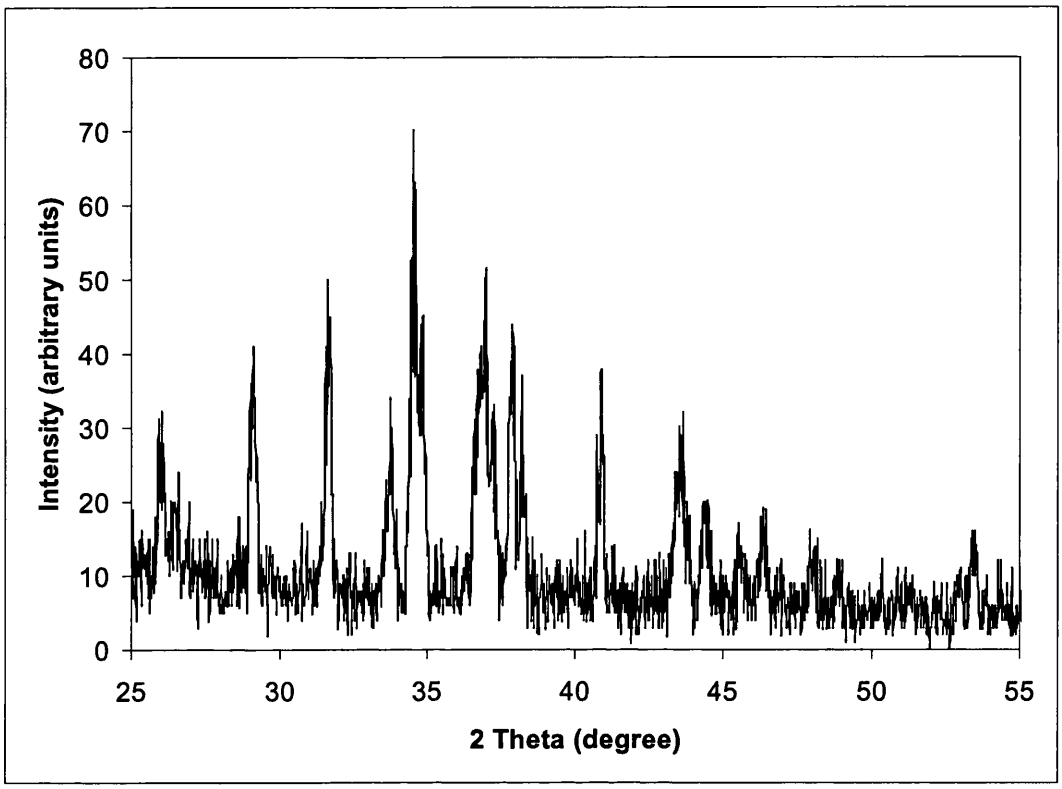

Fig. 2-4 XRD pattern of Ag_2S.

Table 2 Product and XRD data* for silver and copper chalcogenides.

Phase: by XRD	**Colour**	**Unit Cell Params. Lit. Values/Å[60]**	**Unit Cell Params. Observed/Å [a]**
CuS (covelite)	Black	$a = 3.76$ $c = 16.19$	$a = 3.76$ $c = 16.20$
Cu_2S	Black	Characterised using JCPDS file no. 6-0680	
Cu_7S_4	Black	Characterised using JCPDS file no. 22-0250	
CuSe (klockmannite)	Black	$a = 3.76$ $c = 16.19$	$a = 3.76$ $c = 16.20$
Cu_2Se	Black	Characterised using JCPDS file no. 19-0401	
Ag_2S (acanthite)	Black	$a = 4.48$	$a = 4.48$
Ag_2Se (naumannite)	Black	$a = 4.33$ $b = 7.06$ $c = 7.76$	$a = 4.33$ $b = 7.06$ $c = 7.76$

[a] after annealing at 500°C for 24 h. * Unit cell dimensions *a, b, c* in Å (±0.01Å).

The reaction of CuBr with Na_2E resulted in the formation of amorphous powders before annealing. EDAX analysis of the powders gives metal-deficient 1.8:1 copper to sulphur and 1.98:1 selenium atomic ratios. Annealing of the powders results in the formation of crystalline $Cu_{1.8}S$ (digenite) and $Cu_{1.98}Se$ (berzelianite) (Fig. 2-5).

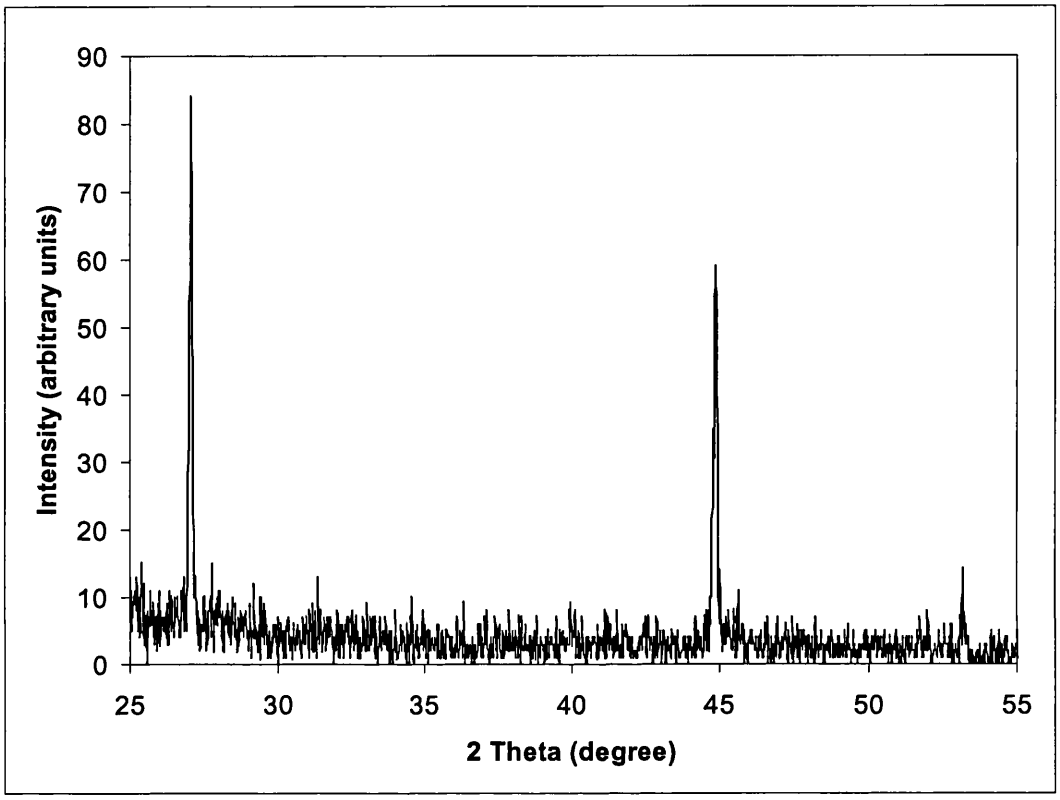

Fig. 2-5 XRD pattern of $Cu_{1.98}Se$.

For the reaction involving $CuCl_2$ (Eq. 2-7) a further number of reactions were performed in an additional number of liquids. These were pyridine, hexane and tetrahydrofuran (THF). The reactions showed that CuS (covelite) was formed regardless of the liquid used. However, with the use of pyridine, the $CuCl_2$ precursor dissolved in the liquid, making it different from the previous reactions using toluene. While the product obtained was found to be crystalline CuS, the yield was reduced to one half of its usual amount. This was due to an adduct formed between the $CuCl_2$ precursor and pyridine which thus immobilized a portion of the copper. The pyridine was found to be a deep green colour. The reactions in hexane and THF produced CuS in similar yields to that of the reaction performed in toluene.

2.2.3 Group 12 - Zinc, Cadmium & Mercury:

The reaction of zinc, cadmium and mercury halides with sodium chalcogenides was performed using the liquid-mediated methatetical route. The reaction schemes are shown in Eqs. 2-9 to 2-11:

$$ZnBr_2 + Na_2E \rightarrow ZnE + 2NaBr\ (E = S,Se) \qquad \text{Eq. 2-9}$$

$$CdCl_2 + Na_2E \rightarrow CdE + 2NaCl\ (E = S,Se) \qquad \text{Eq. 2-10}$$

$$HgCl_2 + Na_2E \rightarrow HgE + 2NaCl\ (E = S,Se) \qquad \text{Eq. 2-11}$$

The reaction of metal halides with sodium chalcogenides in refluxing toluene for 48 h resulted in these cases in the formation of crystalline powders in approximately 90% yield. The powders were washed with ethanol and water and analysis of the water washing showed them to contain sodium halide. Annealing the washed powders resulted in further crystallisation of the products. Similar to all the reactions so far, the precursors were found not to dissolve in the toluene liquid. Some product data is shown in Table 3.

Table 3 Product and XRD data* for zinc, cadmium and mercury chalcogenides.

Phase: by XRD	**Colour**	**Unit Cell Params. Lit. Values/Å[60]**	**Unit Cell Params. Observed/Å [a]**
ZnS	Light grey	$a = 3.76$ $c = 16.19$	$a = 3.76$ $c = 16.20$
CdS	Yellow	$a = 4.14$ $c = 6.72$	$a = 4.14$ $c = 6.72$
HgS (metacinnabar)	Black	$a = 5.85$	$a = 5.85$
HgS (cinnabar)[b]	Red	Characterised using JCPDS file no. 14-1408	
ZnSe	Light orange	$a = 3.76$ $c = 16.19$	$a = 3.76$ $c = 16.20$
CdSe	Deep orange	Characterised using JCPDS file no. 8-0459	
HgSe	Black	$a = 6.08$	$a = 6.08$

[a] after annealing at 500°C for 24 h. * Unit cell dimensions *a, b, c* in Å (±0.01Å). [b] after annealing only.

The product of the reaction of $ZnBr_2$ with Na_2S resulted in a light grey powder which gave an XRD pattern that showed ZnS (sphalerite, zinc blende) (Fig. 2-6). The equivalent selenide reaction gave an orange powder with an amorphous XRD pattern. Annealing at both 250°C and 500°C gave crystalline ZnS and ZnSe. EDAX data for both zinc products gave 1:1 zinc to element atomic ratios.

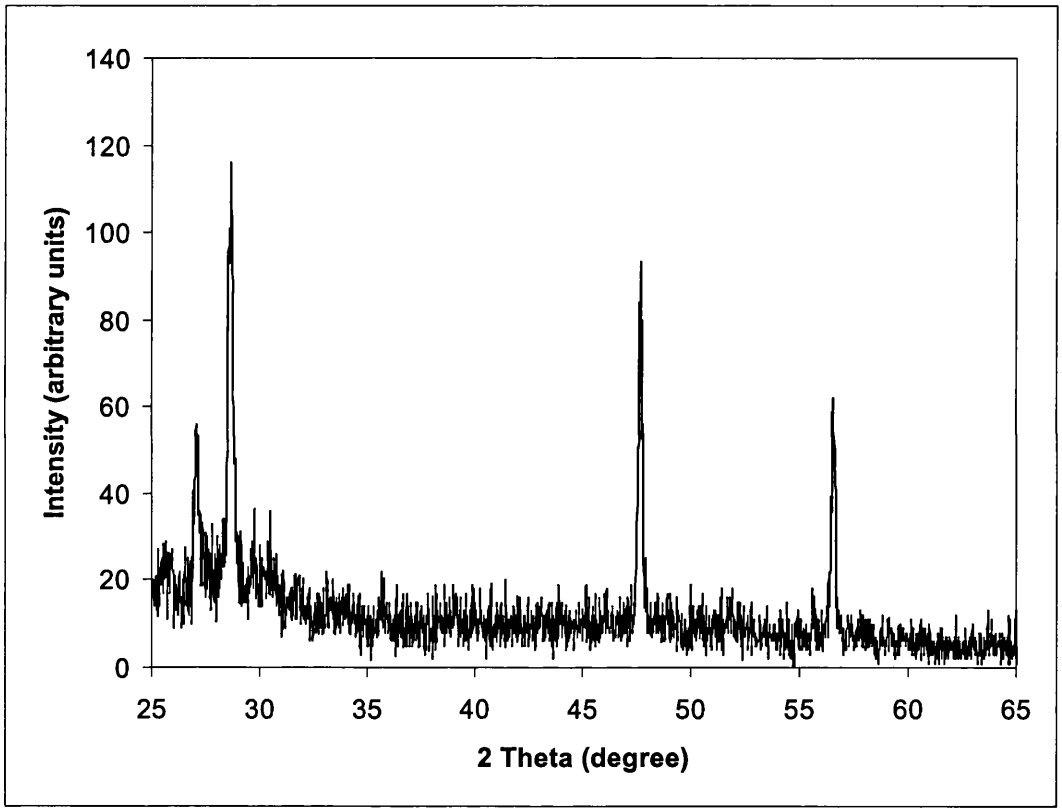

Fig. 2-6 XRD pattern of ZnS.

The product of the reaction of $CdCl_2$ with Na_2S resulted in a yellow powder which gave an amorphous XRD pattern. The equivalent selenide reaction gave a deep orange powder with an amorphous XRD pattern. Annealing at 200°C gave crystalline CdS (greenockite) (Fig. 2-7) and CdSe (cadmoselite). EDAX data for both zinc products gave 1:1 cadmium to element atomic ratios. A further set of reactions aiming towards the synthesis of ternary $CdS_{0.5}Se_{0.5}$ were performed and are described and

discussed in more detail later in this chapter.

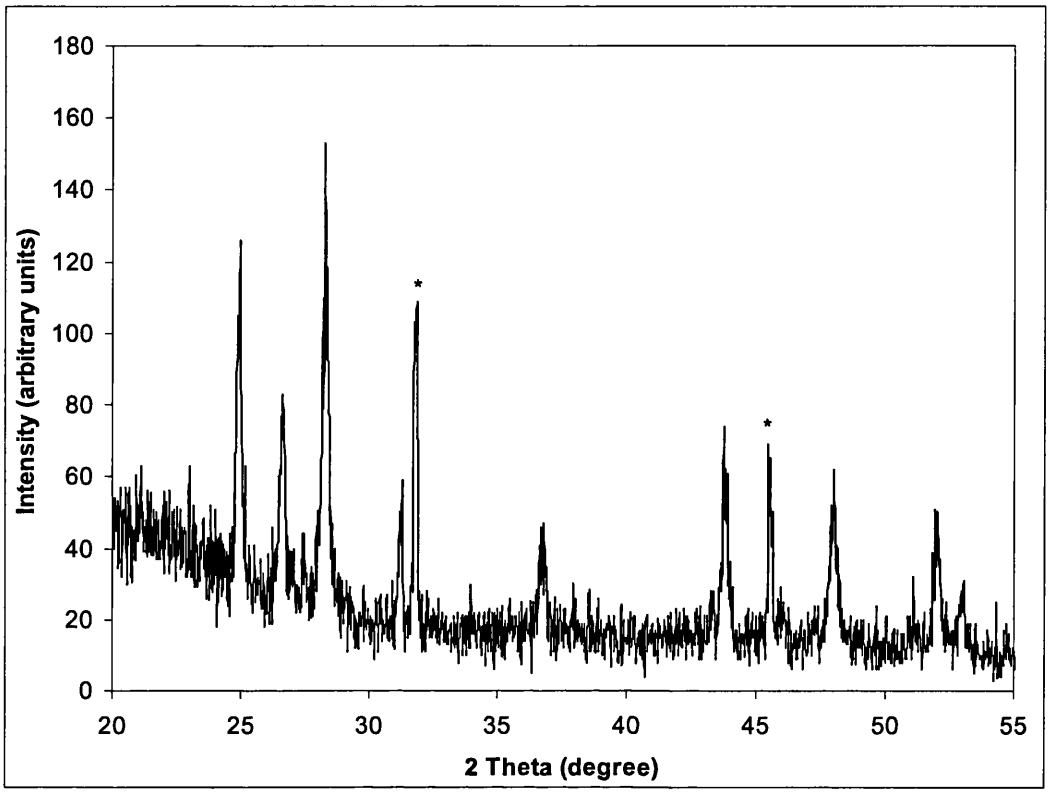

Fig. 2-7 XRD pattern of CdS. * = NaCl peaks

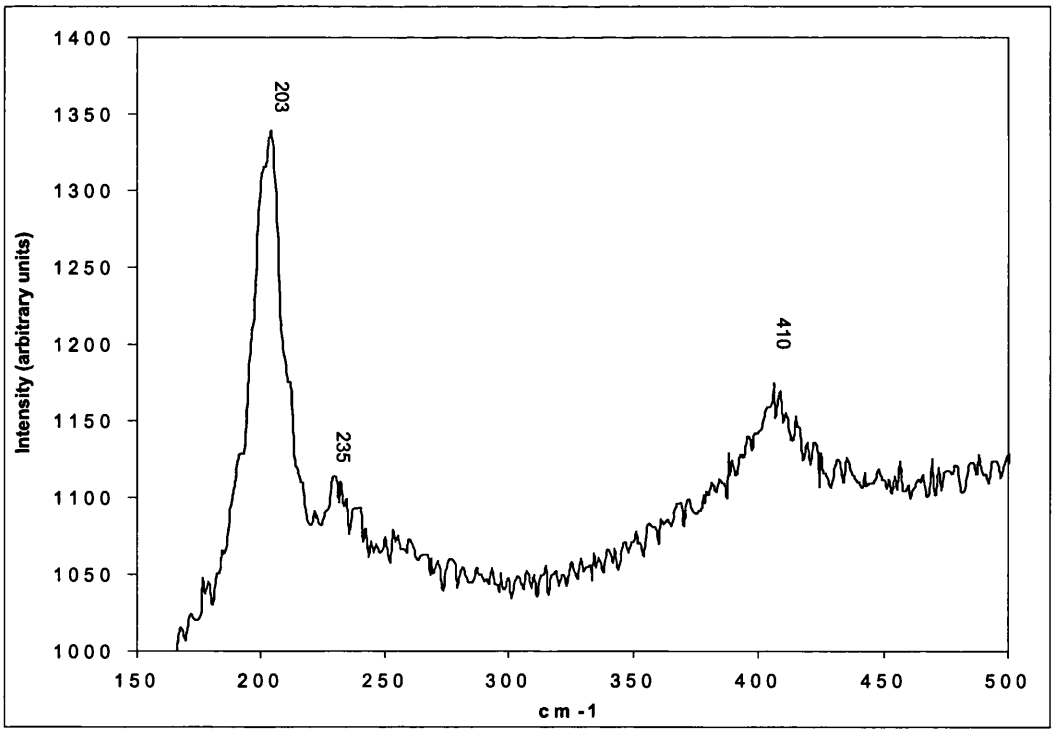

Fig. 2-8 Raman spectrum of CdS.

The product of the reaction of $HgCl_2$ with Na_2S resulted in a black powder which gave the XRD pattern of HgS (metacinnabar) (Fig. 2-9). The equivalent selenide reaction gave a black powder with an amorphous XRD pattern. Annealing of mercury compounds at 500°C resulted in the decomposition of the products to the elements. Annealing at 250°C resulted in the further crystallisation of HgS and in the crystallisation of HgSe (tiemannite). In the case of mercury sulphide a small amount (*ca.* 5%) of a second phase of HgS (cinnabar; also vermillion) appeared as a result of the annealing. Raman microscopy of the mercury (Fig. 2-10) and cadmium (Fig. 2-8) samples confirms the existence of the various phases of sulphide and selenide both before and after annealing. Figs. 2-11 and 2-12 show representative SEM photos for $CdS_{0.5}$ $Se_{0.5}$ and ZnSe, respectively.

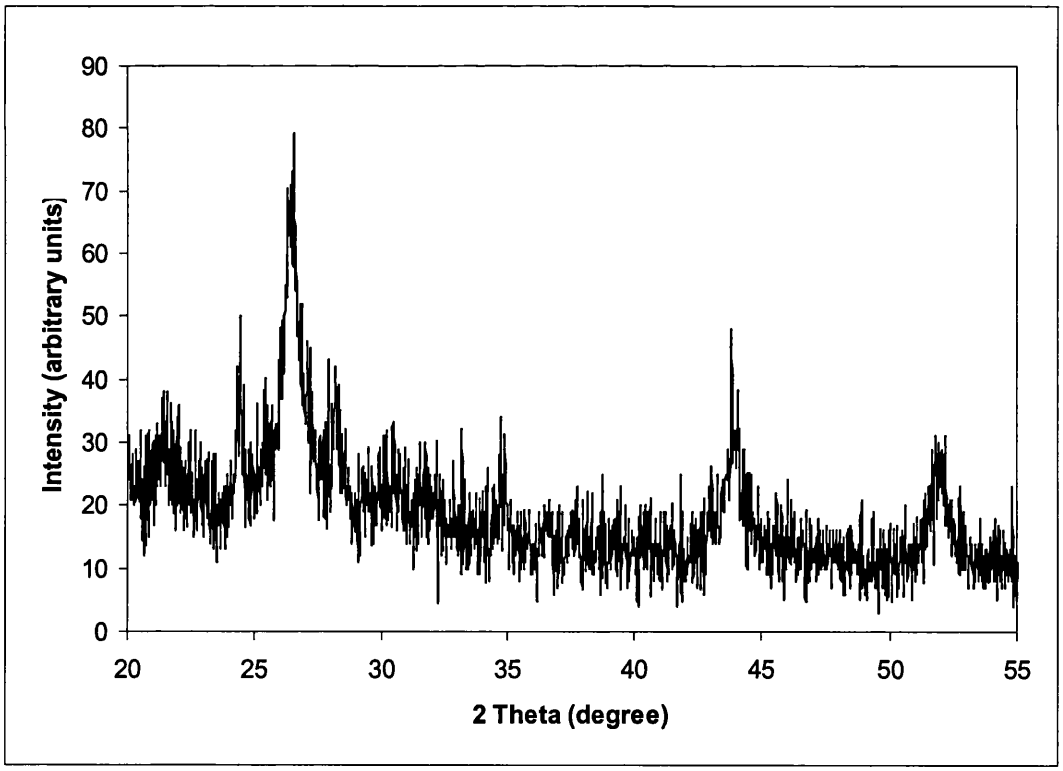

Fig. 2-9 XRD pattern of HgS (metacinnabar).

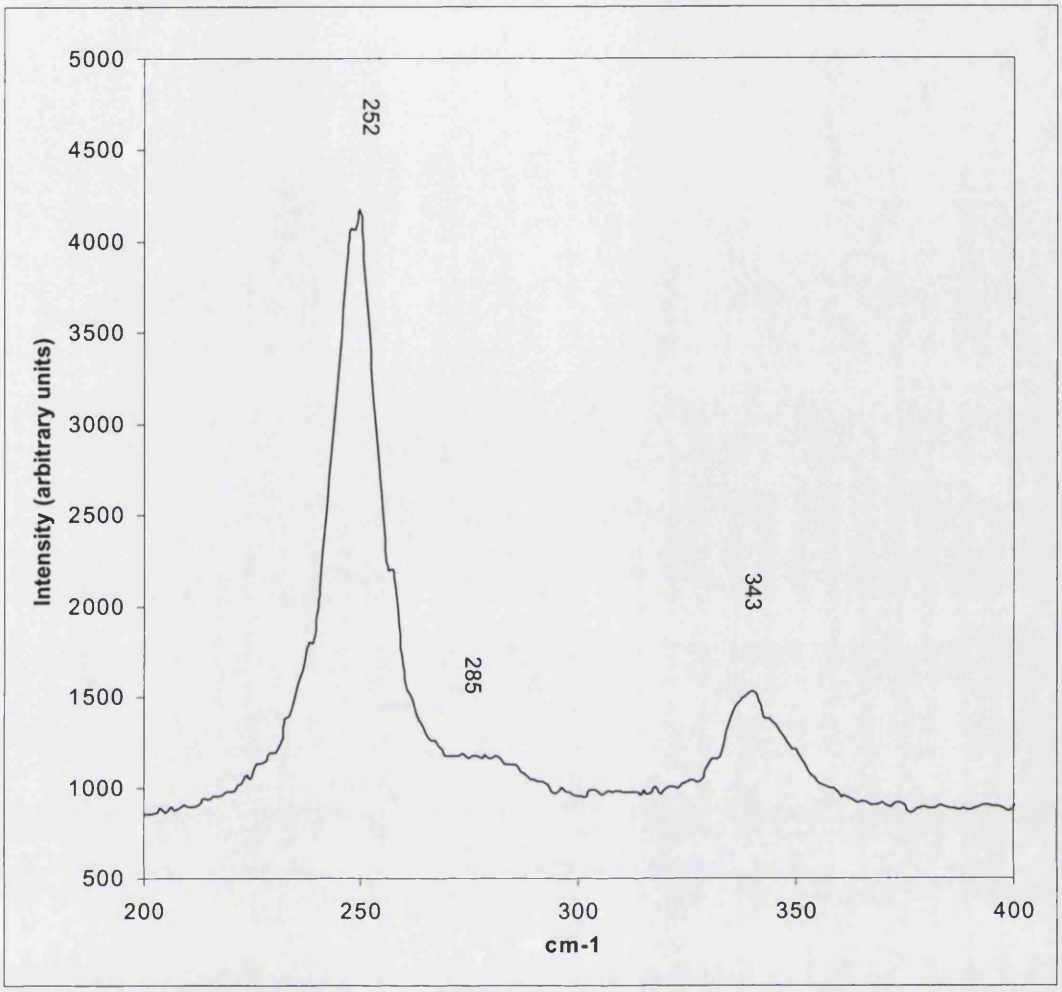

Fig. 2-10 Raman Spectrum of HgS (cinnabar).

Fig. 2-11 SEM of $CdS_{0.5}$ $Se_{0.5}$, annealed.

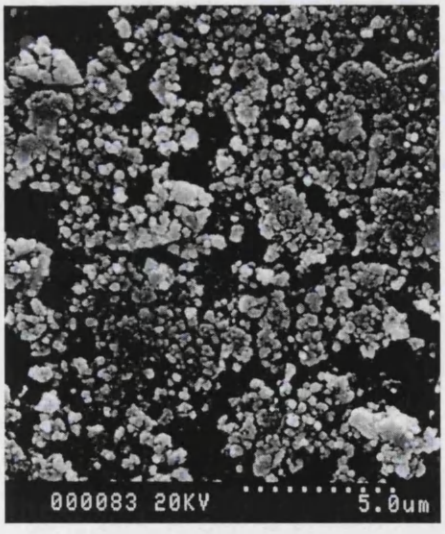

Fig. 2-12 SEM of ZnSe, annealed.

2.2.4 Group 13 - Indium:

The series of indium chalcogenides of the form In_2E_3 (E = O, S, Se, Te) was synthesised using the liquid-mediated metathesis reaction scheme, as shown in Eqs. 2-12 and 2-12.

$$2InCl_3 + 3Na_2O_2 \rightarrow In_2O_3 + 6NaCl + 3/2O_2 \quad \text{Eq. 2-12}$$

$$2InCl_3 + 3Na_2E \rightarrow In_2E_3 + 6NaCl\ (E = S, Se, Te) \quad \text{Eq. 2-13}$$

The reaction of $InCl_3$ with Na_2O_2 or Na_2E (E = S, Se, Te) in refluxing toluene for 48 h resulted in the formation of single-phase In_2E_3 compounds. The colour change of the reactant powders to the colour of the final product indicated that the reaction occured slowly over 24-36 h. Some results are summarised in Table 4. For example, the white colour of $InCl_3$ slowly disappeared as the yellow-green product was formed. Na_2S is a similar yellow-green colour to the product so the reaction progress was judged solely on the amount of white particles seen. It is important to note that the reactants did not appear to dissolve in the refluxing toluene. This meant that the reaction was in fact a dilute stirring slurry of $InCl_3$ particles and Na_2S particles in toluene.

Table 4 Product and XRD data* for In_2E_3 (E = O, S, Se, Te)

Product	Colour	Phase: by XRD[a]	Lattice type	Unit Cell Params. Lit. Values/Å[60]	Unit Cell Params. Observed/Å [a]
In_2O_3	White	In_2O_3	Cubic	$a = 10.12$	$a = 10.11$
In_2S_3	Yellow-Green	In_2S_3	Cubic	$a = 10.73$	$a = 10.78$
In_2Se_3	Red-Brown	In_2Se_3	Hexagonal	$a = 7.13$ $c = 19.38$	$a = 7.12$ $c = 19.37$
In_2Te_3	Black	In_2Te_3 (Te)	Cubic	$a = 18.49$	$a = 18.47$

[a] after annealing at 500°C for 24 h. * Unit cell dimensions *a, b, c* in Å (±0.01Å).
(Minor phases (<10%) in parentheses).

The reactions described above yielded amorphous products in approximately

90 % yield. Annealing the washed powders at 500°C for 24 h resulted in crystalline In_2E_3 products as shown by powder X-ray diffraction (Fig. 2-13 shows In_2O_3). EDAX analysis of the washed powders both before and after annealing showed an indium to element ratio of 2:3, therefore annealing did not affect the element ratios. IR spectra of the powders showed broad bands in the 600 to 400 cm^{-1} region. Examination by XRD of the powders before washing showed them to be a mixture of In_2E_3 and NaCl. Evaporation of the H_2O washings left behind a powder which gave an XRD pattern for that of NaCl. This indicates that the reaction proceeded by a metathetical route.

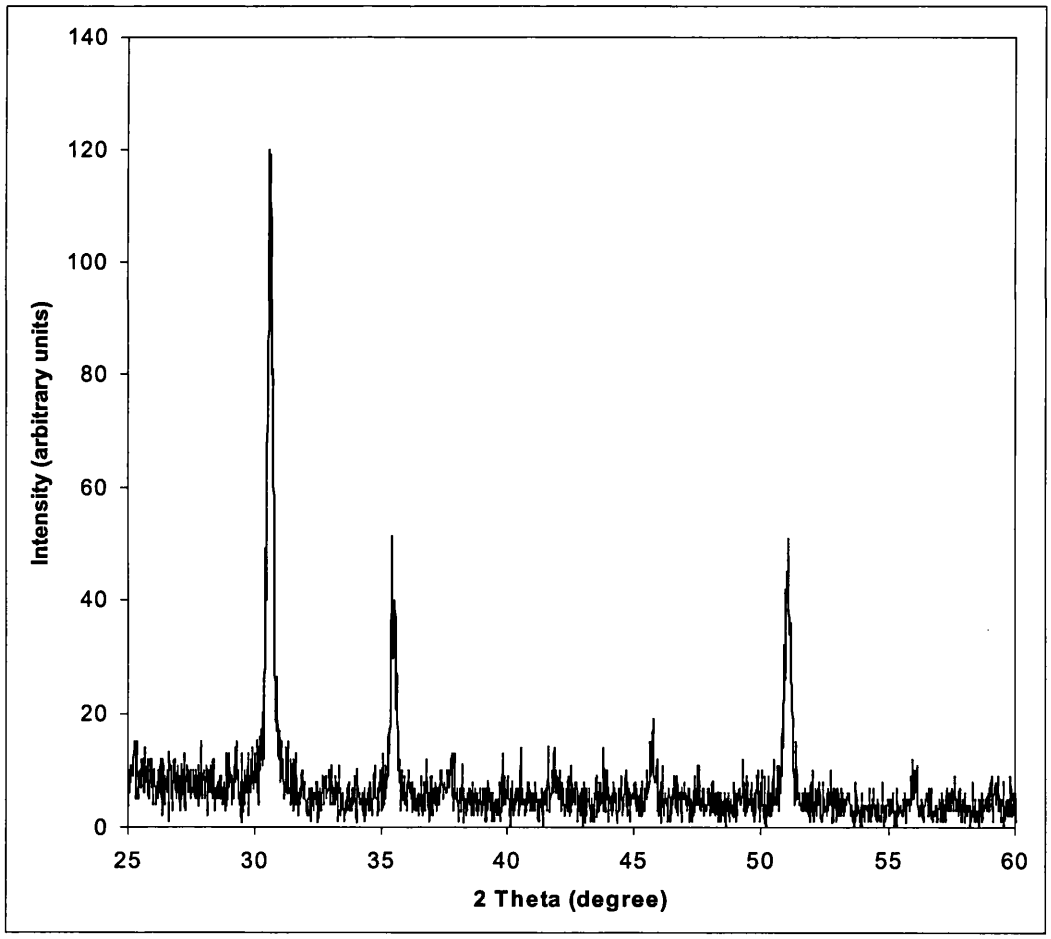

Fig. 2-13 XRD pattern for In_2O_3, annealed.

The powder particles were examined by scanning electron microscopy (SEM) which showed that the morphology and particle size was similar for all the samples (Figs.

2-14 to 2-16). The indium chalcogenides showed small rounded agglomerates with the majority having diameters less than 1 μm. A few agglomerates had larger sizes, up to *ca.* 10 μm in size. Close examination of these agglomerates showed them to have very fine surface features of less than 50 nm diameter.

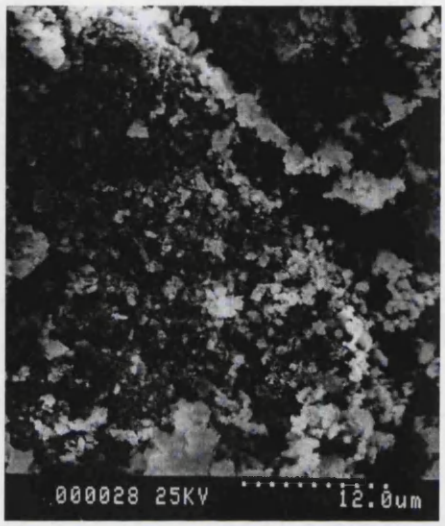

Fig. 2-14 SEM of In_2O_3, annealed.

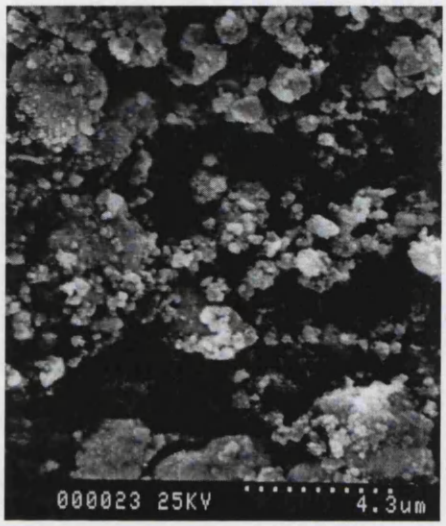

Fig. 2-15 SEM of In_2Te_3 unannealed.

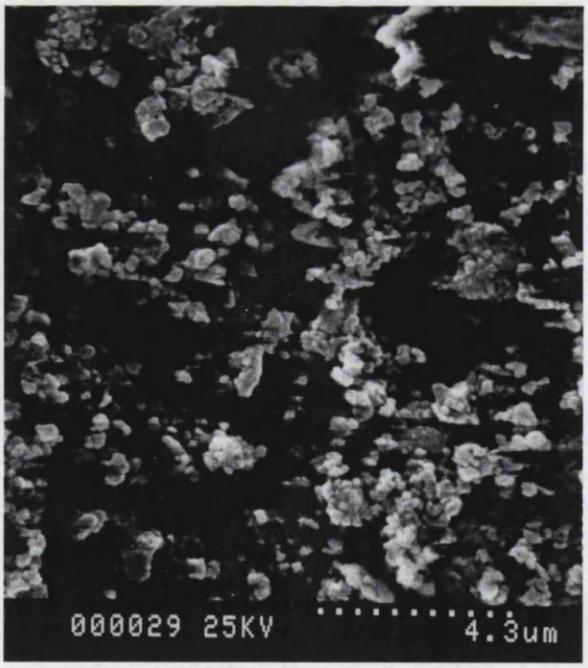

Fig. 2-16 SEM of In_2S_3, annealed.

2.2.5 Group 14 - Tin & Lead:

Tin and lead chalcogenides were synthesised by the liquid-mediated metathetical route employed throughout. Eqs. 2-14, 2-15 and 2-16 represent the chemical equations used:

$$SnCl_2 + Na_2E \rightarrow SnE + 2NaCl \quad (E = S, Se) \quad \text{Eq. 2-14}$$

$$SnI_4 + 2Na_2E \rightarrow SnE_2 + 4NaI \quad (E = S, Se) \quad \text{Eq. 2-15}$$

$$PbCl_2 + Na_2E \rightarrow PbE + 2NaCl \quad (E = S, Se) \quad \text{Eq. 2-16}$$

The reaction of tin and lead halides with sodium chalcogenides in refluxing toluene for 48 h resulted in the formation of crystalline black or dark grey powders in approximately 90% yield. The powders were washed with ethanol and water and analysis of the water washing showed them to contain sodium halide. Annealing the washed powders resulted in further crystallisation of the products. Like most of the reactions described the precursors were found not to dissolve in the toluene liquid. Some product and XRD data are shown in Table 5.

Table 5 Product and XRD data* for zinc, cadmium and mercury chalcogenides.

Phase: by XRD	**Colour**	**Unit Cell Params. Lit. Values/Å[60]**	**Unit Cell Params. Observed/Å [a]**
SnS (herzenbergite)	Black	$a = 3.99$ $b = 4.34$ $c = 11.20$	$a = 3.99$ $b = 4.35$ $c = 11.20$
SnS_2 (berndtite)	Grey	$a = 4.14$ $c = 6.72$	$a = 4.14$ $c = 6.72$
PbS (galena)	Black	$a = 5.93$	$a = 5.93$
SnSe	Grey	Characterised using standard pattern.	
$SnSe_2$	Grey	$a = 3.76$ $c = 16.19$	$a = 3.76$ $c = 16.20$
PbSe	Black	$a = 6.12$	$a = 6.12$

[a] after annealing at 500°C for 24 h. (Minor phases (<10%) in parentheses).

The reaction of $SnCl_2$ with Na_2S resulted in the formation of crystalline SnS (herzenbergite) with an average crystallite size of *ca.* 21 nm. The reaction of SnI_4 with Na_2S resulted in the formation of poorly crystalline SnS_2. Raman microscopy (Figs. 2-17 & 2-18) of the tin samples confirmed the phases detected by XRD (Figs. 2-19 & 2-20). EDAX data shows a 1:1 tin to sulphur ratio for SnS and a 1:2 tin to sulphur ratio for SnS_2. Mild annealing at 300°C of the samples increased their crystallinity.

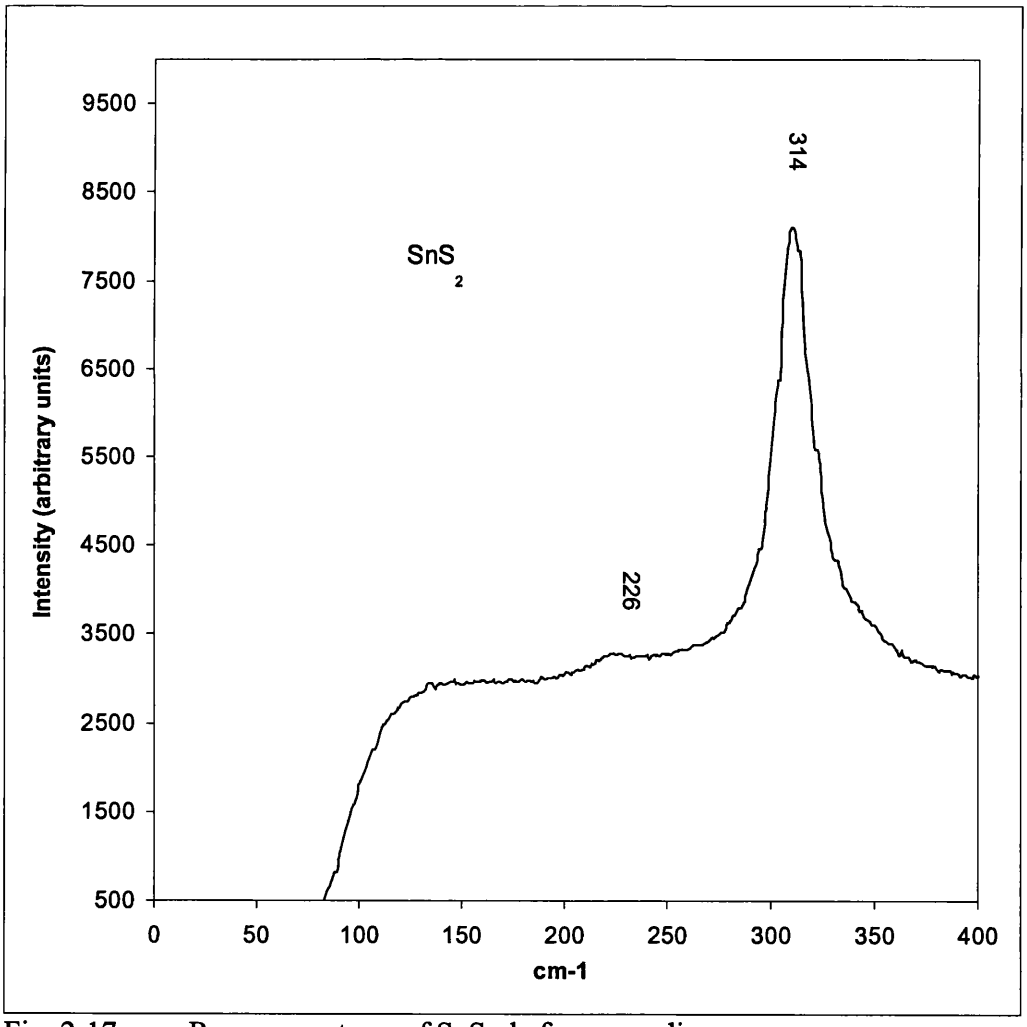

Fig. 2-17 Raman spectrum of SnS_2, before annealing.

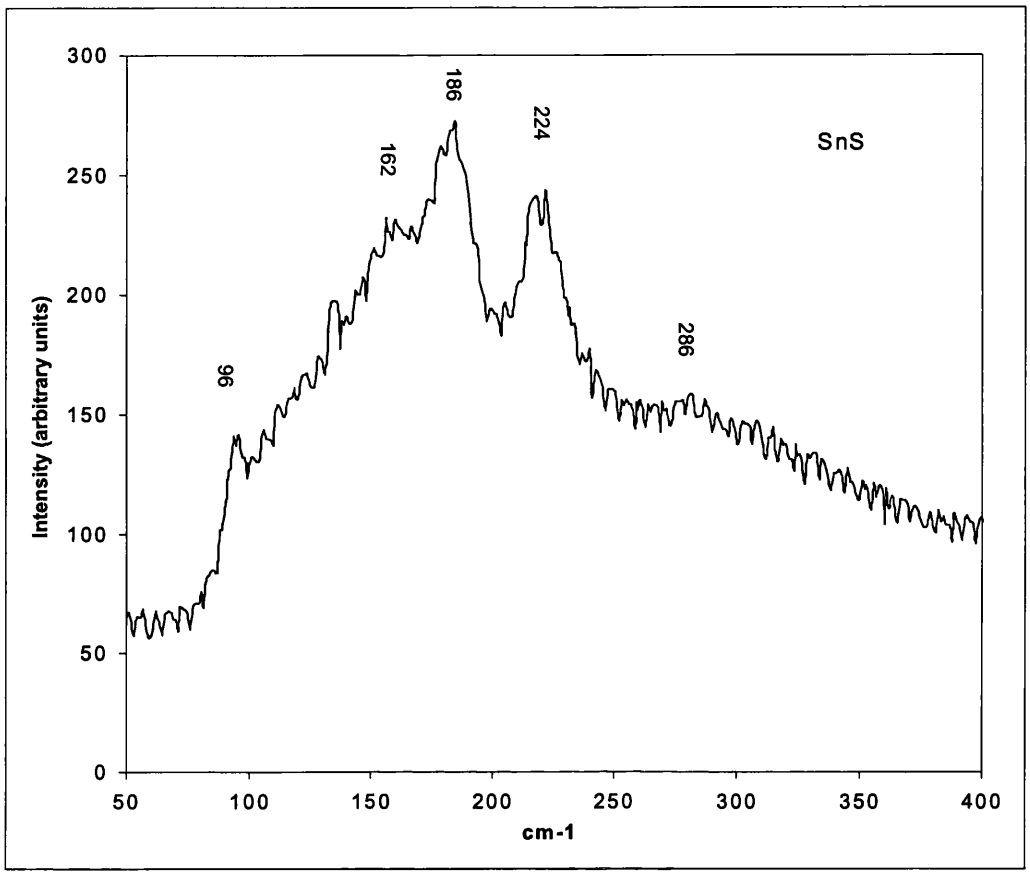

Fig. 2-18 Raman spectrum of SnS, before annealing.

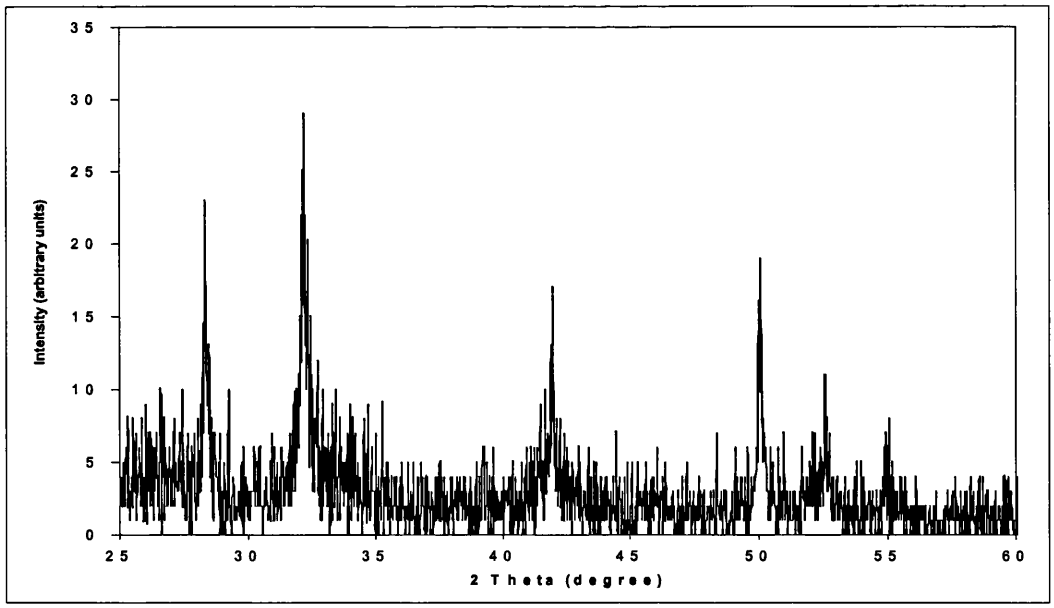

Fig. 2-19 XRD pattern for SnS_2 (berndtite) unannealed.

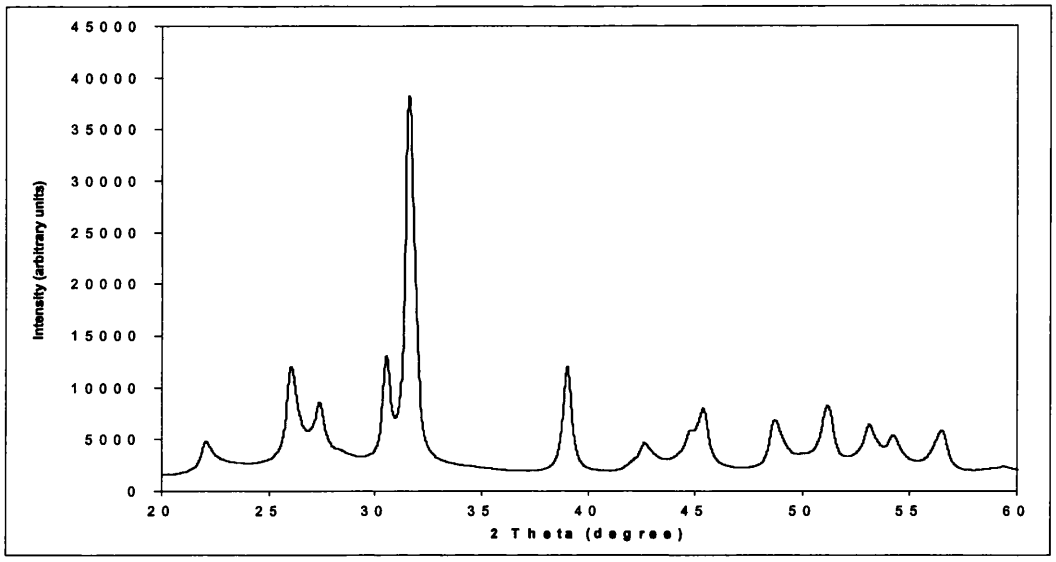

Fig. 2-20 XRD pattern for SnS (herzenbergite) unannealed.

The reaction of $PbCl_2$ with Na_2S resulted in the formation of a product which showed a PbS (galena) XRD pattern (Fig. 2-21). EDAX of the sample showed it to consist of an 1:1 elemental ratio of lead to sulphur. Raman microscopy confirmed these analyses.

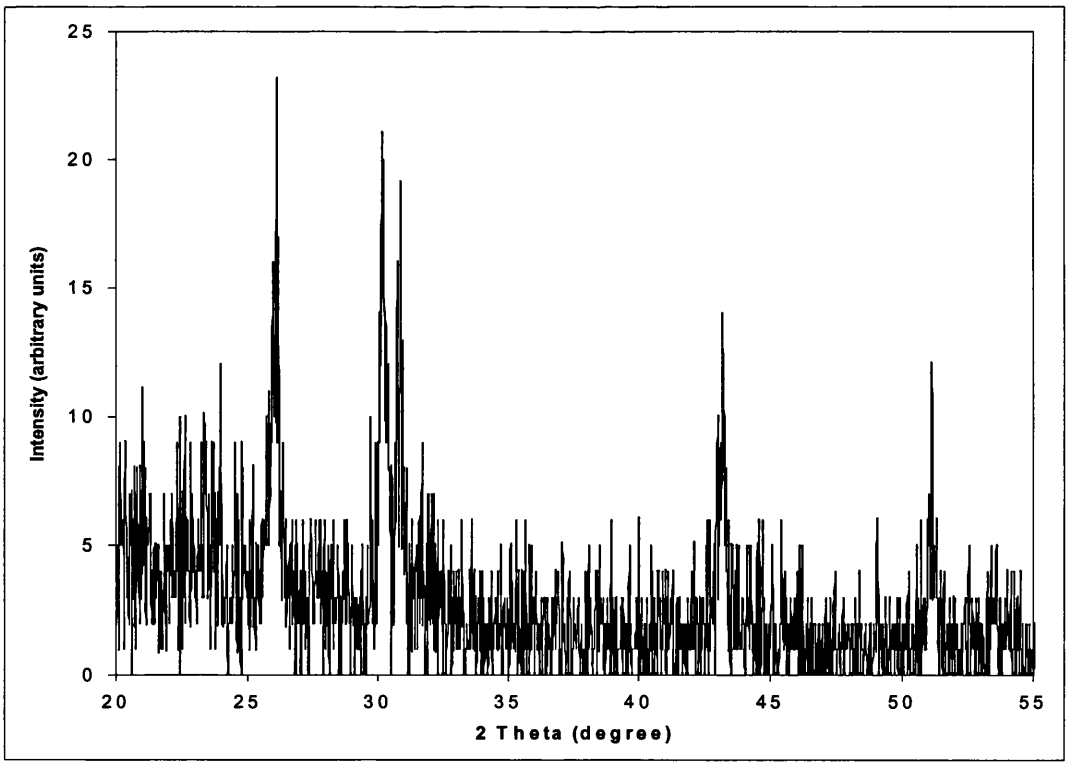

Fig. 2-21 XRD pattern for PbS (galena).

Figs. 2-22 to 2-24 show representative SEM photos of SnSe and $SnSe_2$.

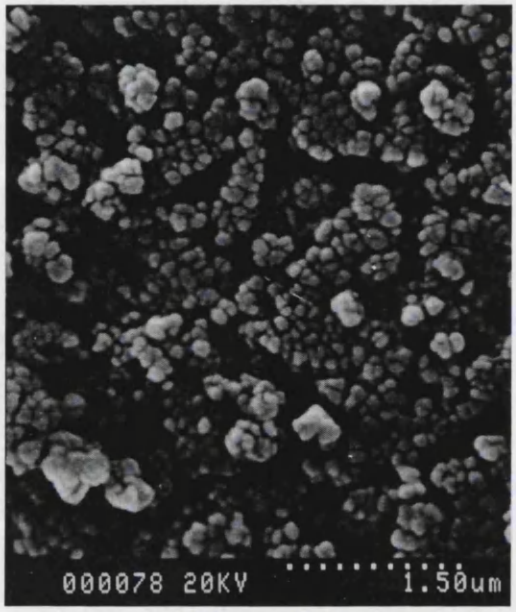

Fig. 2-22 SEM of SnSe, unannealed.

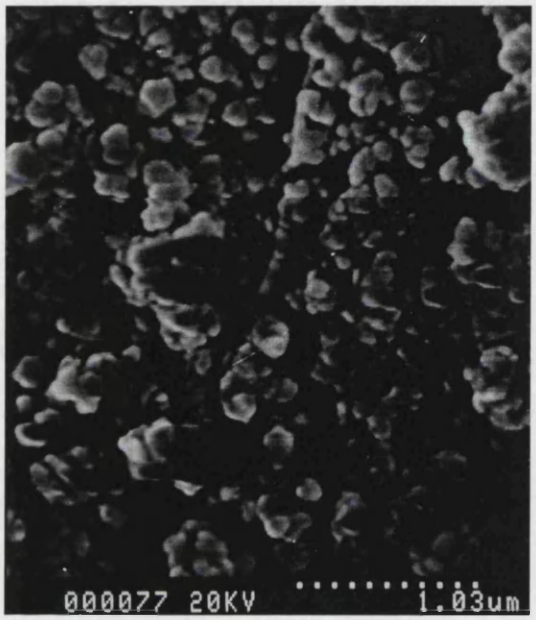

Fig. 2-23 SEM of SnSe, unannealed.

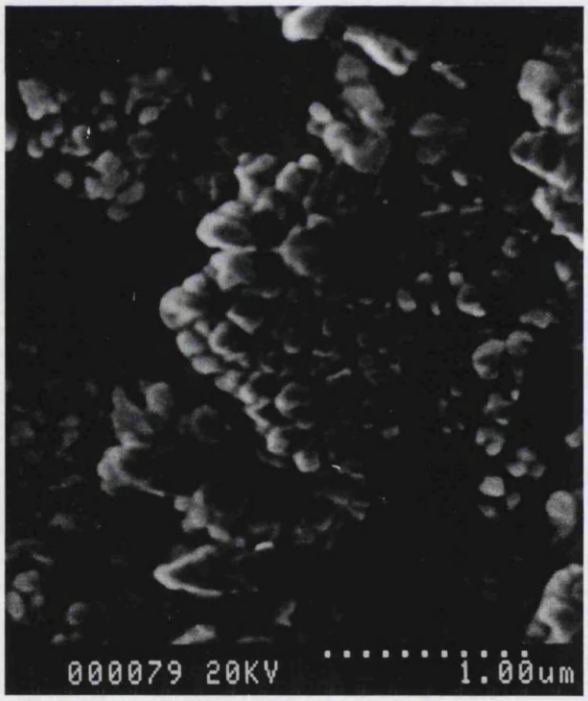

Fig. 2-24 SEM of $SnSe_2$, unannealed.

2.2.6 Group 15 - Antimony & Arsenic:

The synthesis of antimony and arsenic chalcogenides were performed *via* the liquid-mediated metathesis method used throughout. Equations 2-17 to 2-19 show the chemical equations:

$$2SbCl_3 + 3Na_2O_2 \rightarrow Sb_2O_3 + 6NaCl + {}^3/_2O_2 \qquad \text{Eq. 2-17}$$

$$2SbCl_3 + 3Na_2E \rightarrow Sb_2E_3 + 6NaCl \ (E = S, Se, Te) \qquad \text{Eq. 2-18}$$

$$2AsCl_3 + 3Na_2E \rightarrow As_2E_3 + 6NaCl \ (E = S, Se) \qquad \text{Eq. 2-19}$$

The powders obtained from the antimony reactions were found to be X-ray amorphous and could be made to crystallise by mild annealing at 500°C for 24 h (Fig. 2-25 shows the XRD for Sb_2Se_3). Yields were *ca.* 90 %. Details are summarised in Table 6. EDAX results show antimony to element ratios of 2 to 3 both before and after annealing. The powders obtained were shown to contain NaCl before washing and in the evaporated H_2O washings. The particles obtained show a different particle morphology from the indium chalcogenides discussed above. Sb_2O_3 and Sb_2Se_3 were both found to be composed of *ca.* 2 μm angular agglomerates. Sb_2S_3 was found to be composed of needle-shaped particles of approximately 1 by 10 μm dimensions. Sb_2Te_3 was composed of 1 μm spherical agglomerates and some smaller areas of 3 μm angular particles corresponding to elemental tellurium.

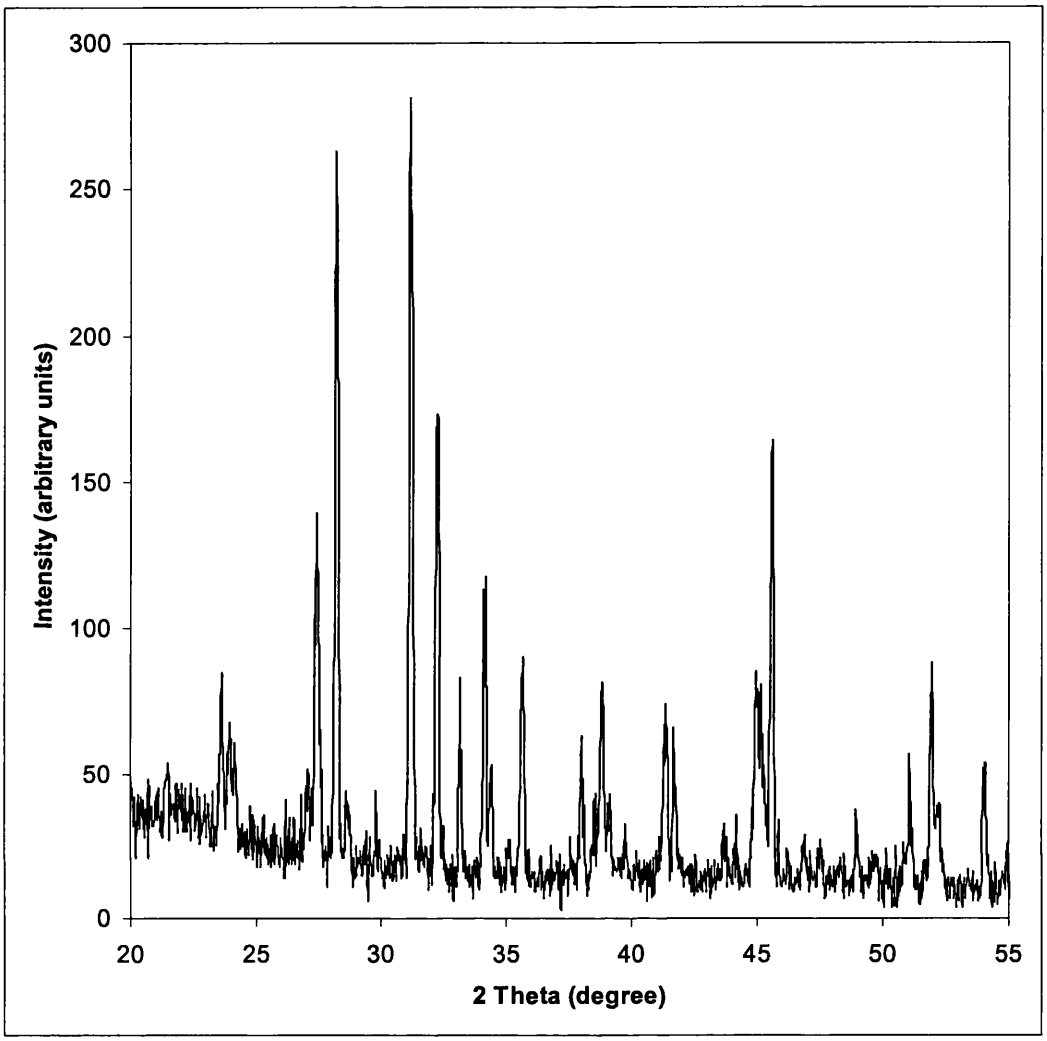

Fig. 2-25 XRD pattern for Sb_2Se_3, annealed.

The elemental tellurium found in both the indium (p. 59) and antimony cases is most likely due to the a small but unquantifiable amount of $NaTe_3$ contained in the Na_2Te precursor. The reagent was measured out as if it were pure Na_2Te and therefore there is an overall excess of tellurium in the reaction system. This is deposited as elemental tellurium during the reaction.

Table 6 Product and XRD data for Sb_2E_3 (E = O, S, Se, Te)

Product	Colour	Phase: by XRD[a]	Lattice type	Unit Cell Params. Lit. Values/Å[60]	Unit Cell Params. Observed/Å
Sb_2O_3	White	Sb_2O_3	Cubic	$a = 11.15$	$a = 11.14$
Sb_2S_3	Brown	Sb_2S_3	Orthorhombic	$a = 11.23$ $b = 11.31$ $c = 3.84$	$a = 11.24$ $b = 11.30$ $c = 3.83$
Sb_2Se_3	Dark Brown	Sb_2Se_3	Orthorhombic	$a = 11.63$ $b = 11.78$ $c = 3.98$	$a = 11.62$ $b = 11.77$ $c = 3.97$
Sb_2Te_3	Black	Sb_2Te_3 (Te)	Rhombohedral	$a = 4.26$ $b = 30.45$	$a = 4.26$ $b = 30.44$

[a] after annealing at 500°C for 24 h. * Unit cell dimensions *a, b, c* in Å (±0.01Å).
(Minor phases (<10%) in parentheses)

No success was had in multiple attempts at synthesising As_2S_3 and As_2Se_3. This was unexpected since in the literature, liquid-mediated metathesis reactions almost always involve at least one soluble reactant. $AsCl_3$ is a liquid at room temperature and dissolves in toluene. A powder was obtained for each reaction but in very low yield (< 10 %) and of inappropriate colour for the intended compound (As_2S_3 is yellow; a black powder was obtained). Even with prolonged annealing this powder did not crystallise. EDAX analysis revealed that there was no or very little arsenic present. Sulphur and selenium were found. Elemental selenium was detected by XRD from the reaction of $AsCl_3$ with Na_2Se.

2.3 *Discussion:*

2.3.1 *Nature of Reactants and Liquid:*

The liquid medium does not seem to solubilise a significant amount of the reactants. This has interesting implications for the reaction. In other reported liquid-mediated reactions it is almost invariably the case that reaction systems are selected by the criterion that at least one component (usually the metal halide), and often both, are soluble.[5,12,13] The reactions investigated here show that insoluble or low-solubility compounds can also be used for the formation of the desired products. The reaction in such cases can be seen as proceeding in two possible ways. The reaction could be a solid-state reaction occurring between the swirling particles in the slurry. As the particles are flowing through the liquid they collide with and abrade against each other. This micro-scale solid-state metathesis reaction is therefore mediated by the liquid medium in which this is occurring. The second option is that the precursors have some limited solubility in the liquid and the reaction occurs between the solubilised portions of the reactions. The reaction would then be limited by either the rate of dissolution (assuming "instant" reaction) or by the rate of reaction.

The attempted synthesis of As_2E_3 (E = S, Se) is interesting in the respect that even though the metal halide is soluble, the reaction did not appear to work. All other reactions in which there appears to be limited solubility of both precursors invariably succeeded. This contradicts the apparent ease which most researchers report in employing soluble precursors. There are a number of possibilities why the reaction does not work. The most likely reason is that during the heating stage of the reaction the flask is open to a nitrogen gas flow and since $AsCl_3$ is a liquid, it is possible that it simply boiled off. This would account for the low arsenic content found in the product. Another possible reason is that since $AsCl_3$ is soluble in toluene, the heat of solvation adds a small, but significant, "extra" barrier to the reaction. It is a barrier that is not present in an equivalent solid-state liquid-mediated reaction. Therefore, when the toluene

is cannulaed off the arsenic precursor is also removed.

2.3.2 Reaction Speed:

The reactions performed *via* the liquid-mediated metathesis route were considerably slower than the equivalent solid-state reactions, which was due to a number of factors. Solid-state metathesis reactions last only a matter of seconds while the fastest liquid-mediated reaction is completed in perhaps a few hours (for silver sulphide).[8] The overall temperature was lower and therefore, for kinetic reasons, it should be expected that the reaction rate would be slower. The reaction would also be slowed down compared with solid-state reactions because the "concentration" of the reactants is significantly lower. If the reaction is seen to be a solid-state reaction initiated by collision and abrasion then the total time that any particle spends in contact with another particle (i.e. the short time of actual collision) is much smaller than the contact of a solid mass of reactants found in solid-state reactions. If the reaction is seen as a solubility-limited process then the reaction would be slowed down significantly because the supply of reactants is limited by the amount of reactant that can fit into the volume of liquid thus leading to a low concentration of reactants. The rate of dissolution could also be a limiting factor.

2.3.3 Reaction Pathway and Completion:

When dealing with an area in which it is difficult to characterise the products there is always the possibility for doubt as to the true nature of the reaction and the products obtained. Given the fact that some samples are amorphous as synthesised, X-ray powder diffraction can not be used to fully identify the product. This leaves the product nature open to some doubt. It could be argued that the product is not a binary material as claimed, but it could be merely a very intimate mixture of elements. It could

also be said that the reagents do not react at the low temperatures used under the toluene reflux conditions. It would then be argued that the reaction is simply initiated at the annealing stage of the process and that it would then be a solid-state reaction.

There are a number of indicators that show that these reactions do proceed *via* a metathetical pathway and that the products obtained, even when X-ray amorphous, are the binary products sought. The first such indicator is that in all reactions, an alkali halide salt is found in the product. This provides evidence that the metathetical pathway proceeds at least halfway to the stage where the salt is formed. The argument that there is an intimate mixture of elements formed which then combine under the annealing conditions is also shown to be untrue. Evidence for this is provided from EDAX which shows an elemental analysis on a *ca.* 1 μm^3 volume scale. The intimate mixture of elements would have to be much finer than this volume if the EDAX analysis were to appear as a binary compound. Elements would most likely segregate and form large enough aggregates to be visible in backscattered electron mode (atomic weight sensitive) and would show up in EDAX analyses as areas of high element concentration. Another piece of evidence used in some cases is the colour of the synthesised product. For example CdSe was a deep orange colour and neither cadmium nor selenium by themselves have these colours so this indicates that the desired product has formed.

Raman microscopy has been used to examine various unannealed samples, the results of which show that these are in agreement with the formation of binary compounds even before annealing. The Raman spectra for both forms of tin sulphide, SnS and SnS_2 are quite distinct from each other and are easily recognisable. Figs. 2-17 and 2-18 show the Raman spectra for unannealed SnS and SnS_2 respectively.[37] These clearly show that the two tin sulphides are formed before annealing and that they are not the result of a heat-induced reaction. Mercury sulphide HgS has two distinct forms: black metacinnabar and red cinnabar, also known as vermillion. Before annealing the HgS sample consisted of only the metacinnabar form. After annealing approximately 5 % of cinnabar was detected both by optical microscope and by Raman microscopy (Fig.

2-10). No cinnabar was detected before annealing and the sample consisted solely of metacinnabar. Lead sulphide was likewise detected by Raman microscopy.

2.3.4 Crystallinity:

The majority of samples were apparently X-ray amorphous in the as-synthesised form. This is a point which can be very difficult to establish beyond doubt. There is a fine line between X-ray amorphous and nanocrystalline samples and using ordinary laboratory-based X-ray sources it can be difficult for the machinery to distinguish extremely small crystallites (< 3 nm) due to the low intensity of reflection and the broadness of the resulting peak. Therefore for all the samples that were found to be initially X-ray amorphous there remains the possibility that these were in fact nanocrystalline. Bearing in mind this *caveat*, it was observed that the samples produced could be annealed under quite mild conditions to produce crystalline samples from the as-produced powders. Fig. 2-26 shows the peak-narrowing associated with annealing for Ag_2S.

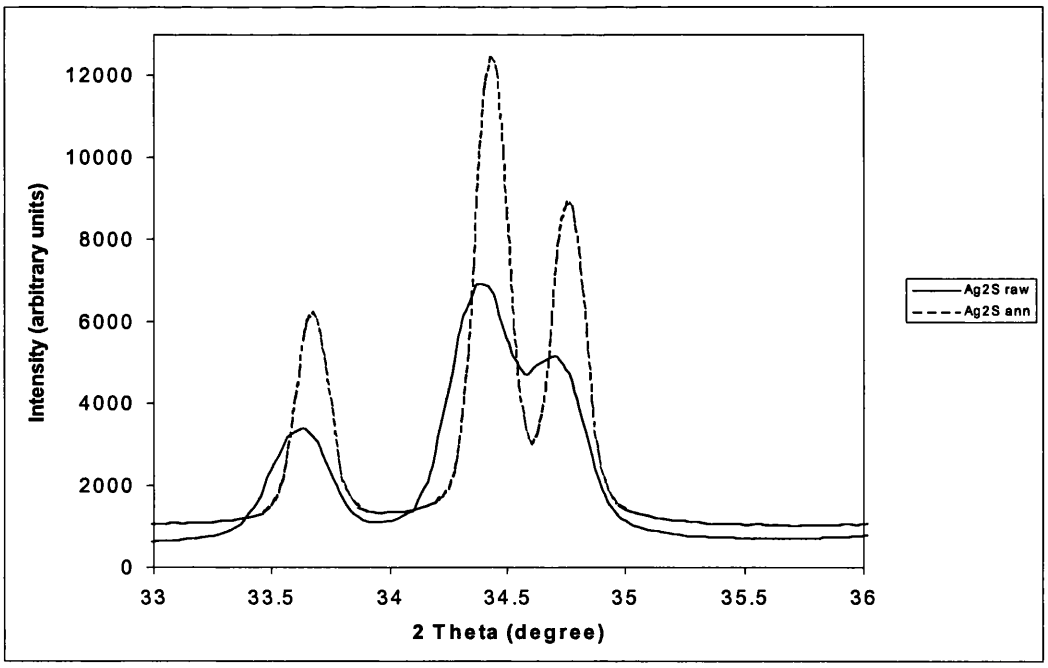

Fig. 2-26 XRD Spectrum of Ag_2S before and after annealing.

2.3.5 *Crystallite Sizes:*

It is possible to obtain an estimate of crystallite size by using the Scherrer equation. This relates the broadness of an XRD peak, its position and the X-ray wavelength to the average crystallite diameter. A modification of the Scherrer equation has been employed to obtain estimates of the crystallite sizes obtained in the reactions performed[61,62]. The modified equation is:

$$D = \frac{1.2\lambda}{B\cos\theta} \qquad \text{Eq. 2-21}$$

Where D = Average crystallite diameter,

λ = Wavelength of incident X-ray radiation (Cu $K\alpha_1$ = 1.5406Å),

θ = Angle of reflection (half of measured peak position (2θ)),

B = Full width at half maximum (FWHM) of measured peak.

Using this equation it is possible to obtain a more accurate notion of the crystallite size of the synthesised powders than is possible using SEM photography alone. Only Transmission Electron Microscopy (TEM) could provide the resolution required to get a direct measure of the crystallite sizes obtained. These measurements are of the as-synthesised samples, if crystalline, and of the annealed samples if not. In_2S_3 as synthesised has an average crystallite diameter of 19 nm. A similar solid-state metathesis reaction produces In_2S_3 with an average crystallite size of 36 nm.[63]

2.3.6 *Annealing & Crystallite Size Control:*

The smaller crystallite sizes obtained lend themselves greatly to further manipulation in terms of more precise crystallite size control. Controlled and selective annealing of the powders obtained has lead to a crystallite size increase proportional to the conditions used.

Annealing tests were performed on In_2S_3, performing a series of annealing experiments at various temperatures for similar amounts of time. The as-synthesised sample was considered as having been annealed at 110 °C since that was the temperature of reaction. Fig. 2-27 shows a graph of the trend observed. This shows that it is possible, by varying the temperature, to get a control of the crystallite size growth.

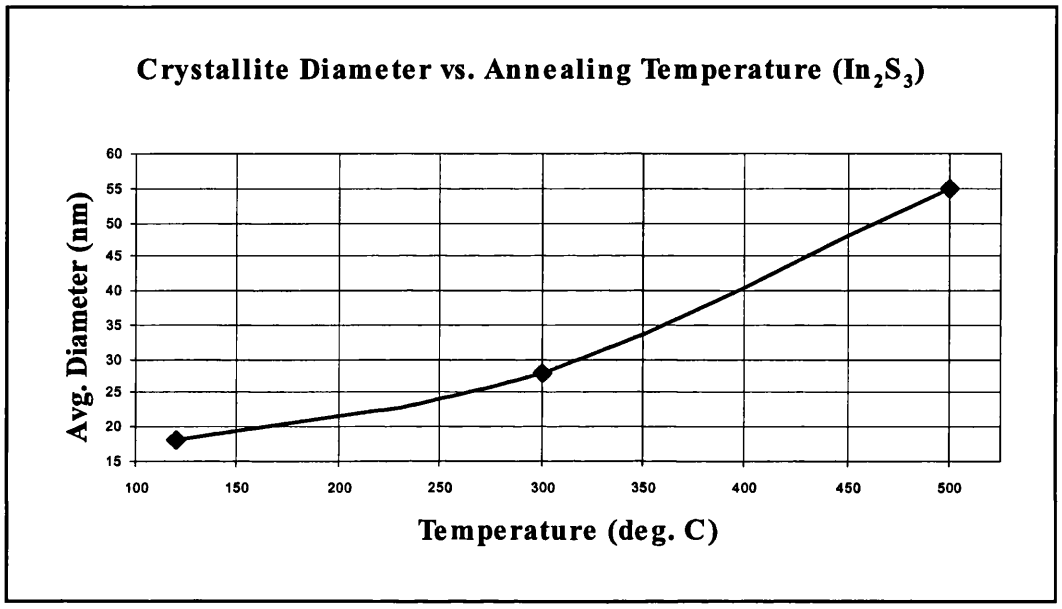

Fig. 2-27 Crystallite Size *vs.* Annealing Temperature (In_2S_3).

An even more striking example of this capability is shown in an annealing study on ZnS. Fig. 2-28 shows the XRD spectrum of ZnS as synthesised. One can see the very broad, almost amorphous, peaks corresponding to ZnS in its Sphalerite (zinc blende) form.

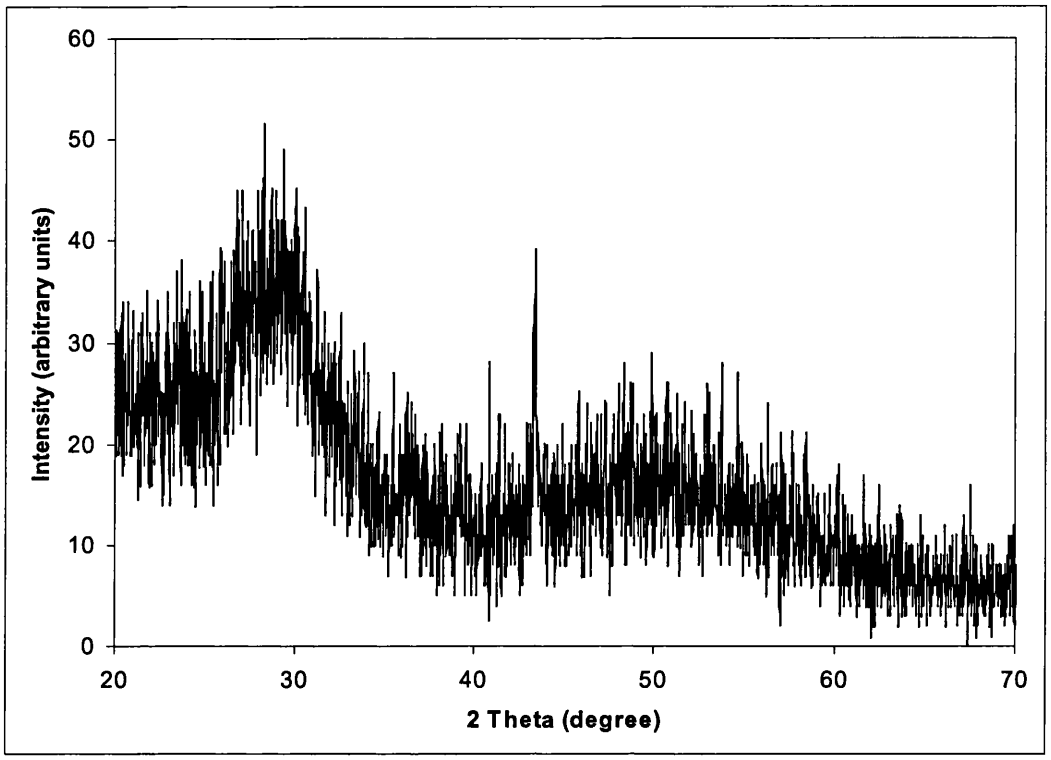

Fig. 2-28 XRD pattern of ZnS as-synthesised.

Fig. 2-29 shows the same sample annealed at 250°C for 60 h. Now one can see the peak at 28.6° sharpen up slightly but it is still relatively broad. The single broad peak in the region 45-55° is now resolved into two distinct broad peaks matching the ZnS (Sphalerite) standard.

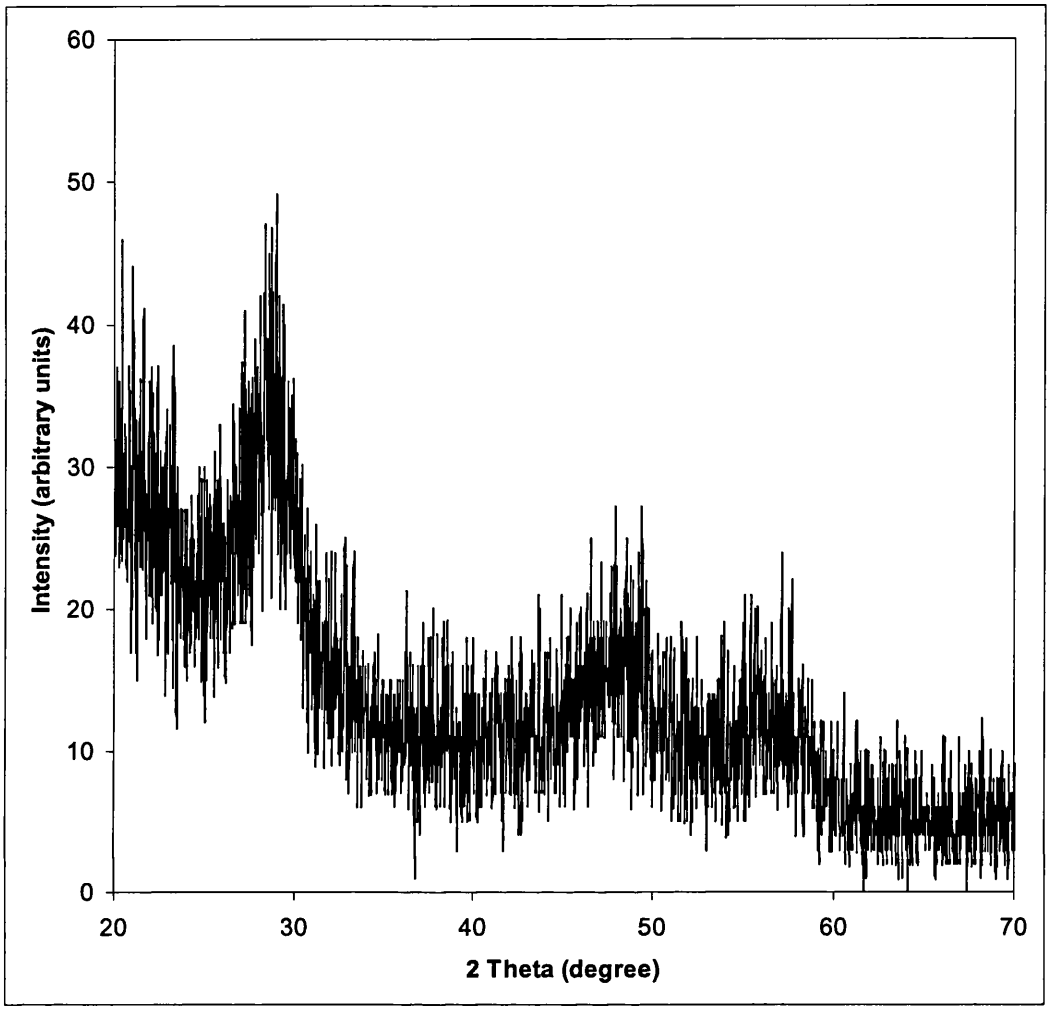

Fig. 2-29 XRD pattern of ZnS annealed at 250°C for 60 h.

Fig. 2-30 shows the same compound annealed at 500°C for 84 h. This spectrum now shows very sharp and distinct peaks corresponding to a highly crystalline sample.

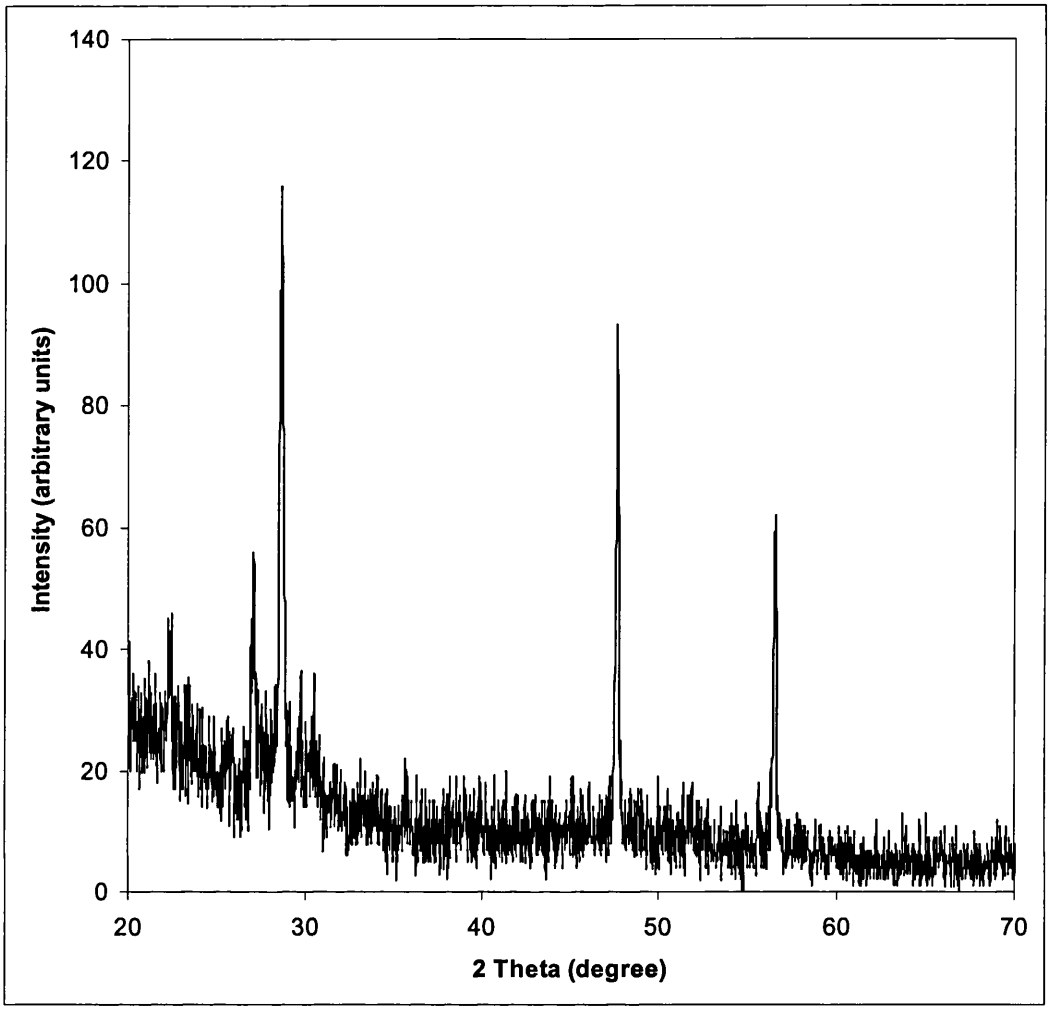

Fig. 2-30 XRD pattern of ZnS annealed at 500°C for 84 h.

Fig. 2-31 shows a graph depicting the crystallite size *vs.* annealing temperature. The change with increasing temperature is much more apparent in this case and shows that once annealing is being used, we are dealing with diffusion control again, and diffusion is exponentially dependent on temperature. In the case of ZnS crystallite sizes from 2.4 nm up to at least 45 nm and probably above are accessible.

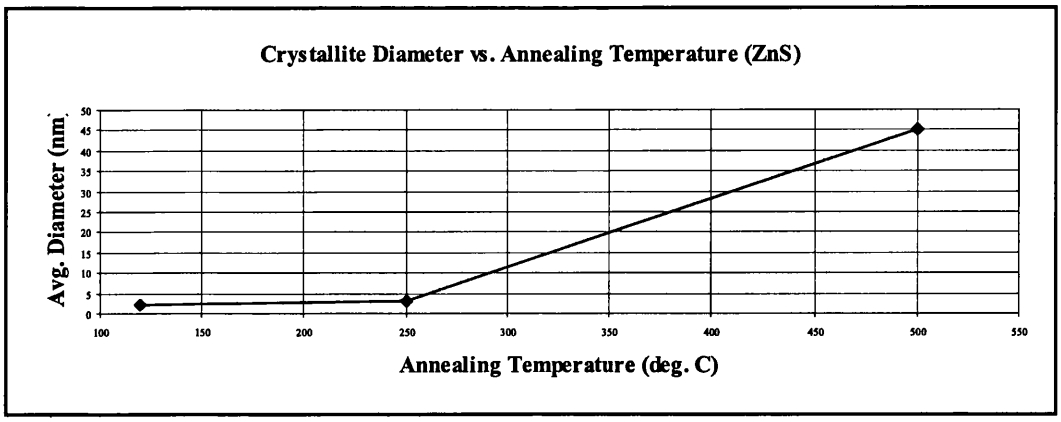

Fig. 2-31 Crystallite Diameter vs. Annealing Temperature (ZnS).

A study on In_2S_3 where annealing at a constant temperature of 500°C for various periods of time was carried out. What became apparent was that once a certain level of crystallisation had been achieved, increasing the time of annealing at that constant temperature did not significantly increase the crystallite diameter. Fig. 2-32 shows a graph of crystallite diameter *vs.* annealing time at 500°C. In order to achieve increased crystallite size it seems that an increase in annealing temperature would be required.

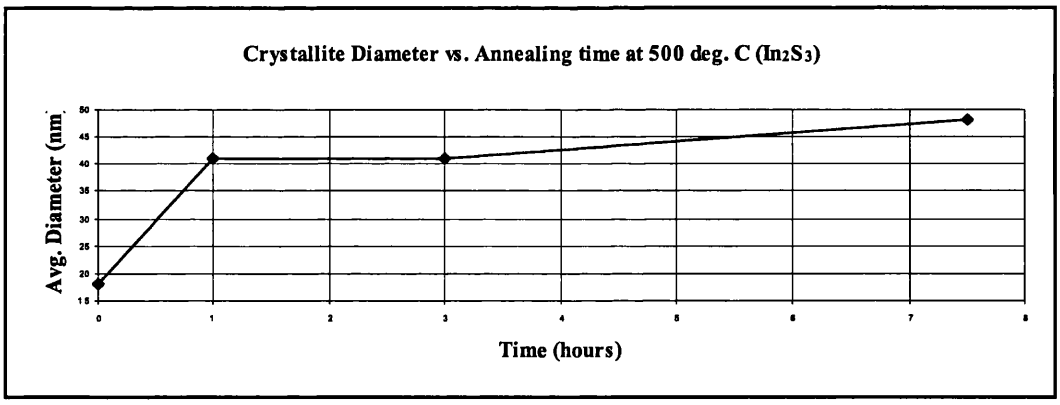

Fig. 2-32 Crystallite Size *vs.* Annealing time at 500°C (In_2S_3).

2.3.7 Redox Chemistry & Phase Control:

It was seen in the previous section that there is some scope for the selection of crystallite sizes by the judicious use of annealing temperatures and times. It is also apparent that these reactions afford a relatively direct route to compounds of a specific

oxidation state of an element.

The reactions involving $SnCl_2$ and SnI_4 showed that the product of the reaction reflected accurately the oxidation state of the precursor compound. Thus it was possible to select which tin sulphide phase was synthesised. The reactions involving copper halides also reflected this maintenance of oxidation state phenomenon. Thus, all of CuS, Cu_2S, CuSe and Cu_2Se were acccessible. It is a noteable feature of almost all of the reactions performed that there was a preservation of the oxidation state of the precursor compound. Only in the case of iron and vanadium was an oxidation state change observed.

A second feature of these reactions is that the products obtained are first of all of a reduced crystallite and agglomerate size but they are also often of a low temperature phase. The case of mercury sulphide shows that either of the two mineral forms, metacinnabar and cinnabar can be synthesised. The black metacinnabar phase is a metastable phase and is therefore rare. The red cinnabar can easily be synthesised either by heating or treatment with alkali polysulphides or mercurous chloride.[64] The liquid-mediated metathesis methodology allows the direct synthesis of the low temperature form of HgS and also allows its easy conversion to its other phase.

2.3.8 Mixed Ternary Chalcogenides:

The synthesis of two mixed cadmium sulphur-selenides was attempted. The synthesis of the binary CdS and CdSe compounds were reported previously in section 2.2.3. The interest in ternary solid-solution formation using compatible binary compounds is spurred on by the 'tuneability' of properties by continuous variation in the mixing elements. Compatible binary compounds are those that share a common crystal structure.

Knowing that the binary compounds form successfully, it was investigated whether there would be competition between the reaction of $CdCl_2$ with Na_2S and $CdCl_2$

with Na_2Se. The first reaction performed was a stoichiometric mix of $CdCl_2$, Na_2S and Na_2Se under the toluene reflux conditions employed throughout. The second reaction involved mixing $CdCl_2$, Na_2S and Na_2Se in a 1:1:1 ratio. Eqs. 2-22 and 2-23 show the two reactions respectively. The second was designed with an excess of Na_2E, (E = S, Se) consisting of 1 eq. each of Na_2S and Na_2Se to allow any preferential reactions to occur and go to completion.

$$2CdCl_2 + Na_2S + Na_2Se \rightarrow 2CdS_{0.5}Se_{0.5} + 4NaCl \qquad \text{Eq. 2-22}$$

$$CdCl_2 + 2Na_2E \rightarrow CdE + 2NaCl + Na_2E\ (E = S, Se) \qquad \text{Eq. 2-23}$$

The ratios of the substituting elements can be measured by two complementary methods. One is the standard EDAX analysis used throughout. The second is applicable only to substitutional solid-solution alloys and uses XRD peak positions as data. Vegard's Law states that the unit cell expansion between one binary compound and the other binary compound is linear between the two extremes. Therefore the *hkl* peak of the ternary compound can be used to quantify the solid-solution composition by the relative distance from each of the binary *hkl* peaks. Vegard's Law assumes that the substitution occurs with a random distribution. Deviations from the law can occur if there are net attractive forces between unlike atoms or there is clustering of ions into segregated domains.

Evidence from both EDAX (before and after annealing) and XRD (after annealing) analysis show similar results. The stoichiometrically matched reaction (Eq. 2-22) showed a 55:45 S:Se ratio by Vegard's Law. EDAX analysis also gives a S:Se ratio of 55:45. When an excess of the Na_2E, (E = S, Se) reagent was used (Eq. 2-23) Vegard's law gives a S:Se ratio of 47:53. EDAX analysis give an S:Se ratio of 48:52, which is within the margins of error (Fig. 2-33).

These results show that in liquid-mediated metathesis reactions, the reactivity difference between these two different atoms, one heavier, one lighter, is not very large.

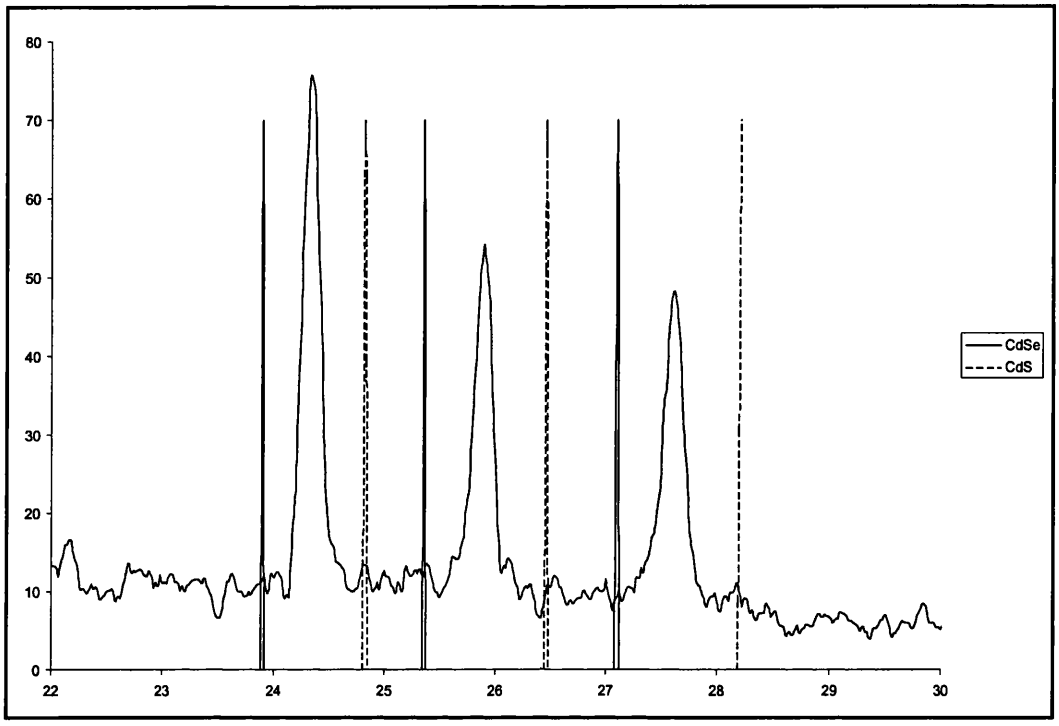

Fig. 2-33 XRD of $CdS_{0.5}$ $Se_{0.5}$ from 1:1:1 reaction.

This indicates that the reaction is not limited to any great extent by diffusion processes. A heavier and large atom would react significantly slower if diffusion was involved. It is more likely that the reaction is controlled by the random reaction of the powders as they swirl in the liquid. Filament-initiated solid-state metathesis reactions show a significant enrichment in the more mobile sulphur atom relative to selenium, which is not seen in these liquid-mediated metathesis reactions.[8]

2.3.9 Transition Metals:

The reactions involving the early transition metals resulted in the formation of sulphide powders which quickly decomposed on exposure to air or moisture to form their corresponding oxides. This can be correlated to the change from the chalcophilic

elements of the late transition metals to the oxophilic elements of the early transition metals. Under the inert conditions employed in the reactions, TiS_2 and VS can form, but as soon as they are exposed to air they react with oxygen and moisture and form their more energetically favourable oxide. The small crystallite sizes that have been observed for the products of liquid-mediated metathesis reactions may be a contributing factor. This would be due to the increased particle surface area exposed to the atmosphere. There would seem to be a transition between chalcophilicity and oxophilicity centred around iron in the first row transition metals, because iron sulphide was partially oxidised while cobalt and nickel sulphides could be exposed to the atmosphere indefinitely.

The two nickel selenide phases observed in the reaction of $NiBr_2$ with Na_2Se are consistent with previous observations. It is known that nickel selenides and tellurides (Ni_xE) can adopt the nickel arsenide structure for values of x between 0.5 and 1.0. This is achieved by progressively removing metal atoms until alternate planes are absent.[65] This gives an apparent $NiSe_2$ structure which is most likely balanced by the formation of polyselenide anions (Se_2^{2-}). At the low temperatures employed for the liquid-mediated reactions the $T\Delta S$ term is small and it is energetically favourable for at least a portion of the metal atoms to form bonds with each other rather than with selenium.

The sulphides of iron, cobalt and nickel were all found to crystallise into slightly metal deficient 1:1 compounds. It is well known that transition metal sulphides adopt non-stoichiometric phases, in fact, stoichiometric unity is rare.[64] The metal deficiency is due to random vacancies of metal atoms throughout the lattice. In the case of iron (II) sulphide this can be balanced by the presence of Fe^{3+} in the lattice. Alternatively, polysulphide anions can also exist to maintain balance. As long as the entropy gain is large enough to balance the enthalpy loss then the $M_{(1-x)}S$ structure can be maintained. It is intersting to note that for cobalt sulphide the stoichiometry was 1:1 before annealing and only after the annealing process did the slightly metal-deficient structure arise. This indicates that the lower temperatures used in the initial synthesis allow a stoichiometry close to 1:1 to be achieved.

2.3.10 Comparison with Liquid Ammonia Metathesis:

A number of the reactions discussed in this chapter have been investigated concurrently by G. A. Shaw, but rather than employing toluene as the medium, liquid ammonia has been used as the reaction medium. Ammonia is condensed into a high-pressure glass reaction vessel and the reagents are added. The vessel is stoppered and allowed to reach room temperature. The reaction then proceeds for a set period of time at room temperature. There are some interesting parallels and divergences that can be drawn between the two different liquids and the results obtained in both. Liquid ammonia is a highly coordinating solvent while toluene is not.

Reactions of silver, zinc, cadmium, mercury, indium and lead halides with sodium sulphide yielded results which were very similar to those that have been presented here. There were a few cases in which different results were obtained. These cases involved a competing reaction between the ammonia and the reactants themselves. For example, it was found that in the syntheses of nickel and zinc sulphide it was necessary to use the chloride and not the bromide. This was because upon dissolution of these bromides, the kinetically stable adducts $Ni(NH_3)_6Br_2$ and $Zn(NH_3)_2Br_2$ were formed, thus immobilising the halides as precursors.

Another restriction on liquid ammonia metathesis reaction was any reaction involving group 14 halides. Apart from $PbCl_2$, it was found that all other group 14 halides undergo ammonolysis, such as silicon tetrachloride which results in $Si(NH)(NH_2)_2$ and ammonium halide. It was found that reactions involving either SnI_4 or $SnCl_2$ resulted in highly crystalline ammonium halide as well as the expected co-produced sodium salt. There was significant contamination of the product with metal amide/imides. One advantage of liquid ammonia metathesis reactions is that they are performed at room temperature and require no external energy input to proceed.

A minor difficulty was encountered in reactions involving copper (II) halides. Liquid ammonia metathesis reactions mimicked toluene liquid-mediated metathesis reactions in that the oxidation state of the precursor was preserved as the major product,

but it was found that when using copper (II) precursors there would be some small contamination with copper (I) species. This was attributed to the increased stability of solvated copper (I) species in liquid ammonia relative to copper (II).

It can be seen from these examples that the role of the solvent can be very important in liquid-mediated metathesis reactions. For the major part of this project toluene has been used as the liquid and as such, it does not partake in the reaction to any noticeable extent. It merely acts as a heat sink to dissipate any released energy, it acts as a particle dispersant to prevent a "critical mass" of reactants from coming together and it may in some lesser way (compared with liquid ammonia) act as an agent for renewing reacting surfaces.

2.4 *Precursor Synthesis:*

Sodium chalcogenides and pnictides were used as the chalcogen and pnictogen source in the reactions performed and reported in this and subsequent chapters. Traditional chalcogen and pnictogen precursors are very often the hydride gases of the element in question, such as H_2S, H_2Se, H_2Te, PH_3, AsH_3 and SbH_3. These are reactive sources of chalcogen and pnictogen elements; (the heavier element gases (H_2Te and SbH_3) have the problem of being thermally unstable at temperatures much above 0°C). However, these compounds are often difficult to handle and require the need for high-pressure reaction vessels. These compounds are also highly toxic and have very unpleasant odours, and being gases can easily spread over large areas if released.

The sodium chalcogenide and pnictide equivalents of these gases are all powders. They are air and moisture sensitive but handling and storage in an inert-atmosphere glove-box alleviates any problems. Of the alkali metal-element precursors employed, only sodium sulphide is commercially available. To obtain all the precursors needed it was necessary to perform the syntheses ourselves. Sodium sulphide was also synthesised to ascertain precursor purity and to maintain uniformity. Sodium chalcogenide (Na_2E; E = S, Se, Te) and sodium pnictide (Na_3E'; E = P, As, Sb) precursors were prepared by two different methods: ampoule oven heating and toluene reflux heating, as described below.

2.4.1 *Ampoule Synthesis:*

Stoichiometric amounts of elemental sodium and element E or E′ were placed in a 25 cm length by 10 mm diameter glass ampoule, evacuated and sealed under vacuum. Total amounts of sodium and element were based on a total yield of *ca.* 1.0 g as specified in Table 7.

Table 7 Chalcogenide and Pnictide Precursor Masses

Target Compound	**Na (mmol)**	**E or E′ (mmol)**
Na_2S	0.580 g (25.66)	0.420 g (13.10)
Na_2Se	0.370 g (16.10)	0.650 g (8.23)
Na_2Te	0.265 g (11.52)	0.735 g (5.76)
Na_3P	0.690 g (30.01)	0.321 g (10.36) (red P)
Na_3As	0.480 g (20.87)	0.520 g (6.94)
Na_3Sb	0.480 g (20.87)	0.845 g (6.94)

The sealed ampoule was heated slowly to 500°C. The reaction of Na and S showed a bright yellow flash of light shortly after the reaction reached 100°C. The reaction of Na and red P showed a similar, but slightly less violent, flash of light. No flashes of light were observed in any of the other reactions, however, they showed a slow darkening of the reaction mass. All ampoule reactions were allowed to proceed for 48 hours after which the ampoule was opened in an inert atmosphere, the fused mass was ground into a fine powder, placed in another ampoule, sealed under vacuum and heated to 400°C for another 4 hours. All precursors were characterised by XRD to confirm their identity.

Caution! These precursors are safe if handled properly, however, exposure to air or moisture will liberate dangerous gases such as H_2E or $E'H_3$. It should also be noted here that these ampoule reactions have the potential to be highly dangerous. In some cases ampoules were found to explode violently. The danger of flying glass and/or the formation of the toxic gases mentioned above after exposure of the ampoule contents to the atmosphere was taken into account. Therefore the reactions were always carried out in an oven inside a fumehood. To reduce the risk of explosion, particularly for the reaction of sodium with sulphur, smaller overall reaction scales were used. The amounts listed in Table 7 are the maximum values for an ampoule reaction. Even reactions where explosion did not occur, cracks could sometimes be seen to develop in the ampoule which often lead to oxygen seepage into the reaction ampoule and product

decomposition.

2.4.2 Toluene Reflux Synthesis:

An alternate method which was found to be safer and more manageable was to perform the precursor reaction in refluxing toluene. Stoichiometric amounts of elemental sodium and element E or E′ were placed in a 120 ml Schlenk flask, to which was added 20 ml of toluene. The total amounts are similar to those shown in Table 7. The flask was heated with stirring in a sandbath to *ca.* 110°C under nitrogen. The reaction was allowed to proceed for 48 hours after which the resulting powder was allowed to settle. The toluene was colourless and clear both before and after the reaction. Reaction completion could be quickly checked by examining whether there were any lumps of unreacted sodium remaining.

During the reaction of sodium with sulphur the toluene took on a slightly yellow colour when the sulphur dissolved upon heating. At *ca.* 100°C a sudden change occured in the reaction flask with the reaction mixture becoming suddenly cloudy with the formed Na_2S product. The reported colour of Na_2S is yellow, but for all cases of this reaction scheme a greenish-yellow coloured solid was obtained. When the products were characterised by XRD they were invariably identified as Na_2S.

During the reaction of sodium with selenium, the selenium did not appear to dissolve. A slow colour change from the deep purple of the selenium powder to a colour that ranged from a pale mauve to a bright purple was observed. This reaction presented somewhat of a problem in that the product outcome was not consistent. In some cases the product XRD showed it to be Na_2Se, but in others an XRD diagram that did not match that for Na_2Se was seen. This could also not be matched to any known compound of sodium and selenium and was thus assumed to not be suitable for further use. No correlation could be made between the different colours obtained and the different XRD diagrams obtained. Since the products were easily synthesised, no further studies to

elucidate the difficulty were performed.

The reaction of sodium with tellurium showed no apparent colour change since both product and precursor are grey. The product was characterised by XRD and was found to be mainly Na_2Te but with some contamination of $NaTe_3$. It was found that this impurity was always present.

All pnictide precursors were formed successfully under the conditions described above. It was also possible to form ternary mixed-pnictide precursors by the same method. These were formed in the following stoichiometries: $Na_3As_{0.5}Sb_{0.5}$, $Na_3As_{0.75}Sb_{0.25}$ and $Na_3As_{0.25}Sb_{0.75}$. These powders were characterised by XRD and using Vegard's law the stoichiometries were approximated. The $Na_3As_{0.5}Sb_{0.5}$ and $Na_3As_{0.75}Sb_{0.25}$ compounds showed good XRDs, while the nominal $Na_3As_{0.25}Sb_{0.75}$ compound was found to be slightly As deficient with *ca.* 18 % arsenic.

All powders could be used as synthesised or annealed before using. All compounds were found to be crystalline as synthesised but some annealing before use could be beneficial in certain circumstances. As noted in the introduction, other researchers observed that the as-synthesised Na_xE powders were found to be more reactive than those which had some annealing. With this toluene reflux method both highly reactive un-annealed and less reactive annealed precursors are easily accessible.

Both the ampoule and toluene syntheses of these precursors work well, but it was found that the toluene method was far more convenient in terms of time taken, safety, and product control. There was no risk of explosion because the liquid medium keeps any excess heating to a reasonable level. It was also found to be very easy to increase the reaction-scale of the precursor synthesis. Up to a 4 g scale was attempted by using a proportionally larger reaction flask and liquid amount.

Kher and Wells report that in their synthesis of Na_3P and Na_3As they found it necessary to employ 36% excess white phosphorus and arsenic powder with respect to sodium.[13] This excess element is then carried on to the reaction itself and they found that they were required to remove excess element from the final product. In the precursor

syntheses carried out for this project, balanced sodium to element ratios were employed. This was found to have no deleterious effects on the products which were found to be stoichiometrically exact and thus no excess element was required to be removed from synthesised products.

2.5 *Experimental:*

2.5.1 *Reaction Methodology:*

The experimental procedure for the reaction of $InCl_3$ with Na_2O_2 is given below. All other reactions, including those involving Na_2S, Na_2Se and Na_2Te, followed a similar procedure with similar amounts and ratios of reactants. Reactions were for the most part based on 0.100 g amounts of the sodium chalcogenide and the metal halide amount was calculated accordingly. The order of addition of the reactants and the reaction conditions were also similar for all the reactions presented.

$InCl_3$ (1.72 mmol) and Na_2O_2 (2.56 mmol) were ground separately with a mortar and pestle inside an inert atmosphere glovebox. The Na_2O_2 was placed in a Schlenk flask to which was added 20 ml of dried degassed toluene using Schlenk line techniques to avoid exposure to either air or moisture. The $InCl_3$ was added with stirring, and the reaction mixture was heated to *ca.* 110°C under nitrogen flow. Once the temperature had stabilised the flask was sealed and allowed to reflux and stir for 48 hours. The resulting slurry was allowed to settle and the toluene was taken off by cannula. The solid was washed with 2 x 20 ml ethanol or methanol, followed by 2 x 20 ml deionized water, and finally by 2 x 20 ml ethanol or methanol. The powder was then pumped to dryness under vacuum. The powder was then collected and stored in air. The resulting ethanol, methanol and water washings were evaporated to identify any sodium halide species.

In the case of the ternary compound, $CdS_{0.5}Se_{0.5}$, Na_2S and Na_2Se were ground together to form an intimate mixture and placed in the Schlenk flask together. Toluene was then added to these and then cadmium chloride. The reason for the addition of toluene to the flask between the two precursors is that in some cases it was found that the two precursor powders would react spontaneously in a solid-state metathesis reaction. To avoid this the toluene was added to prevent direct contact between the precursor powders.

The following experimental conditions and details are valid for this chapter and subsequent chapters. Any deviations will be noted at the appropriate points.

2.5.2 X-ray Powder Diffraction:

Powder X-ray diffraction (XRD) measurements were performed on a Siemens D5000 diffractometer, using Ge monochromated Cu $K\alpha_1$ radiation (1.5406 Å). All spectra were manipulated using the Siemens DIFFRAC-AT v.3.2 software package. All XRDs were recorded at room temperature. Powder samples were prepared as thinly spread layers between two pieces of adhesive tape.

2.5.3 Infra-red Spectroscopy:

All infra-red (IR) measurements were recorded on a Shimadzu FTIR-8700 or a Nicolet 250 Fourier-transform spectrophotometer. Spectra recorded on the Shimadzu FTIR-8700 were manipulated using the Shimadzu Hyper-IR v.1.51 software package. Spectra recorded on the Nicolet 250 were manipulated using the in-built software package. Samples were recorded as KBr discs using Aldrich FT-IR grade KBr as received.

2.5.4 Raman Microscopy:

Raman microscopy was performed on a Dilor XY microscope spectrometer. Excitation was by a 50 mW argon laser (514.53 nm line) using a 300 μm slit width. Samples were prepared as thin layers on or between glass microscope slides. The spectra were calibrated by the Ne plasma line.

2.5.5 *Ultraviolet / Visible Spectroscopy:*

All ultraviolet / visible (UV-VIS) measurements were recorded on a Shimadzu UV-2401PL UV-VIS recording spectrophotometer. All spectra were manipulated using the Shimadzu Hyper-UV v.1.50 software package. Samples were recorded as KBr discs using Aldrich UV grade KBr as received.

2.5.6 *Annealing / Heating:*

All sample annealing and heating operations were performed using Carbolite or Lenton Thermal Designs tube or chamber furnaces. All powder samples for annealing were prepared as sealed evacuated glass or quartz ampoules.

2.5.7 *Scanning Electron Microscopy:*

Scanning electron microscopy (SEM) measurements were recorded on a Hitachi S-580 or a Jeol J-670 scanning electron microscope, both using a tungsten filament. Electron micrographs were recorded on the Hitachi S-580 using Agfa 400-ASA 110 mm black and white film. Photograph developing was performed by the UCL Institute of Archaeology Photographic Division.

2.5.8 *Energy-Dispersive Analysis by X-rays:*

Energy-dispersive analysis by X-rays (EDAX, also called EDS, EDXA) was performed by a Lynx Analytical EDAX attachment to the Hitachi S-580 SEM described above or by a Lynx Analytical Be-window high-resolution EDAX attachment on the Jeol J-670 SEM described above. Calibration was performed with a Cobalt pellet (99.999 %). All data collection, manipulation and ZAF correction was performed using the incorporated ZAF4-FLS software package. EDAX analysis is accurate to approximately

2-3 atom %.

EDAX was performed on various regions across the sample surface, using both area scans and point scans to determine regional homogeneity.

2.5.9 Glassware:

Schlenk Flasks: 25-35 mm diameter, 200 mm length, B24 Quickfit joint, 1/2 mm or 3/4 mm Interkey taps.

Cleaning: Basebath, soap and water and acetone.

Drying: Memmert and Gallenkamp glassware ovens at 150°C.

2.5.10 Solvents:

All solvents were distilled, dried and degassed under nitrogen gas. Drying conditions varied depending on the solvent, as shown in Table 8.

Table 8 Solvents and Drying Conditions

Solvent	**Drying Agent**
Toluene, Aldrich, Low-sulphur 99.5%	Na
Pyridine, Aldrich, Anhydrous 99.8%	As received, stored over sieves.
Petroleum Spirits, Aldrich, 40-60°C	Na
Dichloromethane, Aldrich, 99.9+% HPLC grade	CaH
Benzene, Aldrich, 99%	As received, stored over Na
Diethyl Ether, Aldrich, Anhydrous 99+%	CaH
Tetrahydrofuran, Aldrich, 99+%	Na
Triethylamine, Aldrich, 99+%	As received, stored over sieves.

2.5.11 Experimental Manipulations:

All air-sensitive materials were manipulated and stored under nitrogen in a Saffron Scientific or an MBraun UniLab glovebox. All experimental manipulations were carried out in the previously mentioned gloveboxes or using standard Schlenk line techniques using equipment similar to that described in the literature.[66] Nitrogen gas used in the Schlenk line was purchased from BOC gases and dried through molecular sieves.

2.5.12 Reagents:

All metal halide reagents were purchased from Aldrich Chemical Co. or Merck Chemicals and were of 98 % purity or better. Metal halides were stored under nitrogen and were used as received.

3. *Transition Metal Pnictides:*

3.1 Introduction:

Solid-state chemistry is for the most part concerned with the synthesis and properties of inorganic solids of the form M_xX_z, $M_zM_y'X_z$ etc., containing metallic elements and non-metallic elements. Among these solids, oxides have attracted the majority of interest due to their ease of synthesis and ubiquity[67,68]. In the previous chapter we dealt with the synthesis by liquid-mediated metathesis of a variety of chalcogenides (mainly sulphides and selenides). The tardiness of research into non-oxide solids was due mostly to the relative difficulty of synthesis of these. The liquid-mediated metathesis route showed itself to be a valuable tool in the synthesis of metal chalcogenides.

Another important family of compounds is the pnictides (phosphides, arsenides and antimonides (or stibides)). These have not attracted as much attention as oxides, in particular, and chalcogenides in general. Examples of almost every type of electronic property can be found among the pnictides: MnP and FeP are metallic ferromagnets. The low-spin d^6 $NiAs_2$ and $NiSb_2$ marcasites are semiconducting while the d^5 arsenopyrites (distorted marcasites) would have been metallic but for a structural distortion arising from the highest occupied band of d_{xy} parentage which would be half-filled in the undistorted structure. The d^6 low-spin pyrites, PtX_2 (X = P, As, Sb), are diamagnetic semiconductors while the isostructural d^7 $AuSb_2$ is metallic and even superconducting.[69]

A special feature of pnictide (P, As, Sb) structures is that beside the normal X^{3-} anions, polyanionic compounds containing X-X bonds and polycationic compounds containing M-M bonds are common.[69] Nitrides are, however, different from the other pnictides in that they do not generally form polyanionic compounds, although azides are an exception.[70] The skutterudite ($CoAs_3$) structure, which is unique to the pnictide family containing cyclic X_4^{4-} anions, is related to the ReO_3 structure.[71] Therefore it is not

surprising to find rare earth containing derivatives of the structure RM_4X_{12} (R = rare earth)[72], members of which exhibit superconducting ($LaFe_4P_{12}$)[73], ferromagnetic (UFe_4P_{12})[74] and thermoelectric properties ($LaFe_{4-x}Co_xSb_{12}$).[75] The latter are potential candidate materials for thermoelectric power generation and refrigeration.

Extensive research has been carried out into the properties of nickel phosphide (NiP). It has been evaluated as a catalyst for oxidative dehydrogenation of ethylbenzene.[76] Efforts have been made to understand its crystallisation behaviour[77] and its magnetic behaviour[78], for example, amorphous NiP shows anomalous magnetisation temperature characteristics.[79] It is employed as an interlayer between particles and matrix in aluminium-matrix composites and is being evaluated as an underlayer for magnetic recording media and computer hard drives.[80]

Most metals form pnictides and a wide range of stoichiometries are known, for example metal arsenides have a compositional range from M_9As to M_3As_7.[52] These materials are commonly synthesised by the direct reaction between the constituent elements in evacuated and sealed containers at elevated temperatures.[81] There are various problems associated with this traditional method, among them are volatility of non-metallic constituents, slow diffusion, long reaction duration, incomplete reaction and formation of mixtures of phases.

Recent advances in synthetic methods have produced various novel routes to metal pnictides. Self-propagating high-temperature synthesis (SHS) methods have been employed to form binary compounds[82] and the related solid-state metathesis route has also been successfully used to synthesise metal phosphides, arsenides and some antimonides.[8,83] Another recently-explored route involves the reduction of metal oxoanion compounds to the corresponding metal pnictide. For example, the hydrogen reduction of $Fe_2P_2O_7$ results in the formation of FeP[84] and the reduction of $CoAs_2O_6$ yields CoAs.[85] The electrolytic reduction of fused salts containing alkali-metal phosphates/arsenates and transition-metal oxides and/or chlorides is also known to yield transition-metal phosphides and arsenides.[86]

Other methods employed to synthesise metal pnictides, especially as thin films, have also been employed. Nickel and cobalt phosphides have been synthesised as thin films by plasma arc spraying[87], ion implantation[88,89] and galvanic- and electro-deposition.[90,91] Electroplating has been used to synthesise NiP, NiAs and NiSb thin films[92] while CoP and CoAs thin films have been synthesised by various single- and dual-source chemical vapour deposition methods.[93,94]

This chapter deals with the synthesis of various binary and ternary metal pnictide compounds. With nitrides being quite different in character from the heavier pnictides, no synthetic attempts were made towards the formation of nitrides, and all work was aimed at the heavier pnictides, that is, phosphides, arsenides and antimonides.

3.2 *Results - Synthesis and Characterisation:*

3.2.1 *Group 4 - Titanium:*

The reaction of titanium (III) chloride with binary and ternary sodium pnictides was performed using the liquid-mediated metathetical route according to the reactions shown in Eqs. 3-1 and 3-2:

$$3TiCl_3 + 3Na_3P \rightarrow Ti_3P + 9NaCl + 2P \quad \text{Eq. 3-1}$$

$$TiCl_3 + Na_3As_{0.5}Sb_{0.5} \rightarrow TiAs_{0.5}Sb_{0.5} + 3NaCl \quad \text{Eq. 3-2}$$

The reaction of titanium chloride with sodium pnictides in refluxing toluene for 48 h resulted in the formation of amorphous black powders. The phosphorus sample was washed with absolute ethanol, followed by distilled water. Annealing of the phosphorus-containing sample at 500 °C for 48 h did not achieve crystallinity in the sample.

XRD data for the synthesised powders, before washing, showed them to contain crystalline NaCl. EDAX data for the sodium phosphide reaction showed the product to contain an atomic ratio of titanium to phosphorus of 3 to 1. After washing, EDAX data for the phosphorus-containing sample showed that it contained no chlorine or sodium, within detection limits (0.5 atom %). After annealing, examination of the ampoule showed a surface layer of elemental phosphorus on the inner surface of the ampoule, accounting for some of the excess phosphorus present in the reaction according to Eq. 3-1. SEM showed the sample to consist of sub-micron diameter spherical agglomerates with a narrow distribution range.

The mixed ternary arsenide/antimonide reaction also resulted in a black powder. Upon exposure to the atmosphere, the resulting powder instantly and violently reacted with the atmosphere, showing a bright flash of light and a visible plume of smoke. XRD analysis of the powder after this reaction showed it to contain solely crystalline TiO_2 (rutile) and NaCl (Fig. 3-1). EDAX data confirmed the absence of arsenic and antimony

in the sample after reaction with the atmosphere. No attempts were made to analyse the sample under inert conditions. SEM showed the sample to consist of 1-2 um diameter spherical agglomerates with a narrow distribution range.

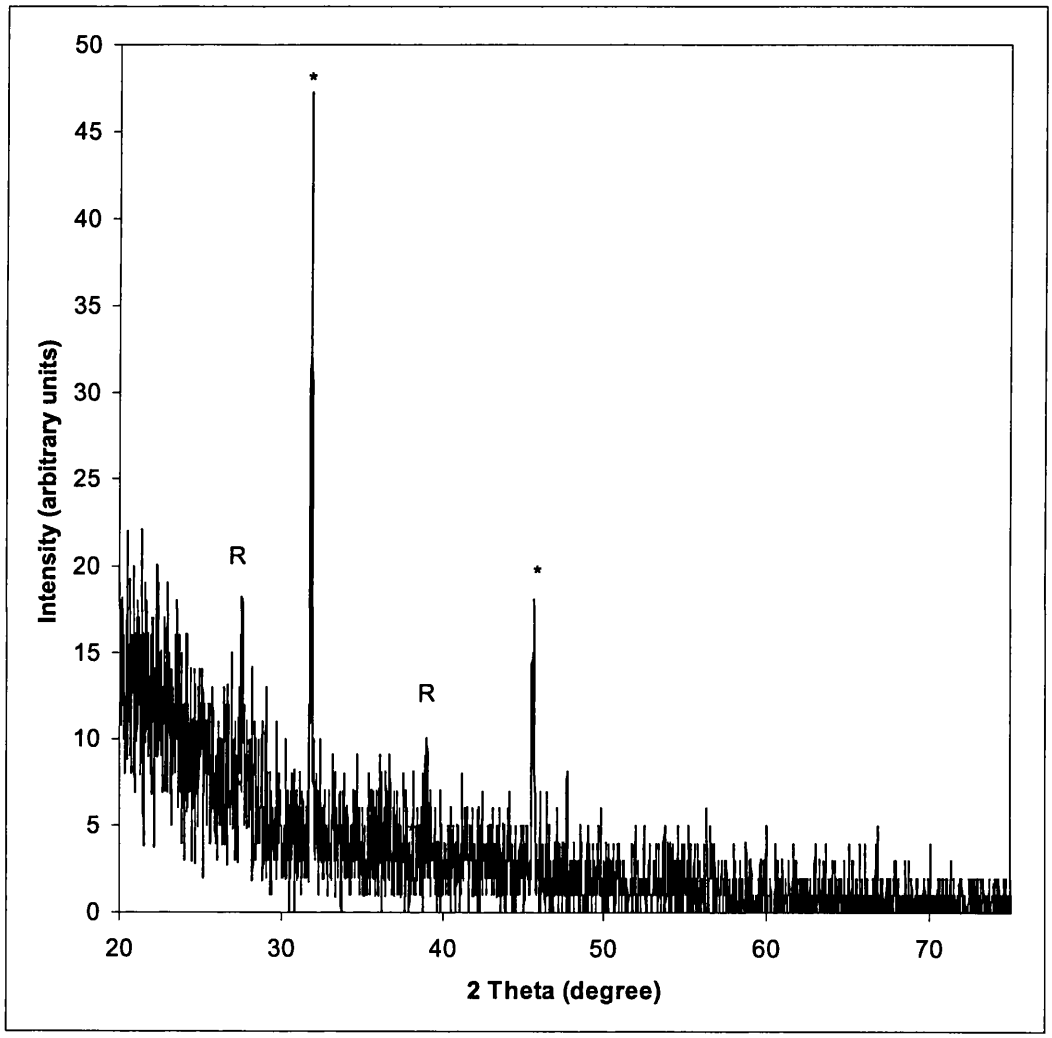

Fig. 3-1 XRD pattern for exposed product from $TiCl_3 + Na_3As_{0.5}Sb_{0.5}$. R = TiO_2 (rutile) and * = NaCl.

3.2.2 Group 5 - Vanadium:

The reaction of vanadium (III) bromide with binary and ternary sodium pnictides was performed using the liquid-mediated metathetical route according to the reactions shown in Eqs. 3-3 and 3-4:

$$4VBr_3 + 4Na_3P \rightarrow VP + V_3P + 12NaBr + 2P \quad \text{Eq. 3-3}$$

$$VBr_3 + Na_3As_{0.5}Sb_{0.5} \rightarrow VAs_{0.5}Sb_{0.5} + 3NaBr \quad \text{Eq. 3-4}$$

The reaction of vanadium (III) bromide with sodium pnictides in refluxing toluene for 48 h resulted in the formation of amorphous black powders. The samples were washed with absolute ethanol, followed by distilled water. The samples were annealed at 500 °C for 48 h.

XRD data for the phosphorus-containing sample showed it to contain VP and NaBr. EDAX data showed that the sample contained an overall vanadium to phosphorus ratio of *ca.* 2:1, with a number of spots consistently showing 3:1 and 1:1. This indicates that there is two phases present in approximately equal amounts, with perhaps a slight excess of V_3P. The annealing conditions employed must have been insufficient to crystallise the V_3P component of the mixture. SEM showed the sample to consist of two distinct particle morphologies, consistent with the formation of two separate phases. One phase was angular with flat surfaces and the other was more irregular, showing small rounded surface irregularities.

XRD data for the ternary arsenide/antimonide sample showed it to be amorphous. EDAX data showed there to be fluctuations in the ratios between the elements. There seemed to be some consistency in the ratio between arsenic and antimony. This ratio was centered around 1.5:1 As:Sb, with some fluctuations (from 1.2:1 to 1.8:1). The average vanadium content in proportion to the pnictide content was 40% (with arsenic providing approximately 36% and antimony, 24%). There were a number of spots which showed an excess of vanadium, but there were no spots which were 100% vanadium. This

indicates that the level of intermingling must be relatively close. It is possible that there is a ternary compound of *ca.* 3:3:2 V:As:Sb composition, with some elemental vanadium interspersed. SEM showed the sample to consist of 3-4 um diameter spherical agglomerates.

3.2.3 Group 8 - Iron:

The reaction of iron (III) chloride with sodium arsenide was performed using the liquid-mediated metathetical route according to the reactions shown in Eq. 3-5:

$$2FeCl_3 + 2Na_3As \rightarrow Fe_2As + 6NaCl + As \qquad \text{Eq. 3-5}$$

The reaction of iron (III) chloride with sodium arsenide in refluxing toluene for 48 h resulted in the formation of an amorphous black powder. The sample was washed with absolute ethanol, followed by distilled water. The sample was annealed at 500 °C for 48 h.

Annealing of the sample caused a shiny silver-coloured mirror to be deposited on the inside of the glass ampoule used for annealing. Upon exposure to the atmosphere, this metallic coating changed from a shiny to a matte black appearance. XRD analysis of the material showed it to be crystalline, metallic arsenic (Fig. 3-2). XRD data for the remaining annealed powder showed it to be amorphous.

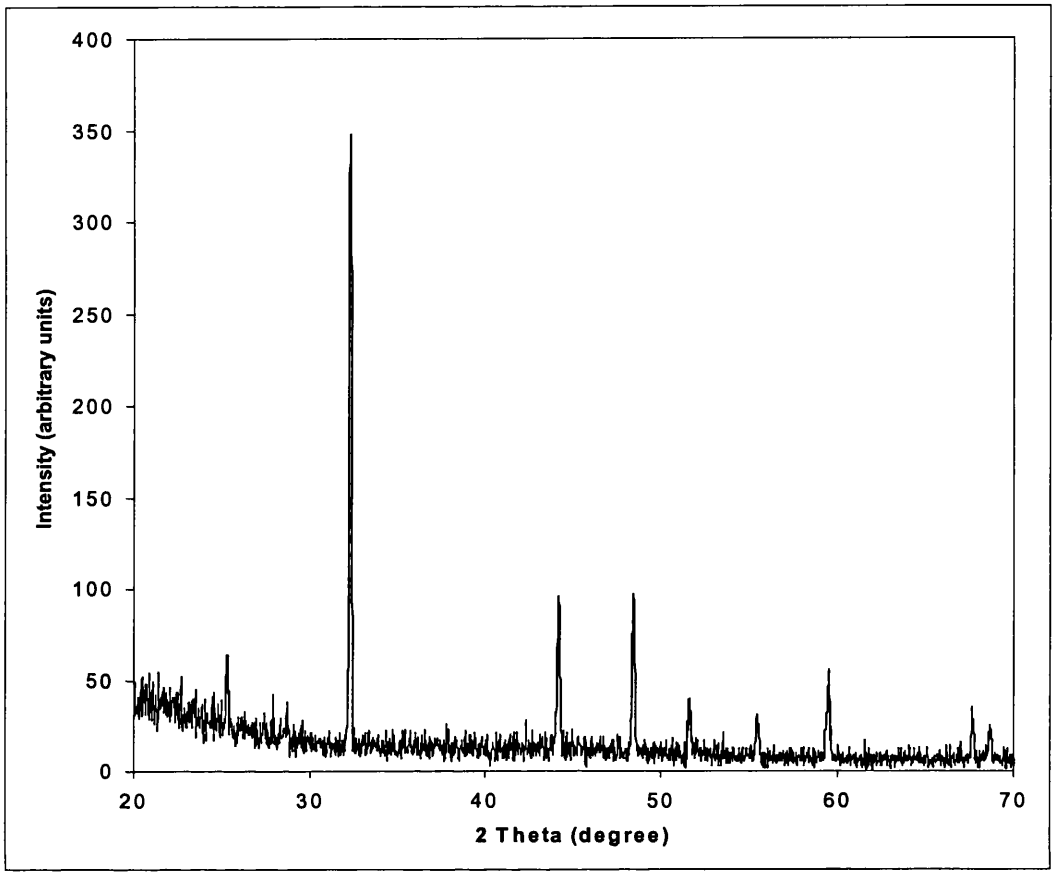

Fig. 3-2 XRD pattern of shiny, metallic component, showing arsenic only.

EDAX data for the amorphous powder, before annealing, showed the majority of the sample consisted of an iron to arsenic ratio of 2:1. A number of spots also showed a higher proportion of arsenic, which would be consistent with an intimate mixture of Fe_2As and elemental arsenic, which is indicated in Eq. 3-5. After annealing, there was only found to be an iron to arsenic ration of 2:1.

3.2.4 Group 9 - Cobalt:

The reaction of cobalt (II) chloride with binary and ternary sodium pnictides was performed using the liquid-mediated metathetical route according to the reactions shown in Eqs. 3-6 and 3-7:

$$3CoCl_2 + 2Na_3E' \rightarrow 2CoE' + 6NaCl + Co, (E' = P, As, Sb) \quad \text{Eq. 3-6}$$

$$3CoCl_2 + Na_3As + Na_3Sb \rightarrow 2CoAs_{0.5}Sb_{0.5} + 6NaCl + Co \quad \text{Eq. 3-7}$$

The reaction of cobalt (II) chloride with sodium pnictides in refluxing toluene for 48 h resulted in the formation of amorphous black powders in approximately 90% yield. The samples were washed with absolute ethanol, followed by distilled water. The samples were annealed at 500°C for 48 h.

XRD data for the phosphorus-containing sample showed it be X-ray amorphous both before and after annealing. The arsenic- and antimony-containing products both gave XRD spectra corresponding to the 1:1 CoAs (modderite) (Fig. 3-3) and CoSb (Fig. 3-3) phases. No XRD spectrum was obtainable from the ternary sample, it showing only an amorphous character both before and after annealing.

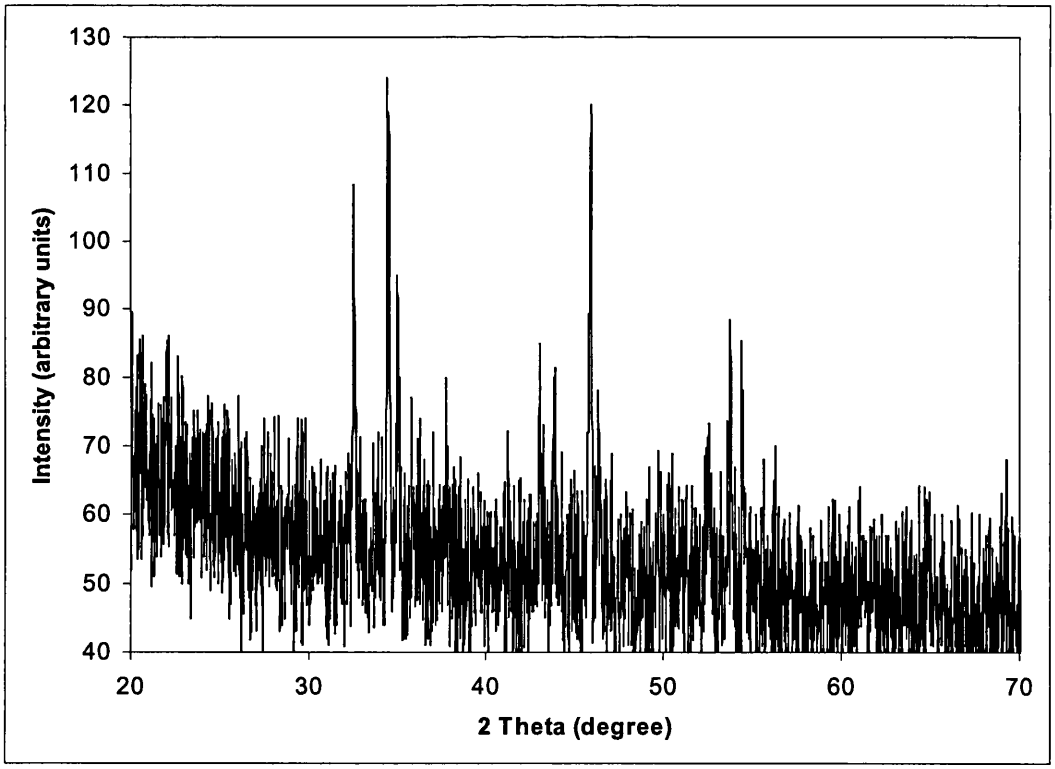

Fig. 3-3 XRD pattern of CoAs, annealed.

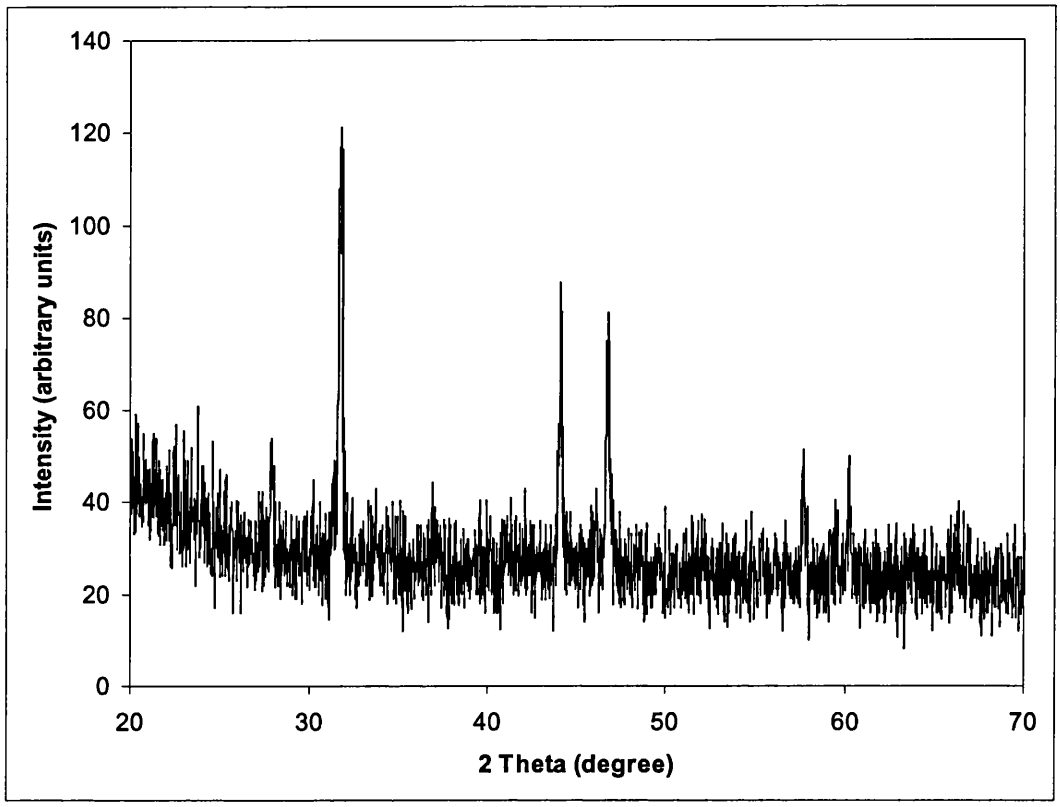

Fig. 3-4 XRD pattern of CoSb, annealed.

The Raman spectrum for the cobalt phosphide product shows peaks at 189, 464, 507, 604 and 666 cm^{-1}. No Raman spectra for cobalt phosphides are recorded in the literature and the recorded spectrum did not correspond to red phosphorus or any of the other obvious possible products, so it is likely that is corresponds to that of 1:1 CoP.

Vibrating sample magnetometry (VSM) data (Fig. 3-5) showed that the samples contained far less elemental cobalt than is indicated in Eq. 3-6. This simply means that Eq. 3-6 is not the best representation of the reaction scheme and that the excess cobalt is partially washed out in the water or ethanol washings and some incorporated into alternate phases.

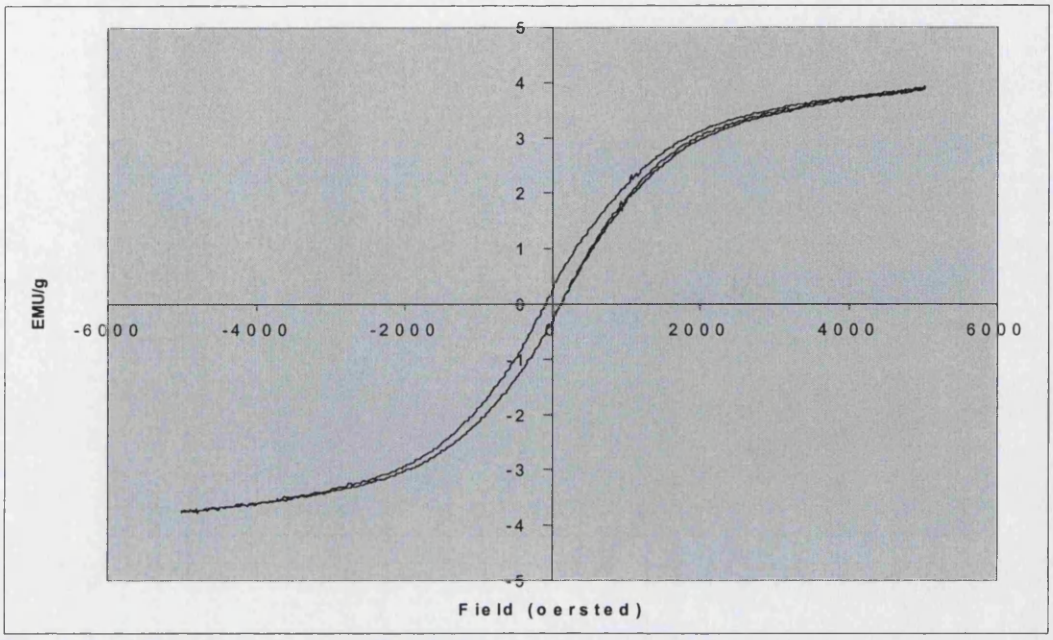

Fig. 3-5 VSM hysteresis loop for CoSb.

EDAX data for the phosphorus sample showed it to contain a cobalt to phosphorus ratio close to 1:1 with a slight excess of cobalt (3-5 %). The cobalt arsenide sample contained a 1:1 Co:As ratio. The antimony sample was shown to consist of a mixture of 1:1 and 2:1 Co:Sb products. The ternary sample prepared from three binary precursors was shown to consist of a nearly 2:1:1 ratio of Co:As:Sb with a slight deviation towards a cobalt-rich product (*ca.* 3%). There was a small number of spots which showed an excess of antimony, but not in consistent amounts, which seems to indicate that there is a component of elemental antimony which is finely divided among the ternary product. It is unevenly scattered in the sample giving rise to the inconsistent readings of excess antimony.

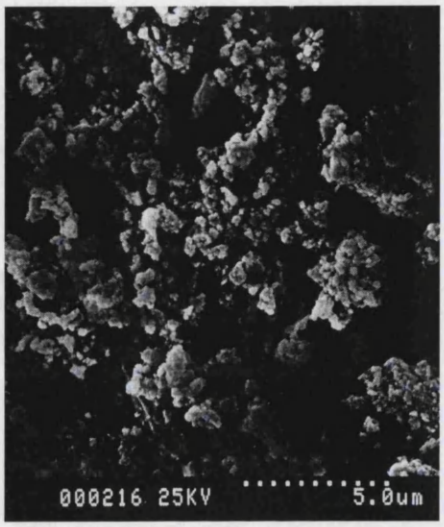

Fig. 3-6 SEM of CoAs, annealed.

SEM imaging of the samples showed that the cobalt phosphide sample consisted of agglomerate up to 3 microns in size, with a relatively small particle size range. The CoAs sample showed a few agglomerates of up to 10 microns with the remainder of the sample consisting of 1-2 micron diameter agglomerates (Fig. 3-6). The cobalt antimonide and ternary samples consisted of large agglomerates with particle diameters up to 100 microns, with a wide range of particle sizes.

3.2.5 Group 10 - Nickel:

The reaction of nickel halides with binary and ternary sodium pnictides was performed using the liquid-mediated metathetical route according to the reactions shown in Eqs. 3-8 to 3-11:

$$3NiX_2 + 2Na_3E' \rightarrow 2NiE' + 6NaCl + Ni, (X = Cl, Br; E' = P, As, Sb) \quad \text{Eq. 3-8}$$

$$3NiCl_2 + 0.5Na_3As + 1.5Na_3Sb \rightarrow 2NiAs_{0.25}Sb_{0.75} + 6NaCl + Ni \quad \text{Eq. 3-9}$$

$$3NiCl_2 + Na_3As + Na_3Sb \rightarrow 2NiAs_{0.5}Sb_{0.5} + 6NaCl + Ni \quad \text{Eq. 3-10}$$

$$3NiCl_2 + 2Na_3As_{0.5}Sb_{0.5} \rightarrow 2NiAs_{0.5}Sb_{0.5} + 6NaCl + Ni \quad \text{Eq. 3-11}$$

The reaction of nickel halides with sodium pnictides in refluxing toluene for 48 h resulted in the formation of amorphous black powders in approximately 90% yield. The samples were washed with absolute ethanol, followed by distilled water. The samples were annealed at 500°C for 48 h. In addition to the three binary nickel pnictides, the synthesis of ternary nickel arsenide antimonides was attempted by two different methods. The first method involved the use of two separate binary pnictide precursors (Eqs. 3-9 & 3-10) in addition to the nickel halide precursor. The second method employed a ternary arsenide/antimonide precursor, synthesised as described in the introductory chapter.

Powder diffraction data for the binary nickel pnictide gave a featureless spectrum before annealing, indicating an amorphous sample. After annealing at 500°C for 48 hours no XRD spectrum was discernible, and only after annealing at 800°C for 48 hours was the sample shown to consist of Ni_3P, which is however not likely its original composition. Evidence for the composition of the sample before annealing is given by EDAX data below. The heavier binary nickel samples were shown by XRD to be NiAs (nickeline)(Fig. 3-7) and NiSb (breithauptite)(Fig. 3-8).

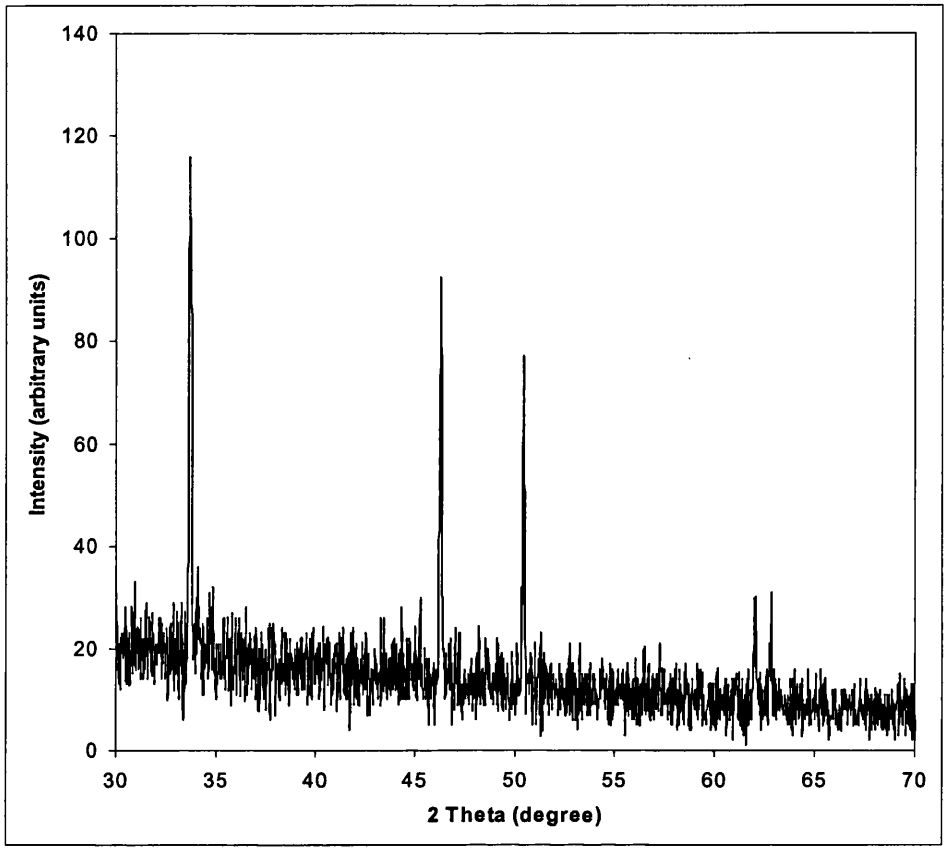

Fig. 3-7 XRD pattern for NiAs (nickeline).

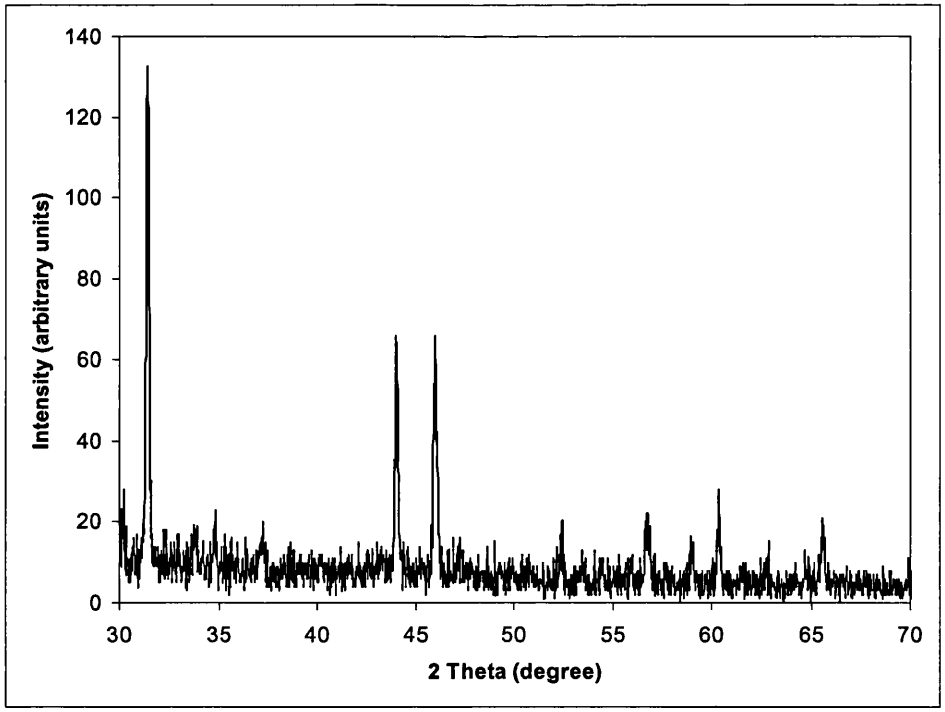

Fig. 3-8 XRD pattern for NiSb (breithauptite).

XRD data for the three ternary samples, before annealing, showed them to be amorphous. Annealing of the $NiAs_{0.25}Sb_{0.75}$ and $NiAs_{0.5}Sb_{0.5}$ samples synthesised from three binary precursors, gave XRD spectra that gave some indication as to the degree of arsenic and antimony incorporation in the ternary products. These XRD spectra also contained peaks which could not be matched to possible by-products such as oxides, binary compounds, halides etc., however they may still be employed to give an approximate indication of the relative quantities of arsenic and antimony within the ternary structure.

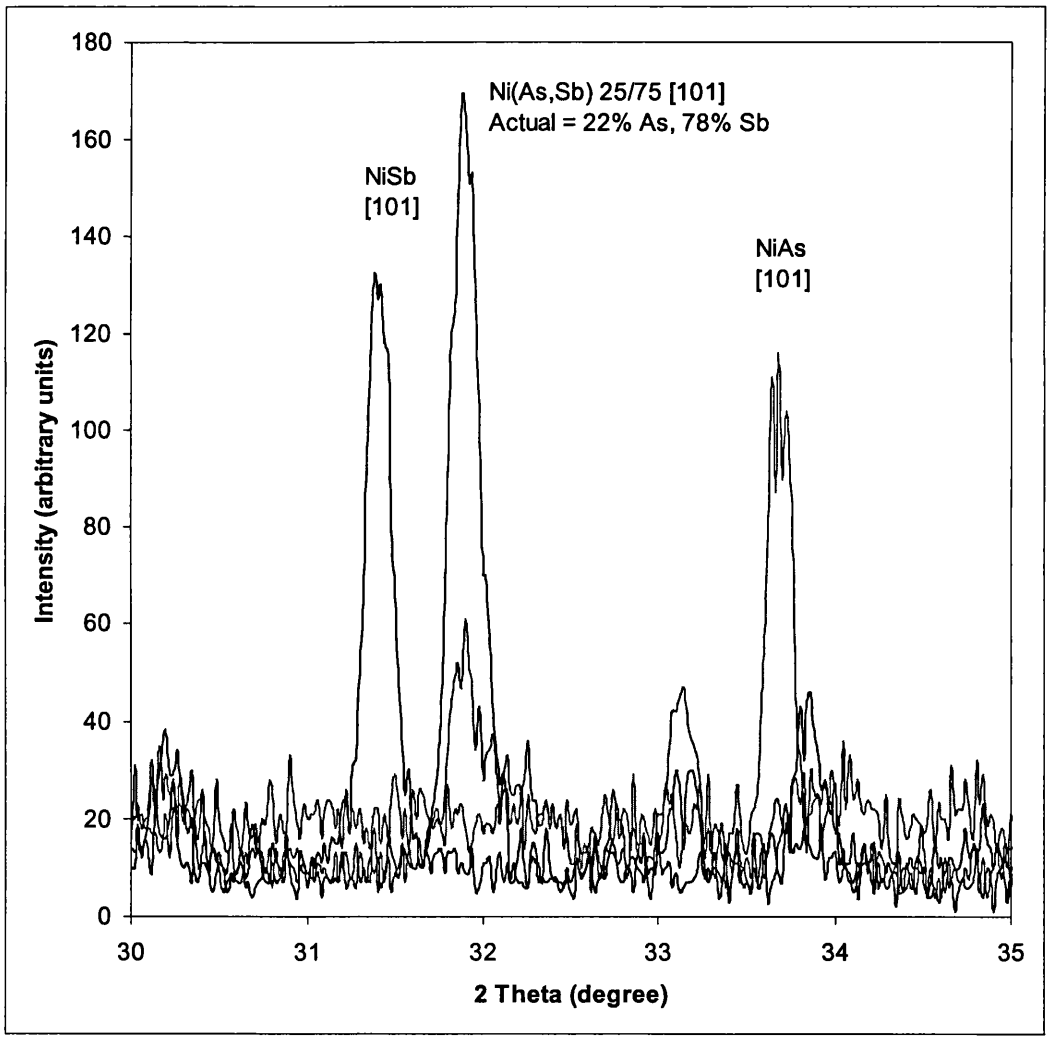

Fig. 3-9 XRD of Ternary $NiAs_{0.25}Sb_{0.75}$ [101] peak.

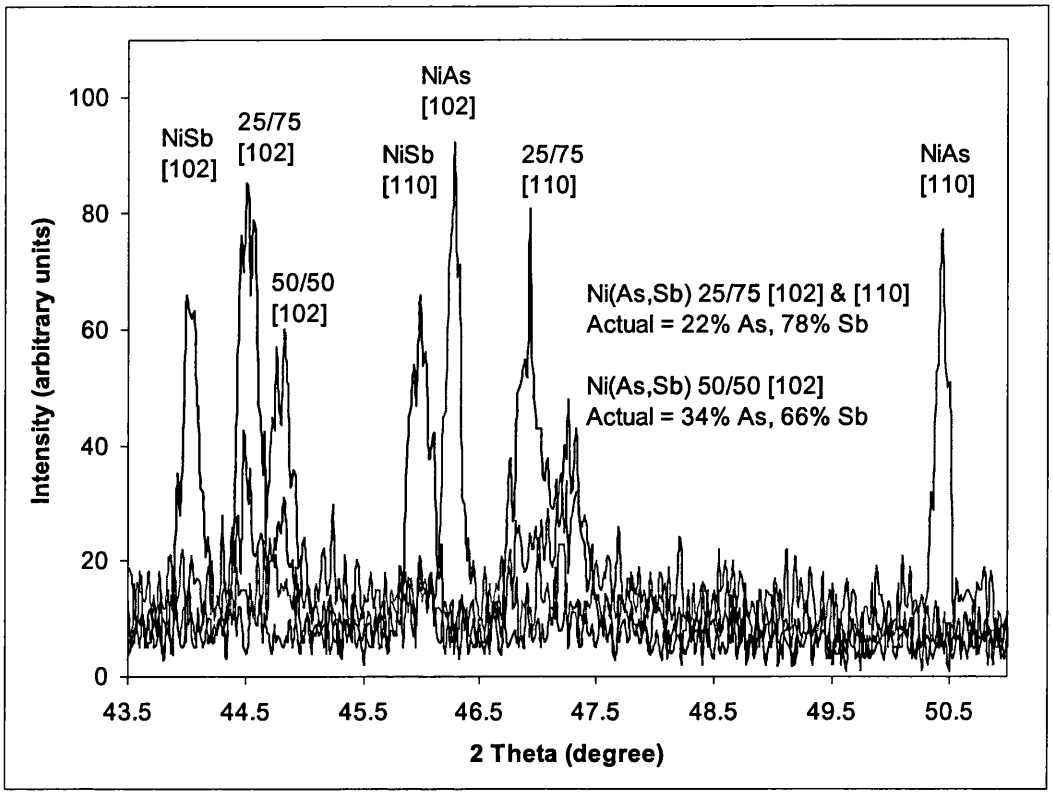

Fig. 3-10 XRDs of Ternary $NiAs_{0.25}Sb_{0.75}$ & $NiAs_{0.5}Sb_{0.5}$ [102] & [110] peaks.

Figs. 3-9 and 3-10 show small portions of the XRD spectra of both $NiAs_{0.25}Sb_{0.75}$ and $NiAs_{0.5}Sb_{0.5}$. It can be seen from the relative position of the $NiAs_{0.25}Sb_{0.75}$ ternary product [101], [102] and [110] peaks, employing Vegard's Law, that they all show that there is approximately 78% Sb and 22% As in the product (with respect to the pnictogen content). This is in quite good agreement with the stoichiometry of the precursors. Only the [102] peak for the $NiAs_{0.5}Sb_{0.5}$ product is visible to any extent and it shows that there is approximately 66% Sb and 34% As, which is a larger deviation from the precursor stoichiometry than the previous case. It will also be noted that many peaks for $NiAs_{0.5}Sb_{0.5}$ are not nearly as strong or in many cases not present at all. Some explanation for this will be give in the Discussion section of this chapter.

Vibrating sample magnetometry (VSM) data (Fig. 3-11) showed that the samples contained far less elemental nickel than would be surmised by Eq. 3-8. Some free nickel was detected, but only a small percentage of what would have been expected. Again, this

indicates that the postulated equation is not the best representation of the reaction scheme and that the excess nickel is partially washed out in the water or ethanol washings and some incorporated into alternate phases.

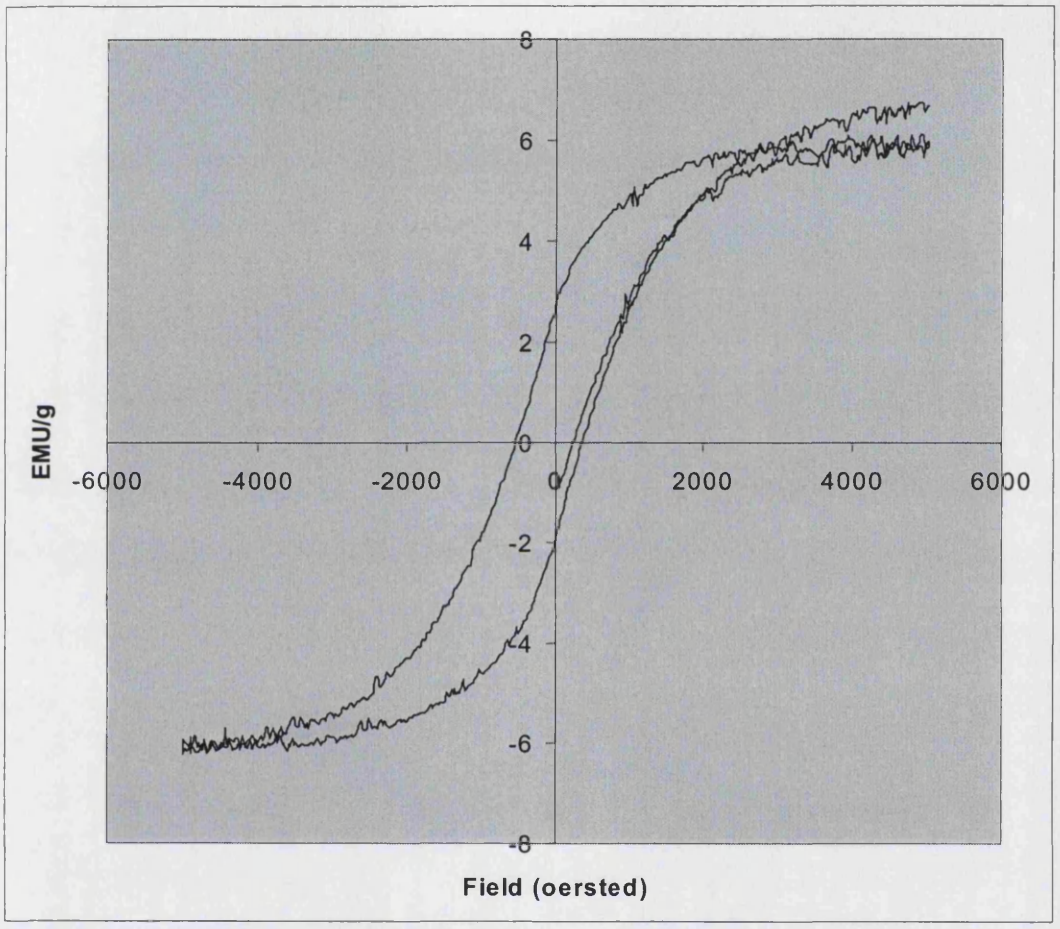

Fig. 3-11 VSM hysteresis loop for NiSb.

EDAX data for the binary phosphide sample showed it to consist solely of 2:1 Ni:P before annealing. After annealing at 500°C the composition was seen to be a mixture of 1:1 and 2:1 Ni:P in approximately equal amounts, and after a full anneal at 800°C the sample was shown to consist of 3:1 Ni:P. It has been previously been observed that heating of NiP and Ni_2P under vacuum at 800°C eliminates phosphorus and forms Ni_3P.[95,96] EDAX data for the heavier pnictide binary compounds showed them to consist of 1:1 Ni:As and Ni:Sb.

EDAX data for the ternary $NiAs_{0.5}Sb_{0.5}$ product synthesised from two binary pnictide precursors showed that it contained a 1:1 ratio of As:Sb and that there was a slight excess of nickel in the product, most likely in the form of elemental nickel. This was finely intermingled with the product so that no areas of high nickel content could be found by EDAX. The ternary $NiAs_{0.5}Sb_{0.5}$ product synthesised from one ternary pnictide precursor showed similar results with a slight excess of nickel and a 1:1 ratio of arsenic to antimony. The ternary $NiAs_{0.25}Sb_{0.75}$ product synthesised from two binary pnictide precursors showed a good match of the nickel to arsenic to antimony ratio of the precursors.

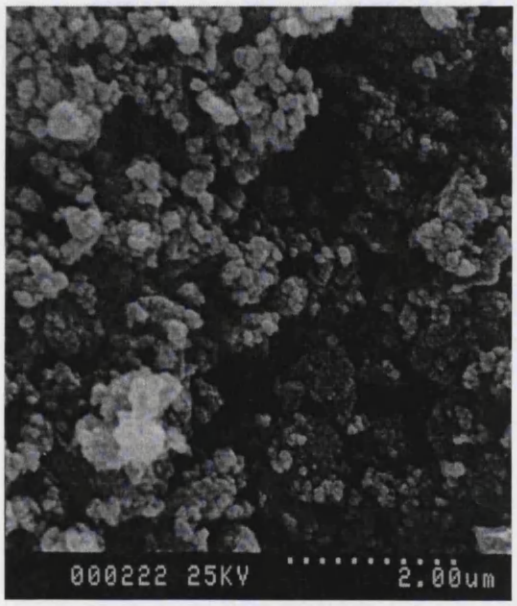

Fig. 3-12 SEM of $NiAs_{0.5}Sb_{0.5}$ unannealed.

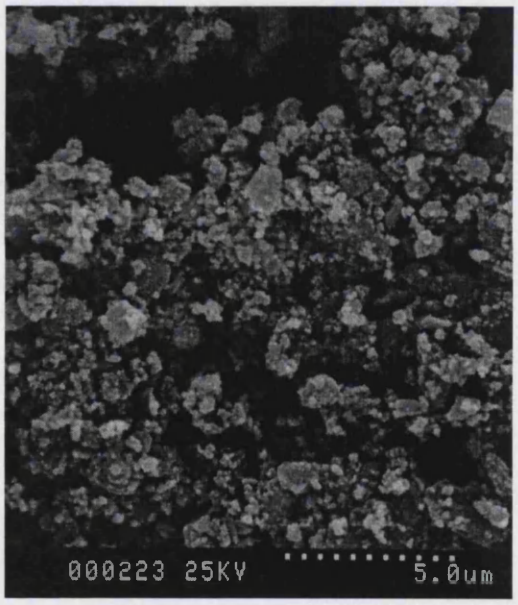

Fig. 3-13 SEM of $NiAs_{0.5}Sb_{0.5}$ unannealed.

Fig. 3-14 SEM of $NiAs_{0.5}Sb_{0.5}$, annealed.

SEM viewing of the nickel phosphide sample showed it to consist of two distinct phases after annealing at 500°C. One consisted of rounded, irregular particles matching the 2:1 Ni:P composition and the other consisted of angular, block-shaped particles corresponding to the 1:1 Ni:P composition. NiAs and NiSb were shown to consist of particles up to approximately 3 microns in diameter with a fair proportion of particles in the sub-100 nm region. The $NiAs_{0.5}Sb_{0.5}$ product from a single ternary precursor showed 3-4 micron spherical particles while the products from two binary pnictide precursors showed small spherical particles of 1 micron diameter or less (Figs. 3-12 to 3-14).

3.2.6 *Group 11 - Copper:*

The reaction of copper halides with binary and ternary sodium pnictides was performed using the liquid-mediated metathetical route according to the reactions shown in Eqs. 3-12 to 3-15:

$$3CuBr + Na_3P \rightarrow Cu_3P + 3NaBr \quad \text{Eq. 3-12}$$

$$3CuCl_2 + 2Na_3P \rightarrow Cu_3P + 6NaCl + P \quad \text{Eq. 3-13}$$

$$3CuCl_2 + 2Na_3Sb \rightarrow Cu_2Sb + CuSb + 6NaCl \quad \text{Eq. 3-14}$$

$$3CuCl_2 + 2Na_2As_{0.5}Sb_{0.5} \rightarrow 2CuAs_{0.5}Sb_{0.5} + 6NaCl + Cu \quad \text{Eq. 3-15}$$

The reaction of copper halides with sodium pnictides in refluxing toluene for 48 h resulted in the formation of amorphous black powders. The samples were washed with absolute ethanol, followed by distilled water. The samples were annealed at 500°C for 48 h.

The as-synthesised copper phosphide powders were X-ray amorphous prior to annealing. The reactions of sodium phosphide with copper (I) bromide and copper (II) chloride, independently, showed XRD data, after annealing, which indicated that both products contained the copper phosphide phase, Cu_3P, and the corresponding sodium halides, NaBr and NaCl, respectively (Fig. 3-15 shows the XRD for Cu_3P from $CuCl_2$). SEM showed both samples to consist of sub-micron diameter spherical agglomerates with a narrow distribution range.

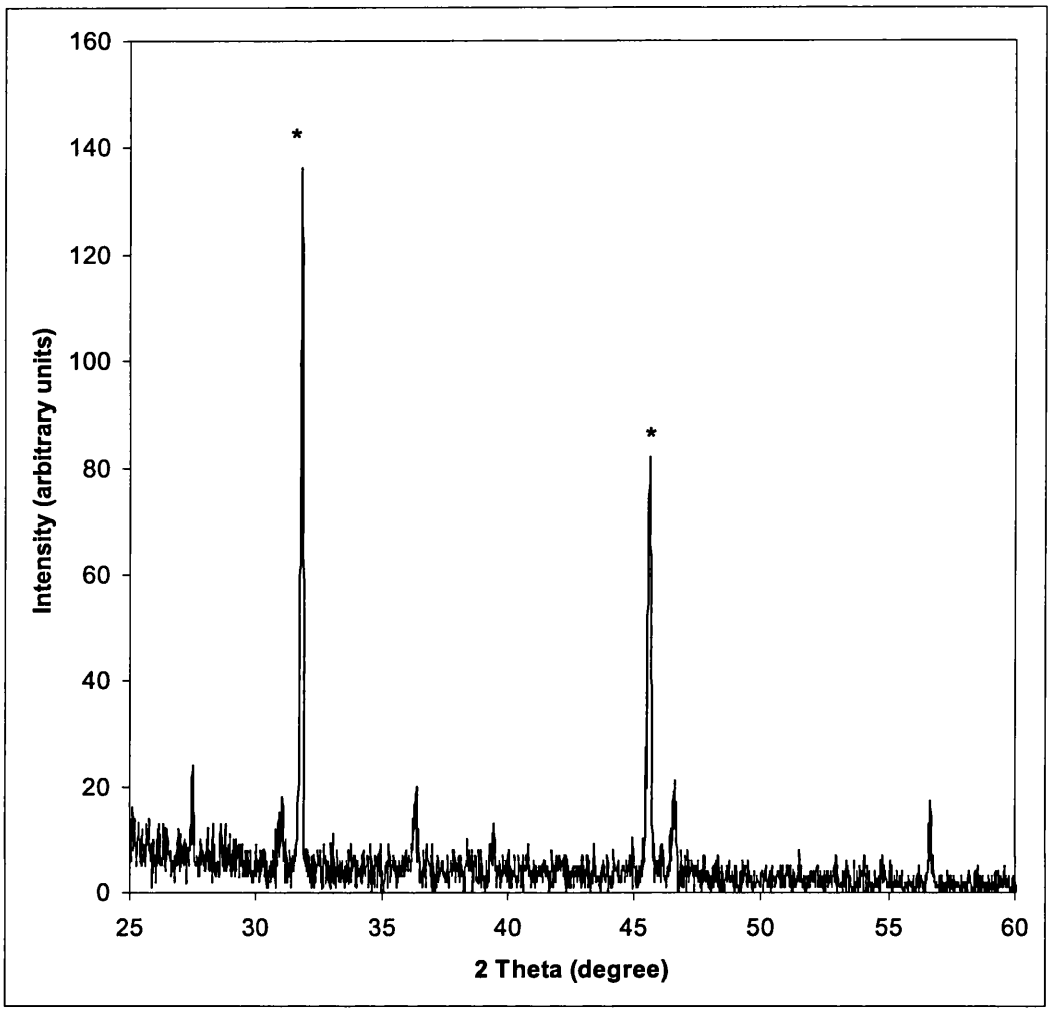

Fig. 3-15 XRD pattern for Cu_3P from $CuCl_2$. * = NaCl peaks.

EDAX data for both reactions showed there to be copper to phosphorus in a 3:1 ratio. The Cu(I) product showed some spots that had slight fluctuations in the Cu:P ratio from 4:1 to 2:1, but the majority of the sample was seen to contain 3:1 Cu:P. This may indicate some incomplete reaction, resulting in elemental copper and phosphorus unevenly distributed in the product mixture or some other copper phosphide phases which did not crystallise under the annealing conditions employed.

XRD data for the binary copper antimonide sample, showed it to be X-ray amorphous both before and after annealing. EDAX data for the sample showed it to consist of two distinct phases: a major phase, with a 2:1 copper to antimony ratio and a minor phase of 1:1 Cu:Sb composition. There was also indication of the presence of

some free, elemental antimony.

XRD data for the ternary arsenide/antimonide sample showed the crystalline phases, after annealing, to be Cu_5As_2 and NaCl. EDAX data showed there to be two distinct elemental ratio regions: One phase showed a 5:2:0 Cu:As:Sb ratio, and a second phase showed an approximate 4:4:3 Cu:As:Sb ratio. This second phase shows a very narrowly defined range of ratios of arsenic to antimony, which gives an indication that they are contained within a single compound rather than being finely intermixed separate elements. SEM showed the sample to consist of 1-2 micron average diameter agglomerates.

3.2.7 Group 12 - Zinc:

The reaction of zinc bromide with sodium arsenide was performed using the liquid-mediated metathetical route according to the reactions shown in Eq. 3-16:

$$3ZnBr_2 + 2Na_3As \rightarrow Zn_2As + 1/3ZnAs_3 + 2/3Zn + 6NaBr \quad \text{Eq. 3-16}$$

The reaction of zinc bromide with sodium arsenide in refluxing toluene for 48 h resulted in the formation of an amorphous black powder. The sample was washed with absolute ethanol, followed by distilled water. The sample was annealed at 500°C for 48 h.

XRD data showed the powder to be amorphous after annealing. No elemental arsenic was seen to form a mirror on the inside of the ampoule, as was the case with the iron reaction, indicating that there is likely no free elemental arsenic in the product. It may be the case that, if finely divided elemental zinc and arsenic had formed, that arsenic may have reacted with zinc under the annealing conditions, instead of forming a silver mirror on the inside of the ampoule.

EDAX data showed the presence of two distinct phases. One phase consisted of

a 2:1 zinc to arsenic ratio and the other phase was an arsenic-rich phase with an approximate composition of 1:3 Zn:As. The relative amounts of these was difficult to assess due to the relatively fine intermixing of the two phases. This uncertainty accounts for the apparent complexity of Eq. 3-16, above.

3.3 *Discussion:*

3.3.1 *Implications of Metathetical (Salt) Balancing:*

It has probably become apparent that one of the factors that may have an effect on the reactions carried out by any metathetical route is the self-imposed requirement that the chemical equation is balanced with respect to the co-produced salt and not with respect to the desired product. This has been done for the reason that it has always been the case for solid-state metathetical reactions, that apart from the energy of the initiation, the entire reaction energy is supplied by the heat of formation of the salt co-produced. In self-sustaining SSM reactions this energy is the most important factor contributing to the completion of the reaction. In the other modifications of metathetical reactions (oven-initiated, those carried out completely in an oven, liquid-mediated, etc) this salt-balancing has been carried over.

Even discounting the energy reasons, which are important for self-sustaining SSM reactions but less so for metathetical reactions where energy is supplied throughout, it can also be argued that salt balancing is important because it is the formation of the salt which leaves the desired element in a reactive state, either in its ionic form or its elemental form. So therefore a balance of say, sodium to chlorine, is important to leave the highest amount of reactive species available. This is of course assuming that a metal in its halide form is not available for reaction.

It can be seen that it may not always be possible to generate an equation that is balanced with respect to both the co-produced salt as well as the desired phase of the product. This is only made slightly easier in cases where the metal halide is available in a wider range of oxidation states, which allows some selection and matching of metal halide with the sodium pnictide. Sodium pnictides are available mainly in the Na_3E' (E' = P, As, Sb) form but Na_2As and Na_4As are also known and sodium sulphides are also available in a number of stoichiometries (Na_2S, Na_2S_3, Na_2S_4, Na_2S_5 etc.).

Even in the cases where the precursors are ideally suited for balancing both with

respect to salt and product there are many cases where the metal does not retain its oxidation state during the course of the reaction and the most conscientious balancing is for nought. A few examples will serve to illustrate the difficulty encountered. In the reaction involving iron (III) chloride and sodium arsenide the reaction was initially written as,

$$2FeCl_3 + 2Na_3As \rightarrow 2FeAs + 6NaCl.$$

(It has been doubled for comparison purposes.) The outcome, however was seen to be,

$$2FeCl_3 + 2Na_3As \rightarrow Fe_2As + 6NaCl + As$$

which shows that the conditions employed in the reaction have a strong effect on the outcome. When using the SMM method the product was $FeAs_2$ and when using liquid ammonia the product was FeAs.

Another example of the vagaries of these reactions can be seen in the case of the reactions to form copper phosphide. The two reactions used were

$$3CuBr + Na_3P \rightarrow Cu_3P + 3NaBr$$

$$3CuCl_2 + 2Na_3P \rightarrow Cu_3P + 6NaCl + P$$

Both reactions resulted in the formation of the same copper product, with seemingly little difference in the quality between the two alternatives. In one case oxidation state has been formally preserved and in the second the oxidation state has changed. Thus it seems apparent that the reaction conditions are more important than the exact composition of the precursors.

3.3.2 Comparison with Other Liquid Media:

There has been some research into metathetical reactions in other liquid media, the most extensive being research into the use of liquid ammonia at room temperature in high-pressure vessels.[31] Ammonia presents a very different environment to the reaction than toluene. The main difference between ammonia and toluene is that ammonia is a strongly coordinating solvent while toluene is a relatively weak

coordinating solvent. The reactions using ammonia were conducted at room temperature, under pressure, while the toluene reactions were conducted at 110°C at atmospheric pressure.

The reactions in liquid ammonia gave results which were quite similar to those obtained in toluene. The reactions to form NiE' and CoE' (E' = As, Sb) in liquid ammonia gave the 1:1 phase of the pnictide in both cases. As with the toluene reactions the nickel samples showed a small excess of nickel in the sample. In the case of the ammonia reactions this was detected as minor peaks in the XRD spectrum and as an uneven elemental composition by EDAX. As with the toluene reactions no significant change in the number or distribution of phases was observed after annealing of the samples.

The reactions in liquid ammonia to form iron and zinc arsenide gave products which differed from those obtained by the toluene reflux method. The iron reaction formed the 1:1 FeAs form, differing from the toluene reaction where Fe_2As and elemental As were formed. This may be due to the use of the higher temperature in the toluene reactions in which a different phase is favoured, or it may be due in part to some form of complexation of the precursors with ammonia which favours the 1:1 product. The zinc reaction in both solvents resulted in multiple phases and elements. The toluene reaction gave Zn_2As, $ZnAs_3$ and Zn while the ammonia reaction gave Zn_3As_2, Zn and As. In both cases there is reluctance for the reaction to go to completion, which may be indicative of the low temperatures used in both cases. The difference between the products in both reactions may again be due to the temperature difference between the two reaction mechanisms, or because of ammonia's coordinating ability. In all reactions in both ammonia and toluene there was observed the formation of a sodium halide which indicated that metathetical reaction had taken place, but as in the case of zinc, the reaction is unable to go to completion.

3.3.3 *Comparison with Solid-State Metathesis:*

Similar reactions using the solid-state metathesis regime have been carried out with the results providing a contrast to the liquid-mediated method.[83] For both nickel and cobalt reactions with arsenic and antimony, the products differed slightly from those achieved by liquid-mediated metathesis. The nickel SSM reactions produced a mixture of $Ni_{11}As_8$ and Ni_5As_2 and a mixture of NiSb and $NiSb_2$, while the cobalt SSM reactions produced a mixture of CoAs and Co_2As and a mixture of CoSb and $CoSb_2$. The reaction to form iron arsenide by SSM formed $FeAs_2$ while Fe_2As and As were formed by liquid-mediated metathesis. The reactions to form zinc arsenide by SSM formed Zn_3As_2 while Zn_2As, $ZnAs_3$ and Zn were formed by LMM.

There is no simple explanation to account for all of these cases but there are a number of possible explanations. In the case of cobalt and nickel there were only single-phase binary compounds formed by both toluene liquid-mediated and liquid ammonia metathesis. The simplest explanation for the appearance of multiple phases in the solid-state reactions is that the higher temperatures employed in solid-state reactions are such that, for these particular reactions, alternate phases are more favourable, whereas under LMM conditions single phases are more favourable. If these reactions proceed by the reductive recombination pathway then it can be seen that in the LMM reactions there is enough energy in the reaction to reduce the precursors to the elements and then only enough energy to form the single-phase binary products formed. In the SSM reactions, however, because of both the much higher temperatures and the much quicker times that once the precursors have been reduced to their elemental form, there are both thermodynamic and kinetic reasons why multiple and alternate phases are observed. The higher temperatures will favour high-temperature phases which are subsequently "quenched" in during the fast cooling occurring in SSM reactions. The faster times will favour the products which form the quickest, whether thermodynamically favoured or not, since, as in the previous example, the reaction cools very quickly. Some combination of these two factors will contribute to the final product.

In the cases of zinc and iron the LMM reactions resulted in multiple phases and elements while the SSM reactions resulted in single-phase products. Again this can be explained by an analysis of the temperatures and time-scale of the reactions. In these cases it is the LMM reactions which give mixed products and incomplete reaction. In these cases it is likely, given the presence of elements, that there is enough energy to reduce the precursors to their elemental forms, but then there is subsequently not enough energy to give a full recombination into a single-phase product. In the SSM reactions there is more heat immediately available to push the recombination to completion.

3.3.4 Redox Chemistry:

The effect of precursor oxidation state was discussed in the previous chapter in relation to chalcogenides and it was observed that most reactions preserved the oxidation state of the precursors, except the reactions involving transition metals. This chapter has dealt exclusively with reactions with transition metal halides and it has been observed that in most of these reactions the oxidation state of the precursors has not been preserved. In case of the reactions to form copper phosphide, the two reactions used were

$$3CuBr + Na_3P \rightarrow Cu_3P + 3NaBr$$

$$3CuCl_2 + 2Na_3P \rightarrow Cu_3P + 6NaCl + P.$$

The first equation is the only example in this chapter where the oxidation state was maintained. In most of the other reactions in this chapter oxidation state changes were frequently observed. It should be noted that when dealing with transition metal solid-state compounds that a strict application of formal oxidation state analysis is not always possible. Many compounds have a more covalent nature and therefore formal oxidation state considerations become less relevant.

It was observed that for many of the reactions, the products consisted of multiple phases and stoichiometries, and in some cases elemental transition metal and/or pnictide. This is in sharp contrast to the previous chapter where chalcogenides were considered where elemental products were rarely found. Pnictides seem to revert to the elements

much more easily than the chalcogenide equivalents. This might have to do with the fact that the heavier pnictogens (As, Sb) have a much more pronounced metallic character than either sulphur or selenium. The position in the periodic table of both arsenic and antimony place them closer to the metallic/non-metallic diagonal line through the p-block than either sulphur or selenium. Tellurium more closely resembles the heavier pnictogens in question, and it was observed in the reactions involving tellurium in the previous chapter that there was found to be some elemental tellurium in the products. It may also be the case, that being more metallic, these elements agglomerate more easily at higher temperatures as those found during annealing or agglomerate more easily at lower temperatures during the reaction itself, and thus precipitate out, effectively removing them from the reaction scheme.

A similar effect has been observed with solid-state metathesis reactions involving progressively heavier pnictogens.[83] There was an increasing trend towards the presence of elemental pnictogen in the products as the heavier pnictogen was used. In SSM reactions to form transition metal arsenides very few reactions showed any elemental arsenic, some reactions to form transition metal antimonides showed elemental antimony and nearly all reactions to form transition metal bismuthides gave elemental bismuth. Therefore, in SSM reactions there is a clear trend towards elemental formation as heavier pnictogens are employed.

Another important consideration is that the pnictide reactions were all carried out with transition metal and not with main group halides. This is likely the main cause of the oxidation state changes observed in the transition metal reactions and not observed in the main group-chalcogenide reactions. The main group halides have more restricted oxidation states than transition metals and therefore during the metathetical reaction process, the main group metals will maintain their oxidation state and proceed *via* the ionic metathesis route, thereby maintaining the elemental proportions found in the precursors, while the transition metal are more easily reduced and proceed by the reductive recombination route.

3.3.5 *Ternary Product Synthesis:*

The attempted synthesis of ternary transition metal arsenide/antimonides was rather less than successful. The vanadium and copper samples were shown to vary widely in the stoichiometry of the final product, indicating incomplete reaction and mixed elemental and binary phases. The titanium product was highly unstable and is discussed in more detail below. Only cobalt and nickel ternary compounds were successfully formed, although not necessarily in the desired stoichiometric ratios, as in the case of nickel. There is an understandable trend that partially accounts for the results obtained. The principle of forming ternary compounds is based on the assumption that with two binary compounds that share a common crystal structure it should be possible to substitute one atom for another atom in the same group and *vice versa*, and form any desired ternary compounds between the two extremes. This theory works very well for some ternary compounds ($NaCl_xBr_y$, $x+y=1$, for example), but breaks down in other cases.

It can then be seen that both copper and vanadium did not form single-phase binary compounds and thus it should not be expected that they would form ternary mixed compounds as easily as those transition metals that formed single-phase binary compounds with similar crystal structures. The reactions involving nickel and cobalt formed binary, single-phase compounds successfully, and were at least partially successful in synthesising ternary mixed compounds.

The copper ternary arsenide/antimonide could not be crystallised but EDAX data showed it to consist of the appropriate ratio of elements. The attempts at forming ternary nickel arsenide/antimonide compounds showed some interesting results. Two particular stoichiometries were attempted: one with equal amounts of arsenic and antimony and one with 75% antimony and 25% arsenic. The sample with unequal amounts of arsenic and antimony was shown by EDAX to contain 4:1:3 Ni:As:Sb and interpolation of XRD peaks showed it to display approximately 78% Sb character and 22% As character. The sample with equal amounts of arsenic and antimony, however,

did not conform to expectations. EDAX data for this sample showed that it consisted of 2:1:1 Ni:As:Sb but interpolation of XRD peaks gave an indication that the sample had only 34% As character and 66% Sb character. This is quite a large deviation from the expected 50/50 ratio aimed for.

The first thing that is noticed is that XRD and EDAX do not appear to agree with one another. This can be explained by noting that EDAX can only detect elemental composition within a certain minimum volume which varies but is on the order of 1 μm^3. Therefore if there are multiple phases mixed together at a level much finer than this, then EDAX will be unable to detect this. It is only able to detect such variations if the distribution is uneven and areas of higher and lower concentration of a certain component are present. The XRD data which shows that there was a far greater amount of antimony incorporated in the ternary sample than arsenic, can be accounted for by two possible explanations. The first reason is that there may simply not be enough energy to complete the complete reaction of the elements after reduction and formation of sodium chloride. The second possible reason is that the Ni:As:Sb phase diagram does not contain a ternary compound of the stoichiometry aimed for.

The second reason is more reasonable since there *was* enough energy to complete the reaction with more antimony than arsenic, and the reaction with equal amounts is not very different from that successful reaction. Also, if there was simply an energetic reason for the failure of the reaction to go to completion it might be expected that annealing of the sample would then supply energy to complete the reaction. Thirdly, the 50/50 sample was approximately halfway between the desired ratio and the 75/25 sample produced, which indicates that the reaction proceeded as far as it was able but at an approximate ratio of 2:1 Sb:As an impediment in the phase diagram was encountered and the reaction could not proceed and the remainder of the reaction resulted in amorphous binary compounds and elements.

One attempt at circumventing this phenomenon was to utilise a ternary precursor with the arsenic and antimony already intermingled on the atomic scale. A $Na_3As_{0.5}Sb_{0.5}$

precursor was synthesised (Fig. 3-16 shows the XRD for the ternary $Na_3As_{0.5}Sb_{0.5}$ precursor) and used in the same manner as the two binary pnictide precursors in a reaction to form ternary $NiAs_{0.5}Sb_{0.5}$.

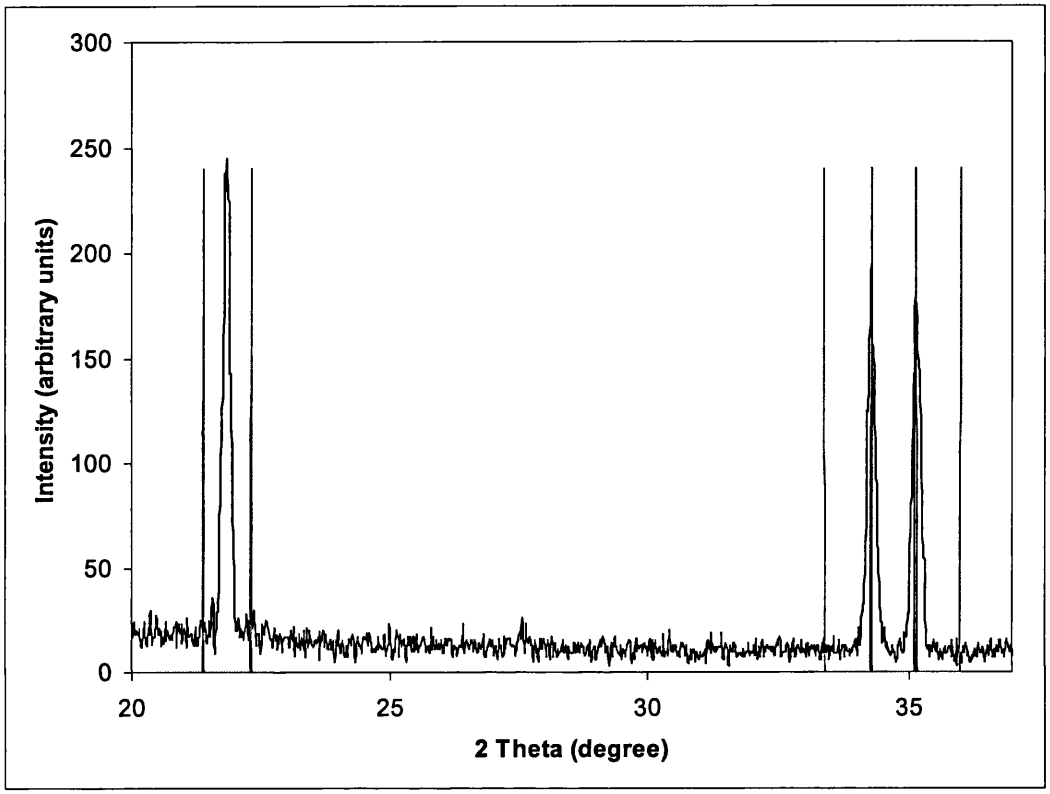

Fig. 3-16 XRD pattern for $Na_3As_{0.5}Sb_{0.5}$. Standards for Na_3As & Na_3Sb shown.

This reaction, however, gave the same results as the reaction using two separate binary pnictide precursors. This indicates that there is an inherent thermodynamic obstacle to the formation of a ternary nickel arsenide/antimonide with equal amounts of arsenic and antimony.

3.3.6 Ternary Titanium Pnictide:

The violent reaction of the ternary titanium arsenide/antimonide sample upon exposure to the atmosphere is interesting and unique. Of all the reactions performed for this thesis project, this was the only example that showed such a spontaneous and violent

reaction with air/water. The only reactions which showed any similarity with respect to instability at ambient and atmospheric conditions were the products of the chalcogenide reactions involving titanium or vanadium halides with sodium sulphide. These reactions also showed a degree of sensitivity to either water or air, but in the case of the chalcogenides, this reaction was seen to occur at a much slower rate and with far less violence.

There are a number of possible reasons for this. As was seen in the case of chalcogenides, titanium and vanadium, the early transition metals, there was a tendency towards instability upon prolonged exposure to the atmosphere. When pnictides were substituted for chalcogenides, however, there is not a direct analogy between the two classes of compounds. In the case of chalcogenides, both titanium and vanadium showed a slow transformation from sulphide to oxide over the course of a few weeks. The titanium sample was perhaps slightly faster than the vanadium sample, but in no way as violent as the pnictide sample.

The analogy breaks down because the vanadium phosphide sample was seen to be stable to air and water, while the titanium arsenide/antimonide was seen to react very violently with atmospheric contact. There are some possible explanations: The difference between the use of phosphorus and arsenide/antimonide as the pnictide is the biggest difference between Ti_3P and the theoretical $TiAs_{0.5}Sb_{0.5}$. As has been seen in all the reactions explored in this chapter, there is a tendency in some reactions for either a variety of stoichiometries of product to be present or of elemental separation. It was also seen that the heavier pnictides had a greater tendency to be found in the elemental state than the lighter ones.

The titanium - arsenide/antimonide reaction could have resulted in elemental titanium and elemental pnictogens, or in a true ternary compound, of whatever stoichiometry. There is some evidence towards the second case. EDAX and XRD examination of the product, after reaction with the atmosphere showed the complete absence of arsenic or antimony. This could be explained if a ternary compound *had*

formed, which upon exposure to air/moisture instantly decomposed to TiO_2 (as observed by XRD) and to the volatile pnictide gases, accounting for their absence. If the case had been that elemental titanium, arsenic and antimony had formed in the reaction mixture, then it would still be possible that very finely granulated titanium (as is likely to result from a liquid-mediated metathesis reaction) would react violently with air, but then it would still be expected to find arsenic and antimony, either as oxides or elements, in the final product mixture. The presence of sodium chloride in the reaction mixture also provides strong evidence that a metathetical reaction has occurred.

As has been stated, the evidence points towards the formation of a ternary compound, which then decomposes violently upon exposure to the atmosphere. This has two possible causes. One is that the ternary titanium arsenide/antimonide is inherently unstable with respect to air or moisture. The second possible explanation is that the particle size of the product is such that the total surface area of the product is great enough to support spontaneous oxidation.

3.4 Experimental:

The experimental procedure for the reaction of $CoCl_2$ with Na_3As is given below. All other reactions, including those involving Na_3P and Na_3Sb, followed a similar procedure with similar amounts and ratios of reactants. Reactions were for the most part based on 0.100 g amounts of the sodium pnictide and the metal halide amount was calculated accordingly. The order of addition of the reactants and the reaction conditions were also similar for all the reactions presented.

$CoCl_2$ (1.04 mmol) and Na_3As (0.695 mmol) were ground separately with a mortar and pestle inside an inert atmosphere glovebox. The Na_3As was placed in a Schlenk flask to which was added 20 ml of dried degassed toluene using Schlenk line techniques to avoid exposure to either air or moisture. The $CoCl_2$ was added with stirring, and the reaction mixture was heated to *ca.* 110°C under nitrogen flow. Once the temperature had stabilised the flask was sealed and allowed to reflux and stir for 48 hours. The resulting slurry was allowed to settle and the toluene was taken off by cannula. The solid was washed with 2 x 20 ml ethanol or methanol, followed by 2 x 20 ml deionized water, and finally by 2 x 20 ml ethanol or methanol. The powder was then pumped to dryness under vacuum. The powder was then collected and stored in air. The resulting ethanol, methanol and water washings were evaporated to identify any sodium halide species.

In the case of the ternary compounds, MAs_xSb_y, (M = Co, Ni) , Na_3As and Na_3Sb were ground together to form an intimate mixture and placed in the Schlenk flask together. Toluene was then added to these and then metal halide. The reason for the addition of toluene to the flask between the two precursors is that in some cases it was found that the two precursor powders would react spontaneously in a solid-state metathesis reaction. To avoid this the toluene was added to prevent direct contact between the precursor powders.

4. *Ternary Chalcopyrites:*

4.1 Introduction:

Copper indium and gallium chalcogenides of the formula $CuME_2$, (M = In, Ga; and E = S, Se, Te;) are chalcopyrite-structured ternary semiconductor materials. Many of the ternary and quaternary sulphides and selenides are potential and actual photovoltaic materials.[97,98,99,100,101] They are ideal candidates for polycrystalline solar-cell materials because of their radiation hardness[102,103], and high conversion efficiency[104,105], which can approach 17%. Solar cells made from these materials approach the efficiency achieved by the best polycrystalline silicon cells, have outstanding outdoor stability and also promise low cost.[106] They also find use as cathode materials of photochemical equipment due to their high performance and output stability.[107]

There have been many reports on the synthesis of this set of materials, which is not unexpected due to their economic potential. The traditional ceramic preparation of bulk $CuInE_2$ is achieved by combination of the elements in a specially strengthened quartz ampoule at 1150°C for 3 days.[108] This can be dangerous as the vapour pressure of sulphur becomes quite high at such temperatures. Other methods employed include evaporation[109], sputtering[110], spray pyrolysis[111], electrodeposition[112] and selenisation.[113] Chemical vapour deposition (CVD) has also been used to synthesise thin films of $Cu(Ga,In)E_2$. Both single source[114] and multi source[115] precursors have been employed. For most of these methods it has been found difficult to maintain the desired stoichiometry during the reaction, especially in deposition from the vapour phase which can yield a copper-deficient $CuIn_5S_8$ phase.[114,115]

This chapter deals in depth with this group of chalcopyrite ternary compounds and considers the products that are achieved from the use of various liquids and other variations in reaction conditions. Since there had been no previous synthesis of these materials by solid-state metathesis reported, these reactions were carried out to allow comparison of the liquid-mediated product and the solid state product.

4.2 Results - Synthesis and Characterisation:

4.2.1 Copper Indium Sulphide:

The synthesis of $CuInS_2$ was carried out by both the liquid-mediated and solid-state metathesis methods according to Eqs. 4-1 and 4-2:

$$CuBr + InCl_3 + 2Na_2S \rightarrow CuInS_2 + 3NaCl + NaBr \text{ (or } 4NaCl_{0.75}Br_{0.25}) \quad \text{Eq. 4-1}$$

$$2CuCl_2 + 2InCl_3 + 5Na_2S \rightarrow 2CuInS_2 + 10NaCl + S \quad \text{Eq. 4-2}$$

The reaction of copper halide and indium chloride with sodium sulphide in refluxing toluene for 48 h resulted in the formation of black powders in approximately 90% yield. The samples were washed with absolute ethanol, followed by distilled water, to remove the co-produced salt. Annealing of the samples was performed at 500°C for 24 h. The reaction of preground and premixed copper halide and indium chloride with sodium sulphide was also carried out in an evacuated, sealed glass ampoule at 500°C for 24 hours. A black loosely fused mass was obtained and was ground into a powder and washed with absolute ethanol, followed by distilled water, to remove the co-produced salt. No post-reaction annealing was performed.

Table 9 X-ray powder diffraction data[a] for $CuInS_2$, after annealing at 500°C for 24-48 h.

LMM, $CuCl_2$	**LMM, CuBr**	**SSM, $CuCl_2$**	**SSM, CuBr**	**Literature[60,116]**
a = 5.516 c = 11.114	a = 5.524 c = 11.106	a = 5.522 c = 11.133	a = 5.519 c = 11.108	a = 5.52 c = 11.12

[a] Unit cell dimensions a, c in Å (±0.004Å).

X-ray powder diffraction (XRD) data for the product from the liquid-mediated metathesis (LMM) reaction with both halides showed the samples to consist of highly crystalline $CuInS_2$ (roquesite) after annealing (Fig. 4-2). XRD data for the pre-annealed

samples showed the presence of $CuInS_2$ with possible traces of CuS. XRD data for the solid-state prepared samples showed them to also be highly crystalline $CuInS_2$ (roquesite). Of the samples prepared from $CuCl_2$ the solid-state product showed the more defined XRD pattern (less peak overlap and better peak resolution/separation), while of the samples prepared from CuBr the liquid-mediated product showed the more defined peaks. Fig. 4-1 shows the better peak separation of the CuBr product over the $CuCl_2$ product from LMM after annealing.

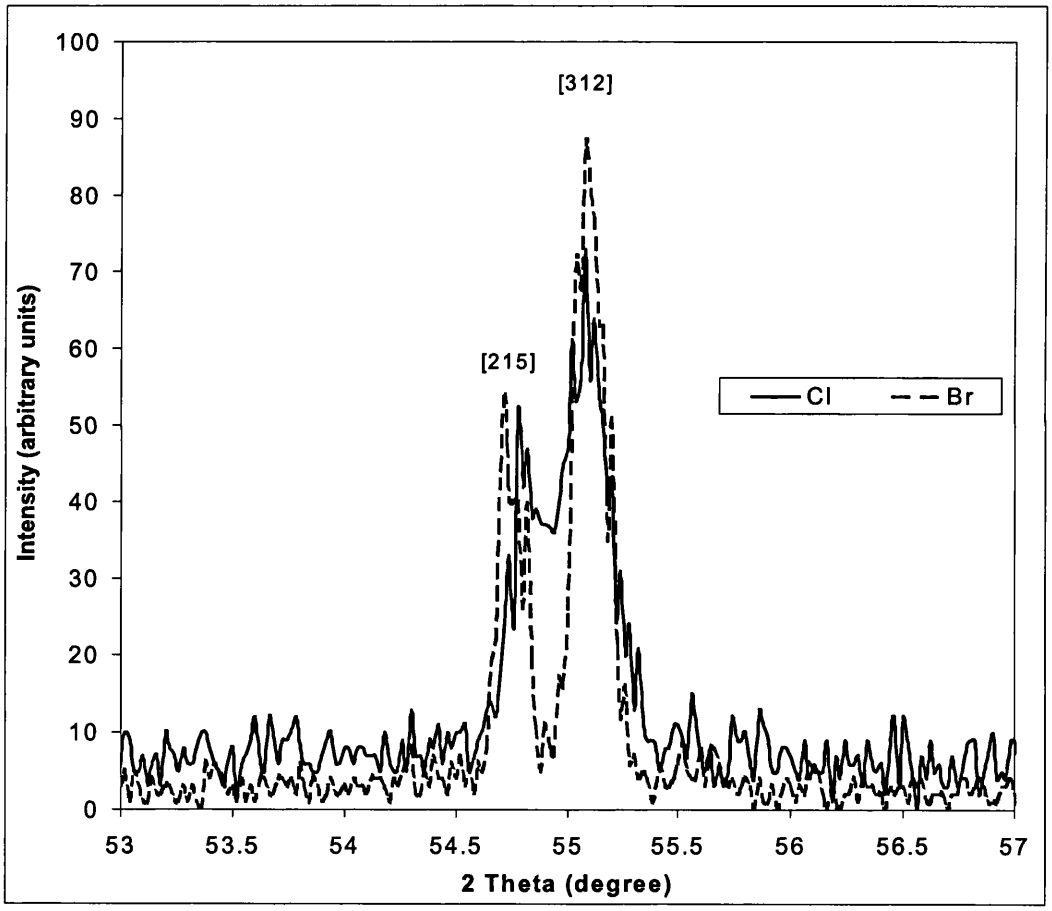

Fig. 4-1 [215] & [312] peaks of $CuInS_2$ from CuBr & $CuCl_2$ by LMM.

EDAX data for the liquid-mediated metathesis product from $CuCl_2$ before annealing showed it to contain mainly a 1:1:2 ratio of Cu:In:S, with the presence of a small amount of 1:1 Cu:S. After annealing solely a 1:1:2 ratio of Cu:In:S was observed. The LMM product from CuBr showed some variance from a 1:1:2 ratio of Cu:In:S with

the presence of 1:1 Cu:S and some spots with a high indium percentage, most likely indicating either elemental indium or some indium oxide/hydroxide. After annealing this variance was eliminated and a 1:1:2 ratio of Cu:In:S was observed throughout. The sample from $CuCl_2$ also showed no Cu:S ratio of 1:1 after annealing. EDAX data for the solid-state prepared samples showed good results for the sample from $CuCl_2$ while the sample from CuBr showed the presence of CuS and In_2S_3 as minor phases to the majority $CuInS_2$.

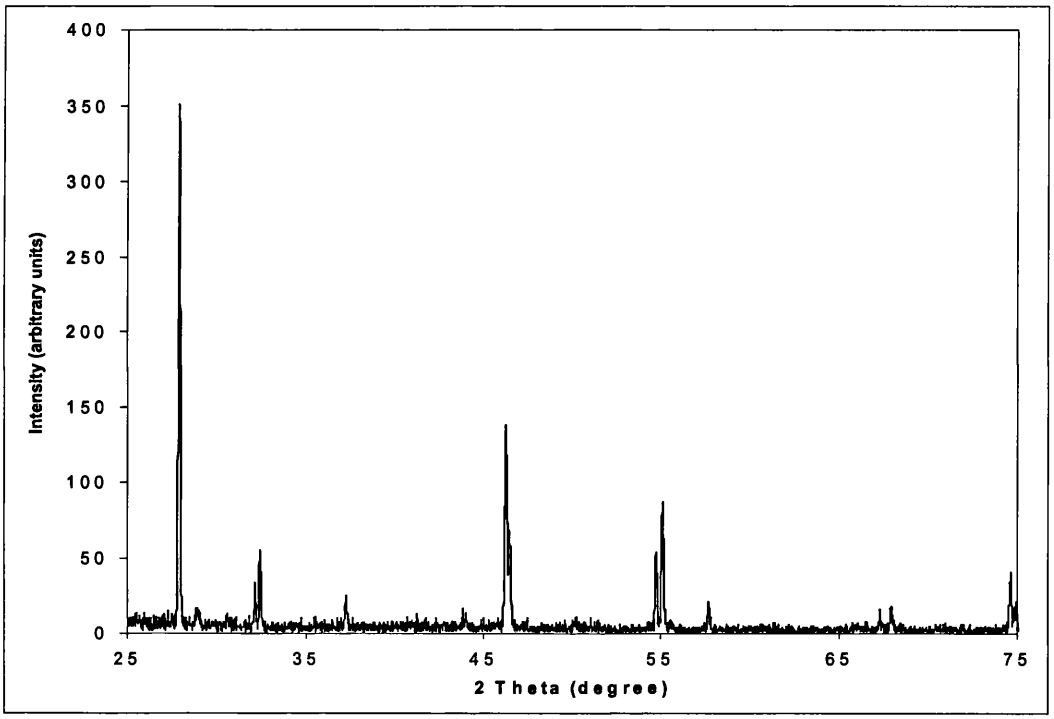

Fig. 4-2 XRD pattern for $CuInS_2$ from CuBr by LMM.

Differential scanning calorimetry (DSC) data for the as-prepared LMM samples showed no exotherms in the region for elemental sulphur or indium.

Particle sizes of the liquid-medaited products were in the 1-4 μm diameter range. Annealing of the LMM sample from CuBr brought about a remarkable change in the morphology of the sample. Before annealing the sample showed particle sizes of 2-5 μm diameter with a variety of shapes. After annealing the sample consisted of incredibly

uniform 1-2 μm diameter, rounded, nearly spherical particles. The samples prepared by SSM also showed roughly spherical particles but in these cases with a much larger range of sizes with a majority in the 5-15 μm diameter range, but some as large as 100 μm in diameter.

4.2.2 Copper Indium Selenide:

The synthesis of $CuInSe_2$ was carried out by both the liquid-mediated and solid-state metathesis methods according to Eqs. 4-3 and 4-4:

$$CuBr + InCl_3 + 2Na_2Se \rightarrow CuInSe_2 + 4NaCl_{0.75}Br_{0.25} \quad \text{Eq. 4-3}$$

$$2CuCl_2 + 2InCl_3 + 5Na_2Se \rightarrow 2CuInSe_2 + 10NaCl + Se \quad \text{Eq. 4-4}$$

The reaction of copper halide and indium chloride with sodium selenide in refluxing toluene for 48 h resulted in the formation of black powders in approximately 90% yield. The samples were washed with absolute ethanol, followed by distilled water, to remove the co-produced salt. Annealing of the samples was performed at 500°C for 24 h. The reaction of preground and premixed copper halide and indium chloride with sodium selenide was also carried out in an evacuated, sealed glass ampoule at 500°C for 24 hours. A black loosely fused mass was obtained and was ground into a powder and washed with absolute ethanol, followed by distilled water, to remove the co-produced salt. No post-reaction annealing was performed.

Table 10 X-ray powder diffraction data[a] for $CuInSe_2$, after annealing at 500°C

LMM, $CuCl_2$	**LMM, CuBr**	**SSM, $CuCl_2$**	**SSM, CuBr**	**Literature[60,116]**
a = 5.780 c = 11.608	a = 5.781 c = 11.613	a = 5.779 c = 11.612	a = 5.776 c = 11.603	a = 5.782 c = 11.619

[a] Unit cell dimensions a, c in Å (±0.004Å).

X-ray powder diffraction (XRD) data for the product from the liquid-mediated metathesis reaction with both halides showed the samples to consist of highly crystalline $CuInSe_2$ after annealing. XRD data for the solid-state prepared samples showed them to also be highly crystalline $CuInSe_2$, with both samples showing crystalline sodium halide before washing. Fig. 4-3 shows $CuInSe_2$ from $CuCl_2$ by SSM and Fig. 4-4 shows $CuInSe_2$ from CuBr from SSM.

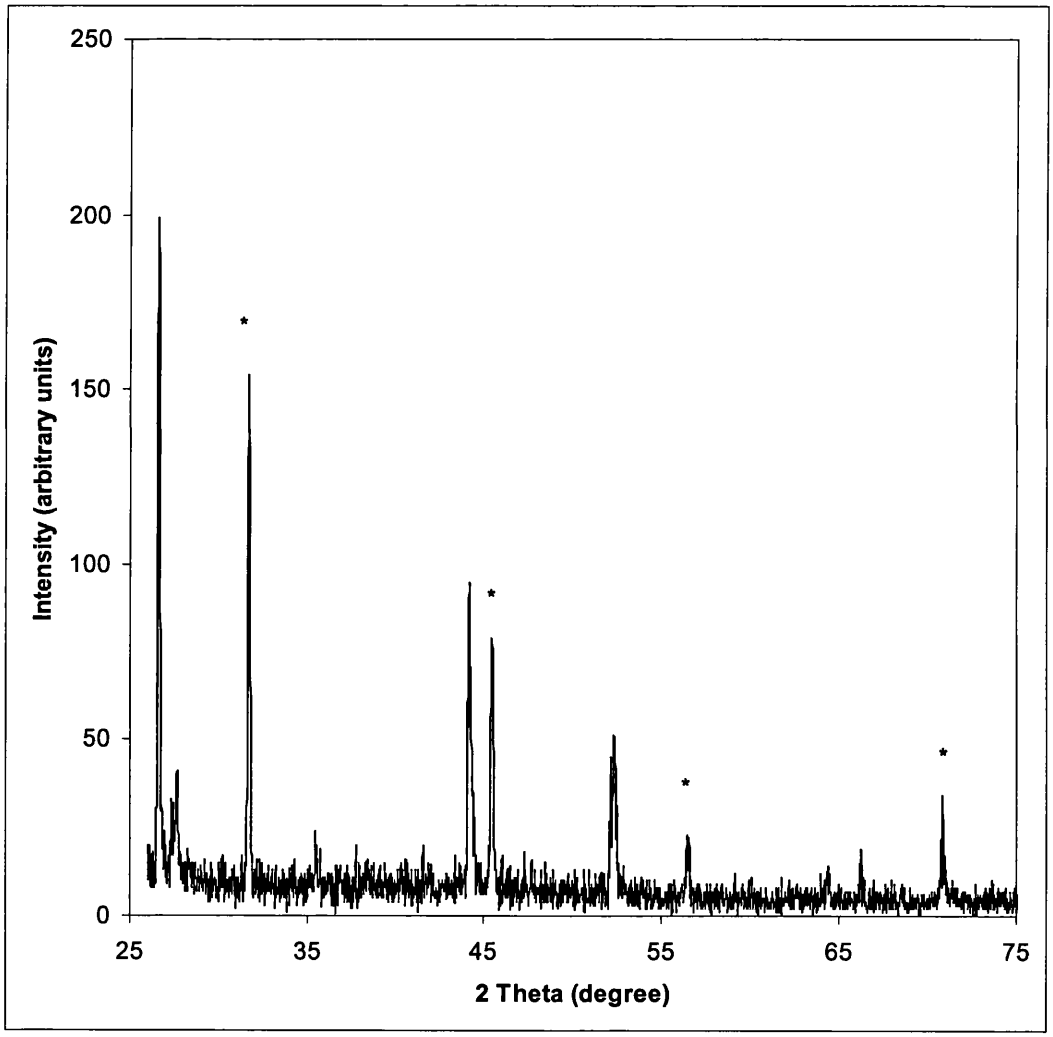

Fig. 4-3 XRD pattern of $CuInSe_2$ from $CuCl_2$ by SSM. * = NaCl peaks.

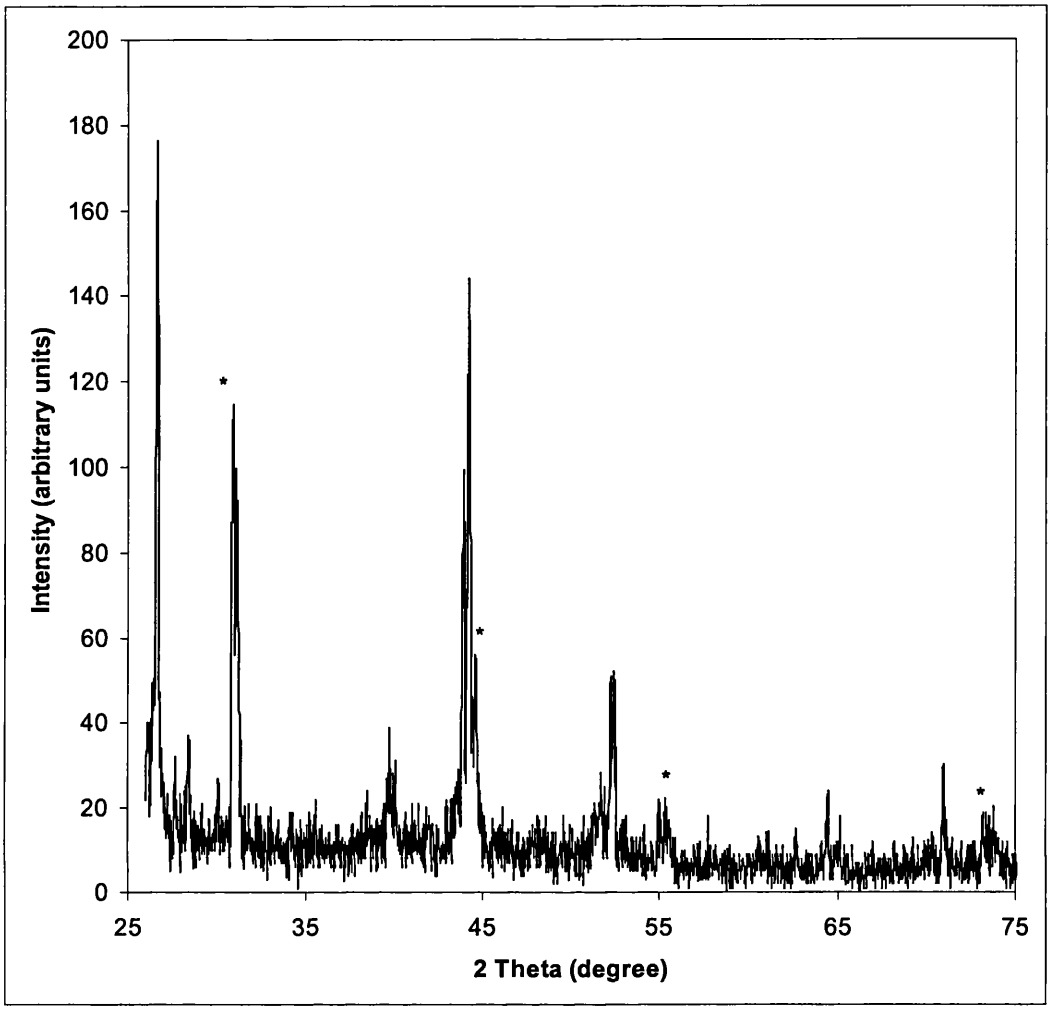

Fig. 4-4 XRD pattern of $CuInSe_2$ from CuBr. * = $NaCl_{0.75}Br_{0.25}$ peaks.

The two liquid-mediated metathesis products showed equally well-defined XRD spectra with little difference between them. The solid-state product from $CuCl_2$ also showed a well-defined spectrum but not as well-defined as that of the liquid-mediated metathesis products. The SSM product from CuBr, while clearly showing $CuInSe_2$, had peaks which were merged into one another.

EDAX data for the liquid-mediated metathesis product from $CuCl_2$ before annealing showed it to contain mainly a 1:1:2 ratio of Cu:In:Se, with a number of spots showing a high selenium content. In what form this appeared was not conluded. The LMM product from CuBr also showed some selenium-rich spots but to a lesser extent

than the $CuCl_2$ sample. After annealing these Se-rich spots were no longer observed and solely a 1:1:2 ratio of Cu:In:Se was observed. EDAX data for the solid-state prepared samples showed them to consist of nearly a 1:1:2 ratio of Cu:In:Se but with a slight copper deficiency. The CuBr sample also showed some evidence for some amounts of Cu_2Se and a copper-rich phase of undetermined composition (oxide/hydroxide).

Differential scanning calorimetry (DSC) data for the as-prepared LMM samples showed no exotherms in the region for elemental selenium or indium.

Particle morphologies for the selenium samples coincided with the sulphur samples, that is 1-3 μm diameter spherical particles for the LMM method and much larger particles for the SSM method. A similarly remarkable change in morphology was observed after annealing for the selenium sample with incredibly uniform 2 μm spherical particles resulting.

4.2.3 Copper Indium Telluride:

The synthesis of $CuInTe_2$ was carried out by both the liquid-mediated and solid-state metathesis methods according to Eqs. 4-5 and 4-6:

$$CuBr + InCl_3 + 2Na_2Te \rightarrow CuInTe_2 + 4NaCl_{0.75}Br_{0.25} \qquad \text{Eq. 4-5}$$

$$2CuCl_2 + 2InCl_3 + 5Na_2Te \rightarrow 2CuInTe_2 + 10NaCl + Te \qquad \text{Eq. 4-6}$$

The reaction of copper halide and indium chloride with sodium telluride in refluxing toluene for 48 h resulted in the formation of black powders in approximately 90% yield. The samples were washed with absolute ethanol, followed by distilled water, to remove the co-produced salt. Annealing of the samples was performed at 500°C for 24 h. The reaction of preground and premixed copper halide and indium chloride with sodium telluride was also carried out in an evacuated, sealed glass ampoule at 500°C for 24 hours. A black loosely fused mass was obtained and was ground into a powder and

washed with absolute ethanol, followed by distilled water, to remove the co-produced salt. No post-reaction annealing was performed.

Table 11 X-ray powder diffraction data[a] for $CuInTe_2$, after annealing at 500°C for 24-48 h.

LMM, $CuCl_2$	LMM, CuBr	SSM, $CuCl_2$	SSM, CuBr	Literature[60,116]
a = 6.20 c = 12.40	a = 6.19 c = 12.40	a = 6.20 c = 12.39	a = 6.19 c = 12.40	a = 6.18 c = 12.36

[a] Unit cell dimensions a, c in Å (±0.01Å).

X-ray powder diffraction (XRD) data for the product from the liquid-mediated metathesis reaction with both halides showed the samples to consist of highly crystalline $CuInTe_2$ and elemental Te after annealing (Fig. 4-5). XRD data for the solid-state prepared samples showed them to also be highly crystalline $CuInTe_2$ and elemental Te (Fig. 4-6). The presence of the elemental tellurium is at least partially explained by the impurities found in the Na_2Te precursor, as was discussed in the Introduction chapter.

However there was also noted a trend in the amounts of elemental tellurium present in the four different samples. Of the four variables involved (LMM *vs.* SSM; & CuBr *vs.* $CuCl_2$) it was clear that the samples prepared from CuBr contained less elemental tellurium than those from $CuCl_2$ and those prepared by SMM contained less elemental tellurium than those prepared by LMM. That the solid-state route produces less elemental tellurium than the liquid-mediated method can be explained by analogy to the previous chapter and previously reported work[8], where it was observed that in LMM reactions the low energy input often caused the formation of elemental metals, particularly with the heavier elements.

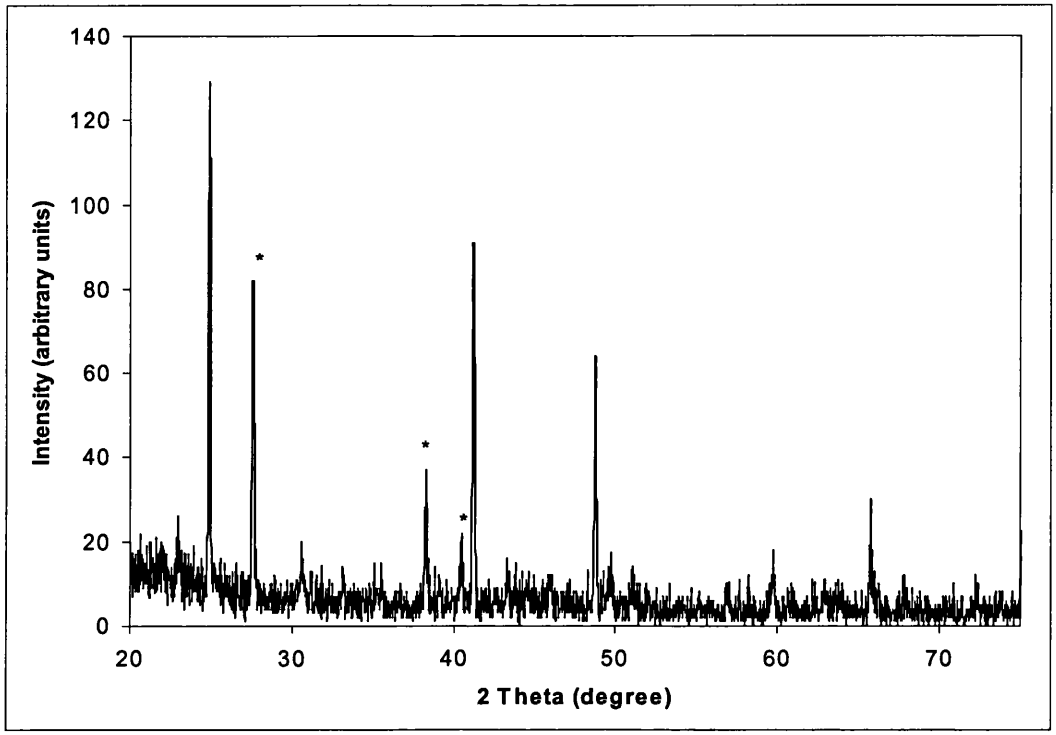

Fig. 4-5 XRD pattern for $CuInTe_2$ from $CuCl_2$ by LMM, annealed. * = elemental Te.

The difference between $CuCl_2$ and CuBr in this case is the clearest example of all these reactions where there is some evidence for the difference between the two balanced equations. It is seen in the equation for $CuCl_2$ that some free tellurium should be present, which is not needed to balance the CuBr-containing equation. The free chalcogenide in the $CuCl_2$ reactions was however *not* seen for the two lighter chalcogenides, but these do not crystallise as readily as metallic tellurium and are thus harder to observe in XRD patterns. EDAX data for the selenium samples showed some Se enrichment prior to annealing to further show that there is a difference between the two equations.

EDAX data for the four samples also confirms the discussion above. The LMM samples showed the presence of 1:1:2 Cu:In:Te as well as spots of 100% tellurium, and the SMM samples did as well. The relative amounts of free tellurium was found to follow the same trend with the LMM $CuCl_2$ sample showing the most and the SSM CuBr sample showing the least.

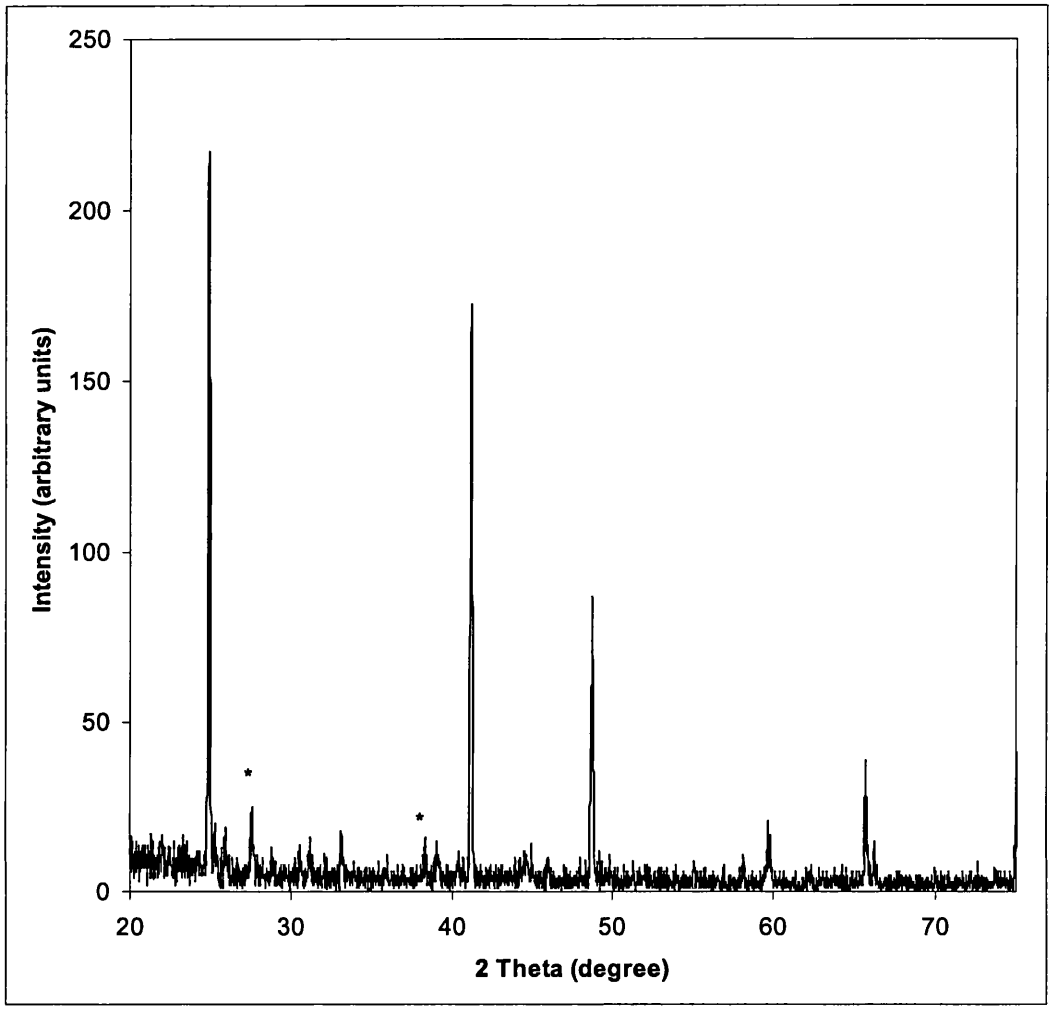

Fig. 4-6 XRD pattern for $CuInTe_2$ from CuBr by SSM. * = elemental Te.
(Note relative elemental Te amounts)

4.2.4 Copper Gallium Sulphide:

The synthesis of $CuGaS_2$ was carried out by the liquid-mediated metathesis method according to Eqs. 4-7 and 4-8:

$$CuBr + GaCl_3 + 2Na_2S \rightarrow CuGaS_2 + 4NaCl_{0.75}Br_{0.25} \quad \text{Eq. 4-7}$$

$$2CuCl_2 + 2GaCl_3 + 5Na_2S \rightarrow 2CuGaS_2 + 10NaCl + S \quad \text{Eq. 4-8}$$

The reaction of copper halide and gallium chloride with sodium sulphide in

refluxing toluene for 48 h resulted in the formation of black powders in approximately 80% yield. The samples were washed with absolute ethanol, followed by distilled water, to remove the co-produced salt. Annealing of the samples was performed at 500°C for 24 h.

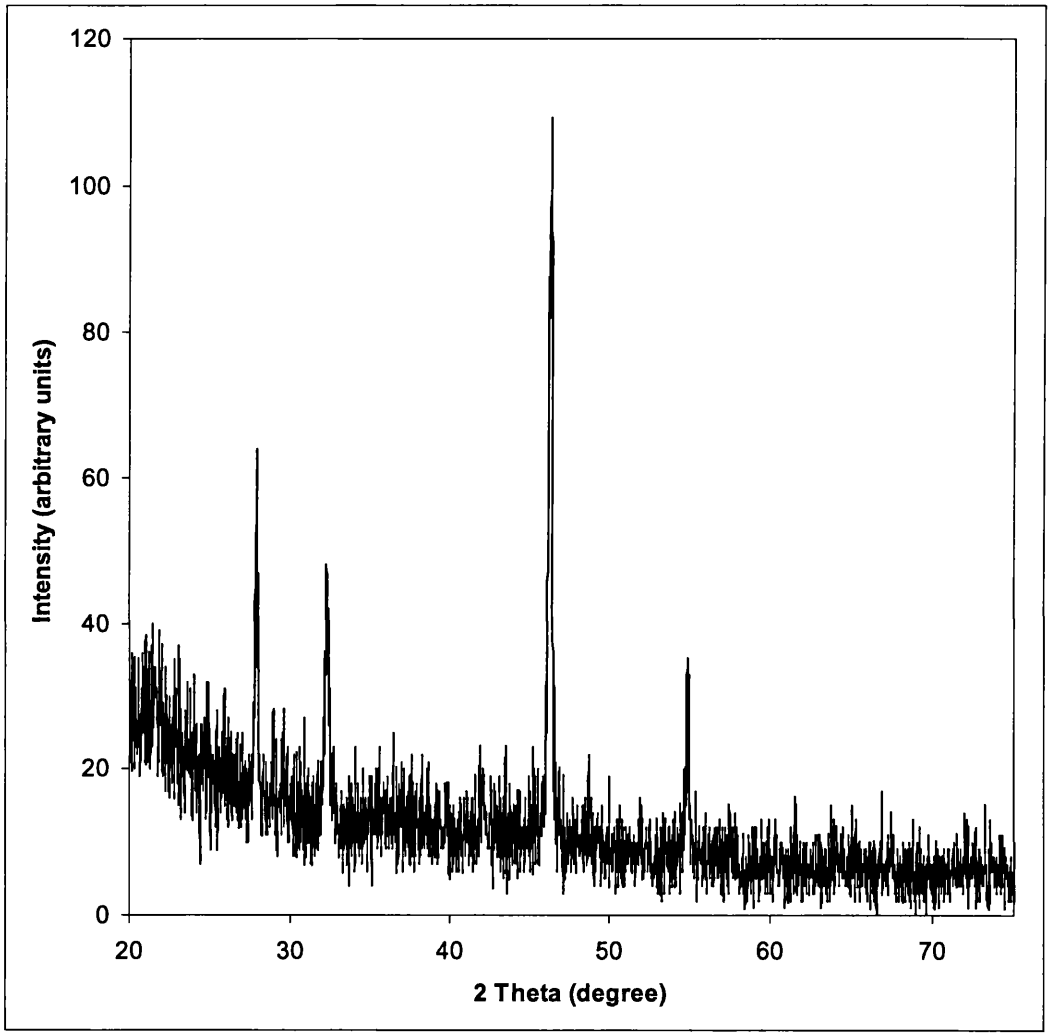

Fig. 4-7 XRD pattern for $Cu_{1.765}S$ (digenite) intermediary.

X-ray powder diffraction (XRD) data for the annealed product from $CuCl_2$ showed it to consist of $CuGaS_2$ (Fig. 4-8) and that from CuBr to be mainly $CuGaS_2$ with a minor phase of $Cu_{1.765}S$ (digenite). The product from $CuCl_2$ before annealing showed it to consist solely of CuS (covellite) and that from CuBr to consist solely of $Cu_{1.765}S$ (digenite) (Fig. 4-7).

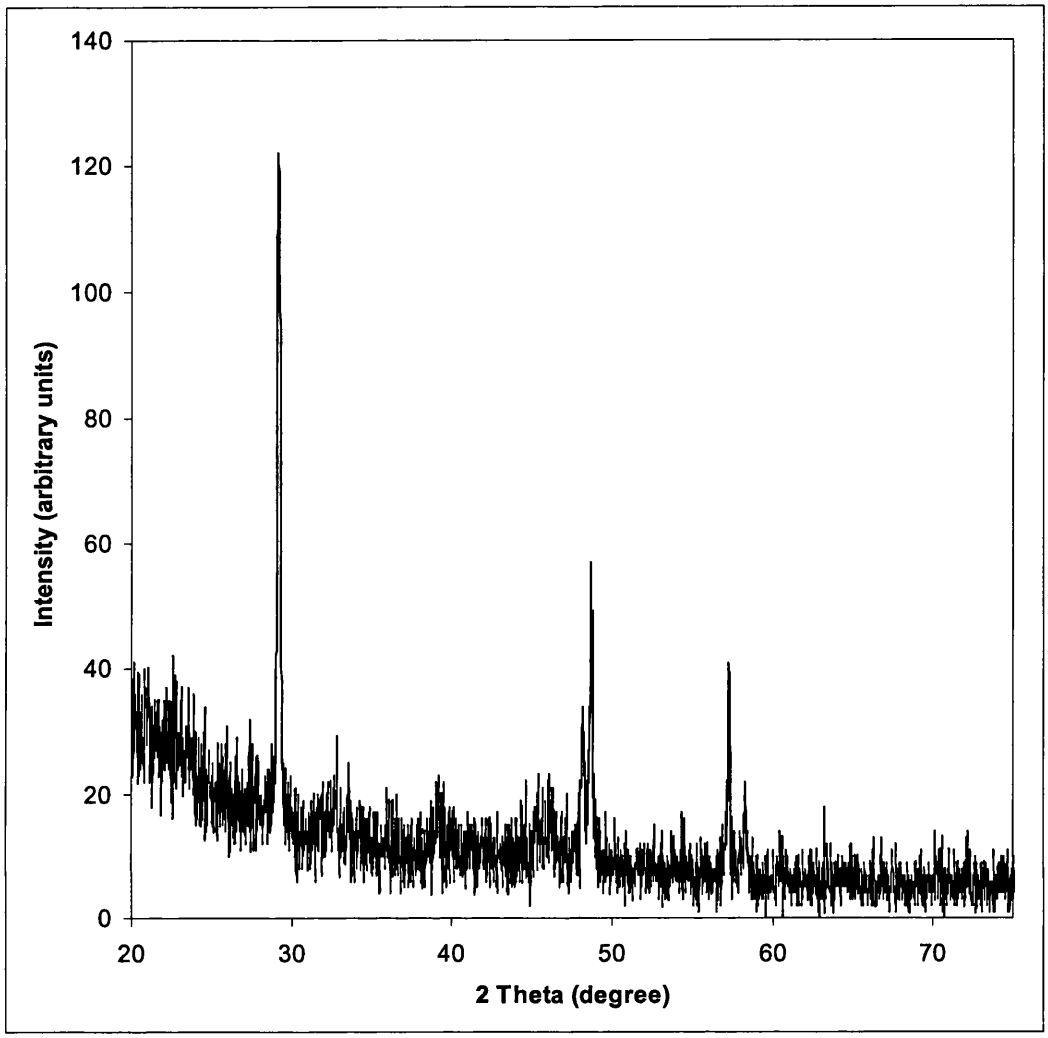

Fig. 4-8 XRD pattern for $CuGaS_2$ from $CuCl_2$.

EDAX data for the products from the gallium reactions showed that most of them consisted of a mixture of 1:1:2 Cu:Ga:S, 1:1 Cu:S and 1.75:1 Cu:S (digenite). The product from $CuCl_2$ was the best result with the highest proportion of $CuGaS_2$, but it still had a deficit of gallium.

4.2.5 Different Liquids:

The synthesis of $CuInS_2$ by liquid-mediated metathesis according to Eq. 4-2 was carried out in a number of different liquids in addition to toluene. The different liquids

used and their boiling points are listed in Table 12.

Table 12 Various liquids and their boiling points.

Liquid	**Boiling Point (°C)**
Ether	34
Dichloromethane (DCM)	40
Tetrahydrofuran (THF)	65-67
Hexane	68-70
Benzene	80
Triethylamine (TEA)	89
Toluene	110
Pyridine	115

The reactions were carried out by the same method employed for the toluene reaction described in section 4.2.1 with the difference being that the reaction was carried out at the boiling point of each liquid to achieve refluxing. Among all the liquids no obvious differences in the reaction progress was observed except for the reaction with pyridine. When $CuCl_2$ was added to pyridine the liquid changed immediately to a deep green colour. After reaction the liquid was found to be colourless, and there appeared to be no significant effect on the final product when compared to the reference toluene reaction.

XRD data for the product from toluene, before annealing, showed the sample to contain $CuInS_2$, with no evidence for the presence of binary CuS. The unannealed product from pyridine also showed only $CuInS_2$ with shorter and wider peaks than observed for toluene. This indicates a slightly smaller average particle size for the pyridine product. The XRD for the products from benzene and triethylamine showed patterns with small, short peaks which corresponded to those for $CuInS_2$, but exact identification of the product was not possible due to the weakness of the pattern. This could indicate that $CuInS_2$ is formed in the reaction but that it is poorly crystallised. All

the products from the lower boiling-point liquids showed amorphous patterns. XRD data for all the products after annealing showed that they consisted of solely $CuInS_2$.

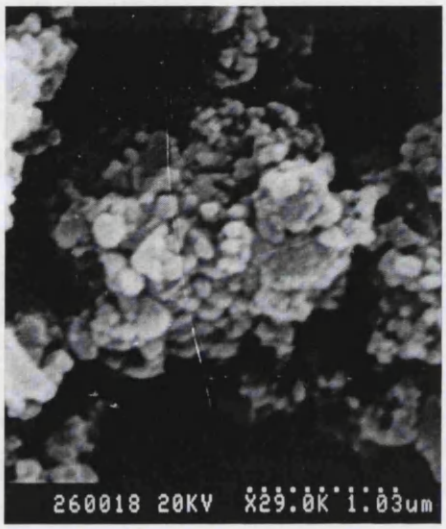

Fig. 4-9 SEM of $CuInS_2$ from pyridine, annealed.

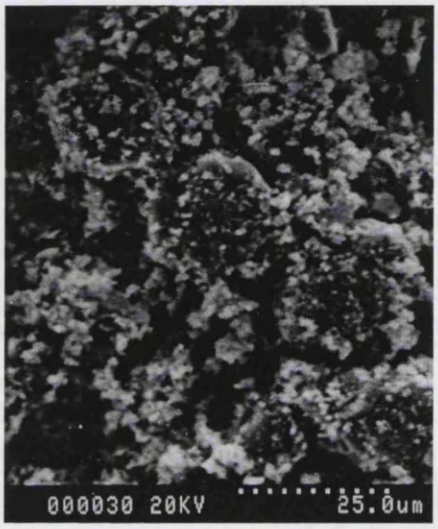

Fig. 4-10 SEM of $CuInS_2$ from DCM, annealed.

(Note scale difference).

EDAX data for the product from pyridine showed it to contain a 1:1:2 ratio of Cu:In:S both before and after annealing, with no evidence for any other stoichiometries. EDAX data for the products from benzene and triethylamine also showed a majority of 1:1:2 Cu:In:S with the benzene sample showing some evidence for the presence of a phase containing only indium and no copper or sulphur. The lower boiling-point liquids gave products which were not phase pure, containing a mixture of $CuInS_2$ and CuS. The lower the boiling point of the liquid used, the higher the proportion of CuS seen in the sample. EDAX data for the products after annealing showed them to contain solely of $CuInS_2$. Figs. 4-9 & 4-10 show SEM photos for $CuInS_2$ after annealing from pyridine and DCM, respectively.

4.2.6 Different Treatments:

The effect of various reaction and post-reaction processing conditions on the final product was explored in relation to the reaction shown in Eq. 4-2. Such factors as reaction temperature, reaction time and annealing time and temperature were explored.

The liquid-mediated metathetical synthesis of $CuInS_2$ from $CuCl_2$ in toluene was attempted without providing external heat, that is, the reaction was performed with stirring only, of the suspended reactants, at room temperature. The product from this reaction was seen by XRD to consist of CuS (covellite) and $In(OH)_3$. The presence of $In(OH)_3$ was found after washing with ethanol and water. Evaporation of the water washings left behind NaCl. Annealing of the CuS and $In(OH)_3$ mixture produced $CuInS_2$ (Fig. 4-11)..

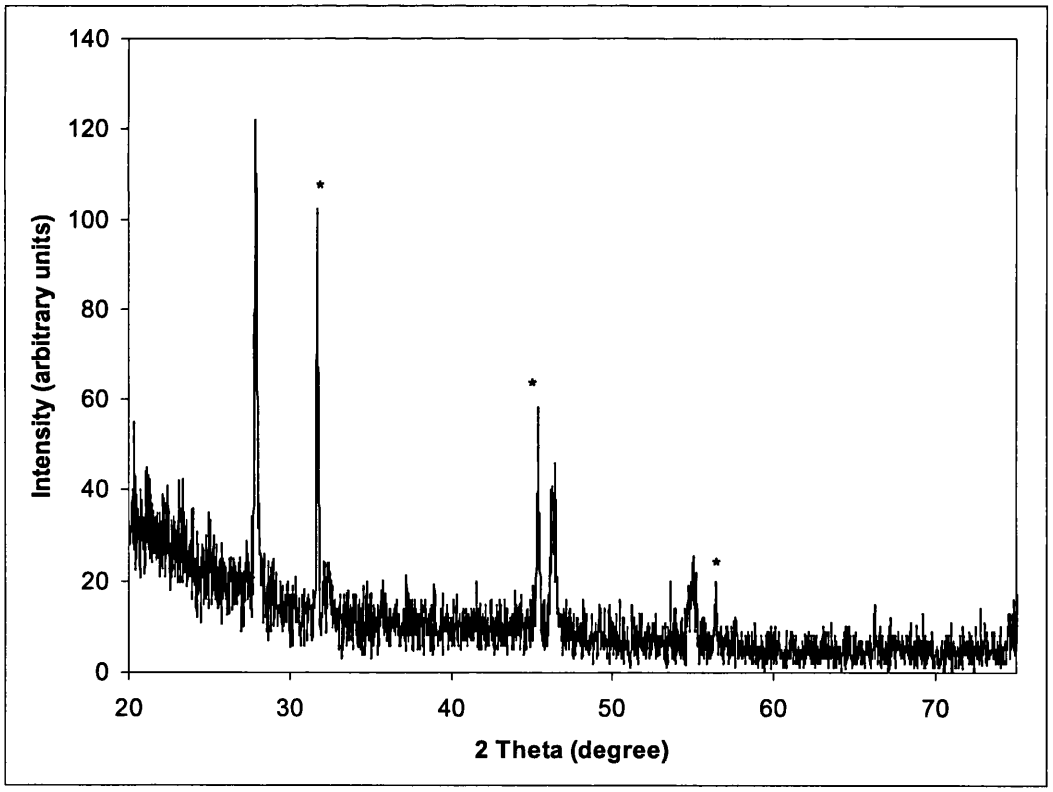

Fig. 4-11 XRD of $CuInS_2$ from room-temperature reaction, annealed. * = NaCl.

The liquid-mediated metathetical synthesis of $CuInS_2$ from $CuCl_2$ in toluene was performed with varying durations. Reaction durations of 2, 6, 12 and 24 hours were

used as well as the standard 48-hour duration. The shortest reaction time gave an XRD spectrum which showed a weak pattern of CuS, while at the 6-hour mark there is evidence for the presence of CuS and some $CuInS_2$. After 12 hours there is still evidence for the presence of CuS and $CuInS_2$ with the proportions being reversed in favour of the ternary phase. After 24 hours there is only $CuInS_2$ seen in the XRD spectrum. EDAX data for the above reactions mirror the findings from XRD, with the shorter time reactions showing spots of 1:1 Cu:S and spots of high indium content. As the reaction time is increased there are more and more spots with a 1:1:2 ratio of Cu:In:S.

The effect of annealing temperature and time-scale on the product crystallinity was also explored. Annealing at 200°C for 1 hour produced a product which showed very little difference from the product before annealing. Increasing the temperature to 500°C had a marked effect on the crystallisation of the product. Annealing for as short a time as 5 minutes produced a distinct crystalline pattern of $CuInS_2$ (Fig. 4-12).

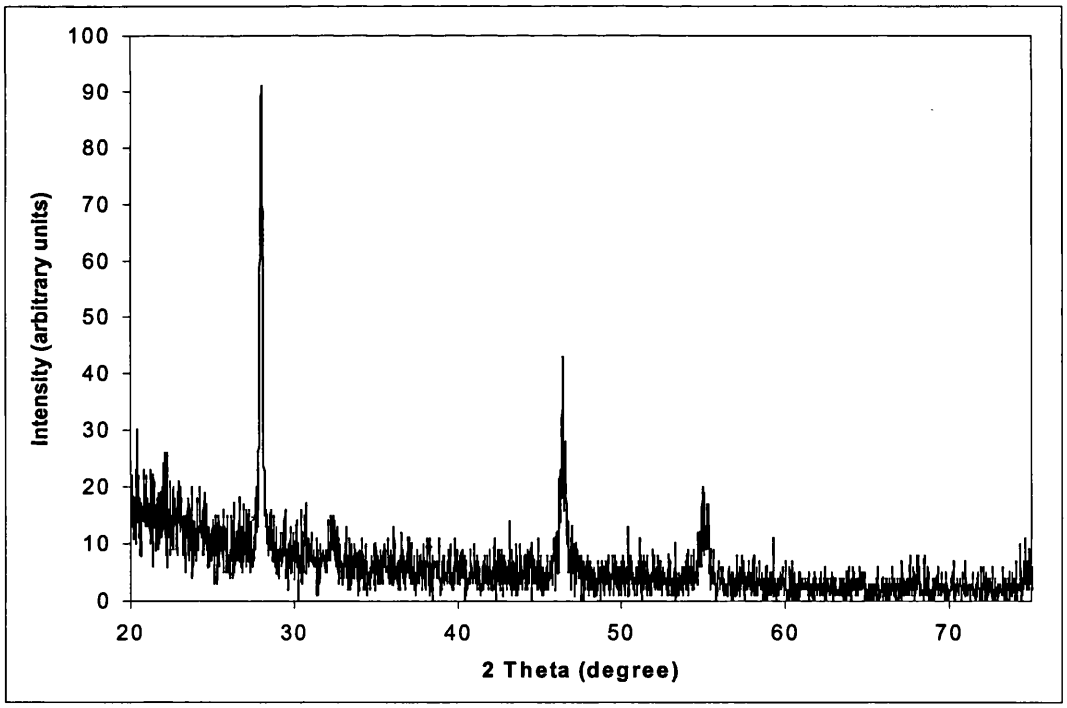

Fig. 4-12 XRD of $CuInS_2$ annealed at 500°C for 5 min.

Further annealing at 500°C did not result in a marked increase in crystallinity, except perhaps slightly sharper peaks and better separation of adjacent peaks.

4.3 *Discussion:*

4.3.1 *Different Liquids:*

Substituting different liquids for toluene in the reaction to form $CuInS_2$ seemed to have no obvious liquid-specific effect on the composition of the product. The products that resulted from the use of the different liquids were all either $CuInS_2$ or a combination of $CuInS_2$ and CuS. It seems quite clear that the differences in the product composition with the different liquids can be correlated to the boiling point of the liquid, and thus the temperature of reaction for each liquid. The two lowest boiling point liquids (Ether, 34°C; DCM, 40°C) contained mostly CuS (covellite) and some $CuInS_2$, while those with intermediate boiling points (THF, 65-67°C; Hexane, 68-70°C) contained more $CuInS_2$ than CuS. Once those liquids with boiling points in the 80°C region (Benzene, 80°C; Triethylamine, 89°C) are reached the product consists of $CuInS_2$ only. The highest boiling point liquids used (Toluene, 110°C; Pyridine, 115°C) also produced solely $CuInS_2$. The main difference between the last two sets of liquids is that the higher boiling point liquids yield products which are slightly more crystalline in the as-synthesised state.

Within each pair of liquids of similar boiling points there is one liquid which is polar or has an active group which has lone pairs and capable of binding or coordinating to metal groups, and one which is non-polar. Within each pair of liquids the main difference between the products is seen in the SEM micrographs of the products. The liquid with the polar or coordinating group produced a product with particle sizes slightly smaller than those from the non-polar liquid. The difference becomes more apparent as the temperature of the liquids increase.

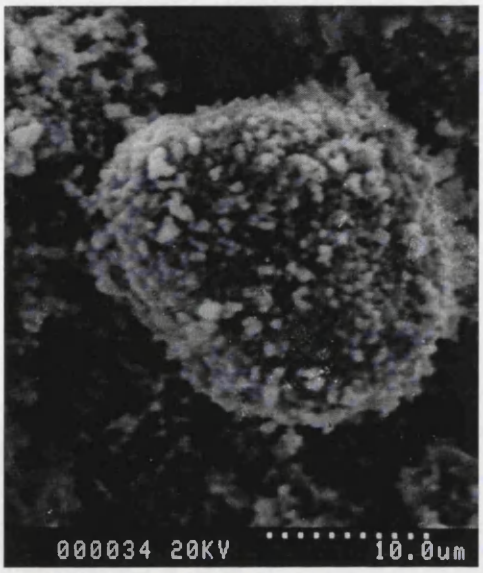

Fig. 4-13 SEM of $CuInS_2$ from ether. *(Note scale difference).*

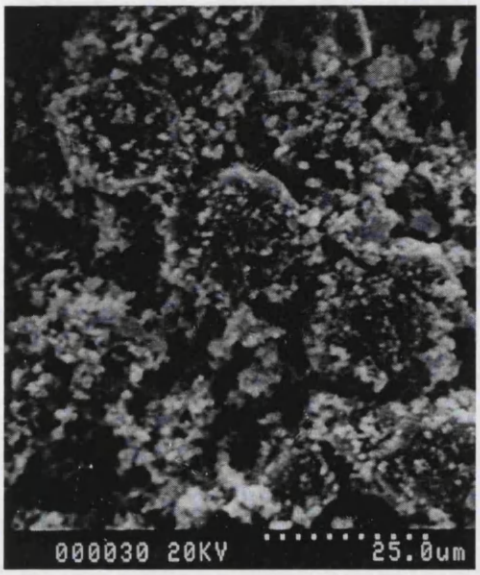

Fig. 4-14 SEM of $CuInS_2$ from DCM.

Figs. 4-13 & 4-14 show the difference between the product from ether and dichloromethane, respectively. One can see that the products consists of large agglomerates on which one can see very fine surface features, which correspond to individual crystallites. The difference between these two liquids is not particularly striking but one can see that the agglomerate is slightly smaller and the surface features appear smaller in the ether sample.

Fig. 4-15 SEM of $CuInS_2$ from THF. *(Note scale difference).*

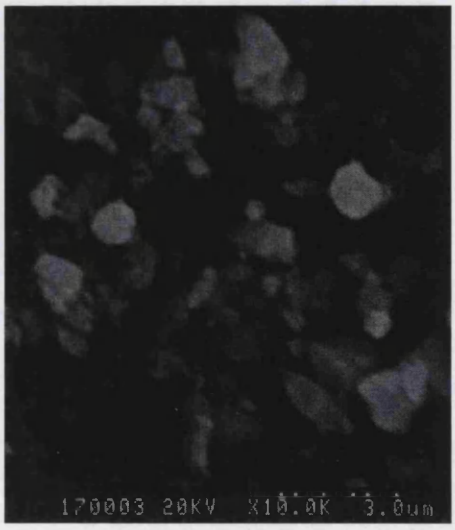

Fig. 4-16 SEM of $CuInS_2$ from hexane.

Figs. 4-15 & 4-16 show the difference between the product from THF and hexane, respectively. One can see that the product from THF consists of sub-micron particles with a relatively high uniformity. The hexane sample shows a wider particle-size range with many of them in the 1.5-2 micron particle range.

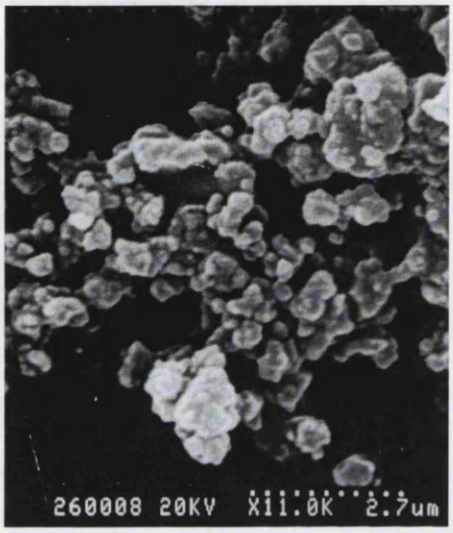

Fig. 4-17 SEM of $CuInS_2$ from toluene.

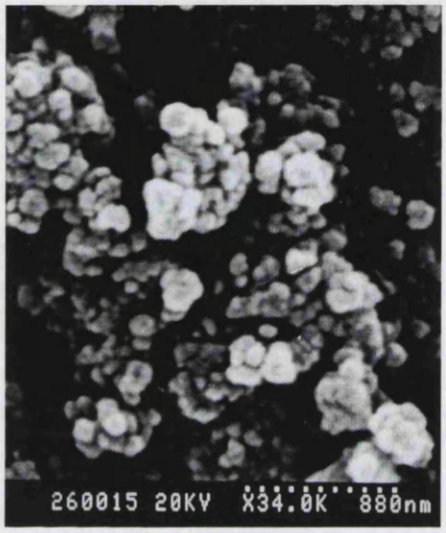

Fig. 4-18 SEM of $CuInS_2$ from pyridine.

(Note scale difference).

Figs. 4-17 & 4-18 show the difference between the product from toluene and pyridine, respectively. One can see that the product from pyridine consists of very small, uniform particles of approximately 100 nm diameter, agglomerated into slightly larger groups. The toluene sample shows a different morphology of agglomerates, many of them in the 1.5-2 micron particle range.

The dependance of both individual crystallite and agglomerate behaviour on the liquid used can be partially seen from the reactions carried out in toluene and pyridine. These two liquids have similar boiling points (110°C *vs.* 115°C) and therefore the difference in reaction temperature is not likely the major factor in the difference found between the products. The major difference seen is therefore likely to be the result of the lone pair found on pyridine.

Similar observations by other groups on the effect of various liquids were discussed in the introductory chapter. Kher and Wells found that, in the synthesis of GaAs and GaP, when substituting 1,4-dioxane for toluene that no noticeable change in particle size was observed but when using flexible multidentate liquids such as mono- or diglyme, there was a noticeable particle size reduction.[13] Another group performed the reaction of $SnCl_4$ and Na_2S in an autoclave at 150°C in toluene and THF.[16] They found that even the monodentate THF had the effect of reducing the crystallinity of the product.

A third group of researchers report that in their synthesis of $CuInSe_2$ from elemental selenium, $CuCl_2 \cdot 2H_2O$ and $InCl_3 \cdot 4H_2O$ that the product in diethylamine at 180°C for 36 hours has similarly sized spherical particles as toluene at 110°C.[117] In pyridine they only found copper selenide, indium selenide and elemental selenium, while ethylenediamine gave 5x50 μm needle crystals. According to the authors, the added bidentate functionality of the diamine forced a different crystal growth orientation. They selected the use of alkylamines for their strong basicity, strong chelating ability and their ability to absorb the excess heat of the reaction. Toluene was chosen specifically for its weak polarity and its lack of reactivity. The authors explain that the use of elemental selenium was made possible by the reactivity of the amine. Firstly, it allowed the selenium to dissolve and secondly, selenium undergoes a nucleophilic attack by the amine to activate it to further reaction.

Within the resolution range possible for scanning electron microscopy (SEM) it is possible to observe directly that the agglomerates of the products are distinctly different (Figs. 4-17 & 4-18). To truly observe any particle size difference among individual crystallites it would be necessary to utilise the greater resolution of transmission electron microscopy (TEM).

4.3.2 Reaction Pathway:

An interesting parallel to this temperature-dependent product composition is seen in the liquid-mediated reaction using toluene but supplying no external heat. The product from this reaction was CuS only. This shows that the temperature of reaction is crucial in promoting the further conversion of the binary sulphide and indium compound into the ternary $CuInS_2$. (After washing the presence of $In(OH)_3$ was also detected, but the exact form of indium in the product before washing was not determined). This is also supported by the observation that regardless of the liquid or temperature employed, or of intermediate products found, after annealing all the products were found to be ternary $CuInS_2$.

The reactions in which the duration of reaction was limited from 2 to 24 hours also shows that this conversion requires a certain period of time to go to completion. Until approximately 12 hours into the reaction, the main product found is CuS, after which time there is found a higher and higher proportion of $CuInS_2$ until about 24 hours of reaction, when there appears to be only $CuInS_2$ present.

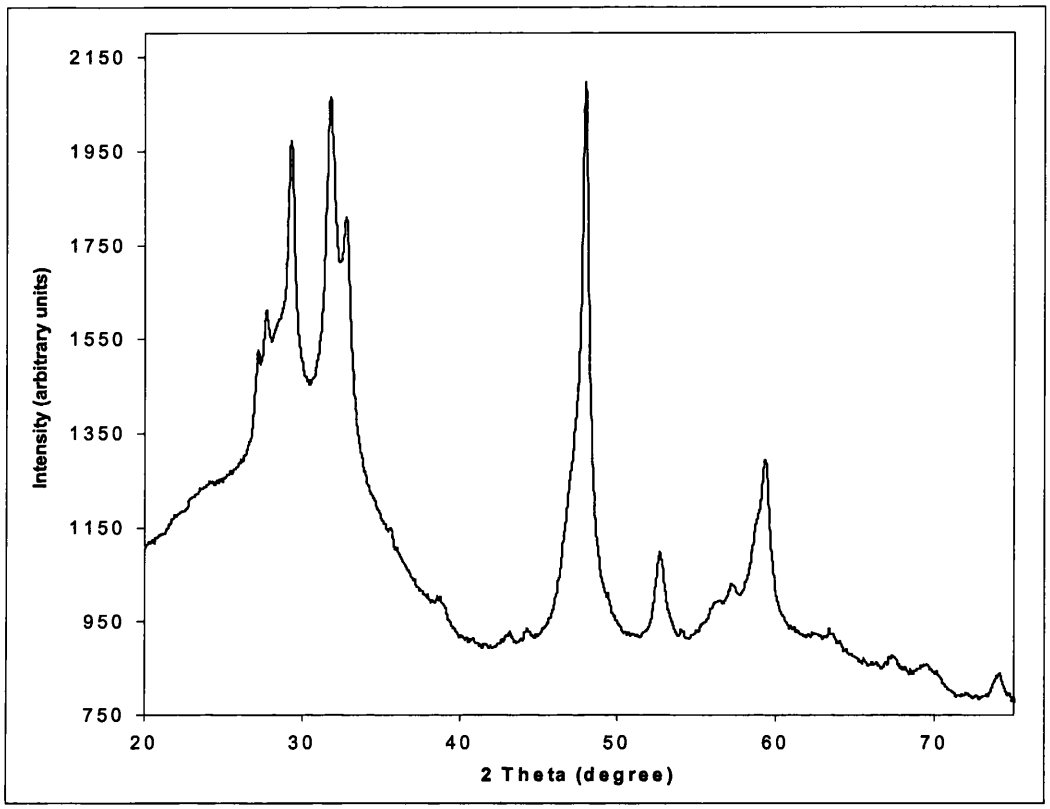

Fig. 4-19 XRD of $CuGaS_2$ unannealed, showing CuS (covelite) only.

In the case of the formation of $CuGaS_2$, the intermediate compound appears to be $Cu_{1.765}S$ (digenite) when CuBr is used and CuS (covelite) when $CuCl_2$ is used (Fig. 4-19). This means that the copper halide does not change oxidation state when it reacts with Na_2S to form the intermediate binary copper sulphide. The oxidation state change must therefore happen when the binary copper sulphide reacts with the gallium-containing compound at the later stage in the reaction. After annealing CuGaS2 is formed (Fig. 4-20). This may well also be the case with the $CuInS_2$ reactions described above (shorter reaction times and the room temperature reaction), but since only $CuCl_2$ was employed as the copper precursor, only CuS as the binary intermediary would naturally be found.

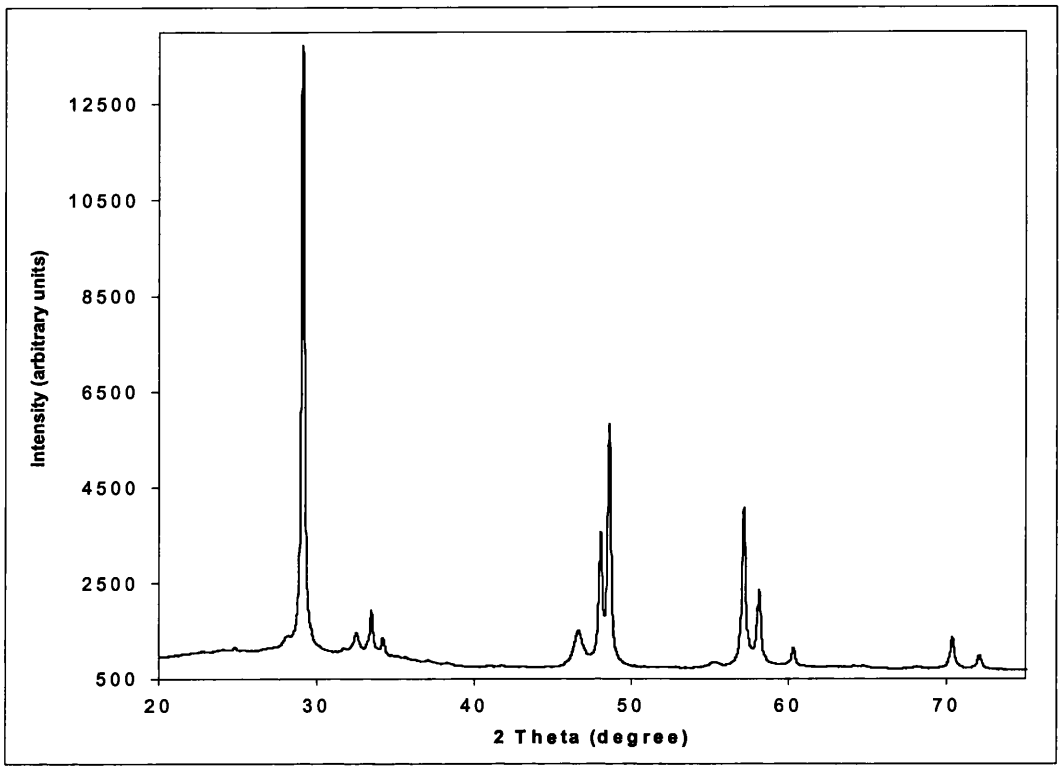

Fig. 4-20 XRD of $CuGaS_2$ after annealing.

Therefore, through the data found for the reactions using different liquids and that of toluene at room temperature, it can be seen that the reaction discussed passes through a distinct copper sulphide binary intermediary as well as some form of indium-containing compound, which with both time and heating eventually convert into the ternary product, $CuInS_2$.

4.3.3 Solid-State vs. Liquid-Mediated Metathesis:

For each reaction of the synthesis of $CuInE_2$ (E = S, Se, Te) both the liquid-mediated and solid-state metathesis methods were applied. The two methods are remarkably different in their conditions and timescales, and therefore it should be expected that the products will show some significant differences. Solid-state metathesis proceeds with high temperature and fast reaction time while liquid-mediated metathesis follows proceeds with low temperature and longer reaction times. Despite these differences in reaction conditions, the final products from all the reactions to form

$CuInE_2$ (E = S, Se, Te) were the same, irregardless of which metathetical method used.

The main difference between the SSM and LMM products is in the particle morphology. The SSM sample showed particles with a variety of shapes and sizes. Most of the particles were in the 5-15 μm diameter range and of a rounded, roughly spherical shape. In addition to these, there were also seen some particles with flat faces and sharp angles, as well as some very large particles of 50 to 100 μm in diameter (See Fig.4-22). The LMM sample showed particles which were uniformly rounded and near-spherical, with 1-2 μm diameters. (See Fig. 4-21). In both SEM micrographs there can also be seen very small, irregular particles scattered around and on the surface of the larger particles. These may correspond to individual crystallites in the nanometer size-scale.

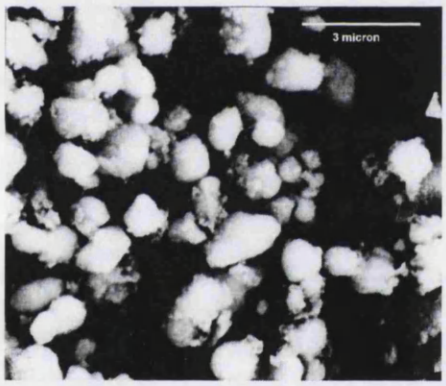

Fig. 4-21 SEM of $CuInS_2$ from toluene, annealed

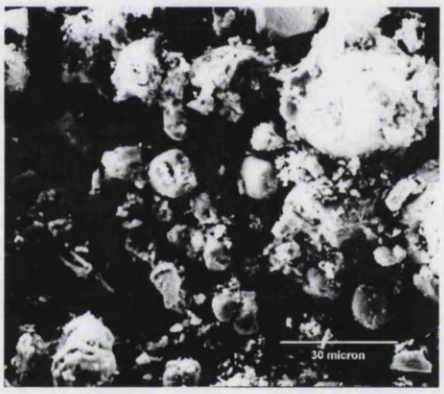

Fig. 4-22 SEM of $CuInS_2$ by SSM

(Note scale difference).

The reason for this marked difference in particle morphology between the two methods is not at first sight obvious. It should be remembered that both samples have been through a similar annealing treatment. The liquid-mediated sample was annealed at 500°C for 48 hours after being washed and dried. The solid-state sample has, in effect, also been annealed for the same period of time since that is the duration that the reaction was left in the furnace. The difference then is due to the reaction conditions themselves. The LMM product, before annealing, consists of smaller particles than those obtained in

the SSM reaction. The process of annealing the LMM product does not increase the size of the particles significantly, instead it simply seems to increase the crystallinity of the particles without causing undue particle growth. This leads to the conclusion that the heat-dissipating ability of the liquid in LMM reactions keeps the particle size of the product from becoming overly large by keeping the excess heat of the reaction from contributing to particle growth. In SSM reactions this heat is in direct contact with the reaction mixture and must contribute to particle growth.

Another difference in the two methathesis methods is the time needed for the reaction to go to completion. An SSM reaction was performed where the product was removed after only five minutes of reaction at 500°C and it was found to consist of fully crystalline $CuInS_2$ with no by-products. As was reported for the liquid-mediated reactions at least 24 hours were needed for the presence of binary intermediaries to subside and pure $CuInS_2$ to result. This shows a prominent difference in the reactions because of the different temperatures used in each method.

4.3.4 Halide Effect:

No direct analysis of the effect of the effect of the metal halide chosen was carried out within these experiments. However an interesting effect was noted with respect to the use of the two different halides employed. It should of course be borne in mind that the comparison is between CuBr and $CuCl_2$ and therefore the effect may also be obscured by or enhanced by the difference between Cu(I) and Cu(II). No effect on the product seems to be seen when comparing the use of bromide or chloride in liquid-mediated reactions, but there was an interesting effect with the solid-state reactions.

The EDAX data for the products which were synthesised with CuBr seemed to show more variable results, than those synthesised from $CuCl_2$. This means that the variability in the atomic ratios could be larger or that the product contains small amounts of binary side-products. This effect is observed for $CuInS_2$ and $CuInSe_2$, but not for

$CuInTe_2$. The cause of this increased level of undesired by-products could be attributed to two possible reasons. The first is that bromide being larger than chloride, the diffusion of these two elements through the reaction mass will be different. It could be that the slower diffusion rate of bromide is enough to retard the reaction enough to promote the continued existence of binary by-products or to cause the ternary product to have slightly varying ratios of elements in it. This diffusion cause would also explain that the effect is not observed in the liquid-mediated reaction. A second, and related, reason could be that in the reactions containing CuBr, the indium precursor is $InCl_3$, which means that the co-produced salt will be $NaCl_{0.75}Br_{0.25}$. This mixed-halide sodium salt may be more difficult to form due to the presence of the two different-sized halides. This may in turn produce less energy and result in the presence of by-products. It is ironic how the "non-stoichiometric" $CuCl_2$ reactions (see Eq. 4-2) provide a cleaner EDAX result when compared to the similar CuBr reaction, because Cu(II) has to convert to Cu(I) before going on to form $CuInS_2$ and there is a theoretical excess mole of sulphur per 2 moles of $CuInS_2$.

4.3.5 Gallium Reactions:

It became apparent in the gallium reactions that $GaCl_3$ behaved quite differently from $InCl_3$ in the reactions of this chapter. First of all $GaCl_3$ is very soluble in toluene, which $InCl_3$ is not. Also, because of its reputation for being particularly sensitive to air and moisture, it was placed in the Schlenk flask in a glove-box, then taken out and the toluene syringed on top of this. There then remained the option of whether to add the Na_2S next or the copper halide. Both methods of addition were used, and there seemed to be no reaction between the dissolved $GaCl_3$ and Na_2S when these were added to each other at room temperature. The order of addition didn't seem to affect the product outcome significantly.

The gallium reactions required much more careful handling of the reaction

preparation. The first attempt with CuBr resulted in a product which lacked completely in gallium. The product from $CuCl_2$ did contain gallium but scattered through the sample in varied amounts. The gallium compound may have been exposed to air and decomposed or it may have been that the solubility of $GaCl_3$ in toluene affects its reactivity. Repeating the experiment under stricter conditions then resulted in much better results with the $CuCl_2$ product being completely $CuGaS_2$, but the product from CuBr still contained some $Cu_{1.765}S$ (digenite). There are two possible reasons for the sensitivity seen in the gallium reactions: One which was mentioned earlier is that $GaCl_3$ is known to be more sensitive to moisture and air exposure and that careless handling will cause it to decompose and that washing of the samples supposedly also washes away the gallium-containing component.

A second possibility is that the solubility of $GaCl_3$ in toluene affects the energetics of the reaction. It was discussed in Chapter 2 that the solubility of $AsCl_3$ may have been responsible for the inability to form As_2S_3, and that the energetics of a reaction with dissolved species were different from those with suspended reactants. It was seen that $CuInS_2$ reactions proceeded *via* a CuS intermediary which then reacted with the indium reactant to form the ternary compound. There was evidence for the existence of binary intermediaries in the gallium reactions as well. If the assumption is made, therefore, that the gallium reactions also proceed *via* a binary intermediary, then it could be that either the rate or the endpoint of reaction of the binary copper sulphide with gallium chloride is affected by the gallium reactant being dissolved. Whatever the reasons for the differences between the different attempts, it is clear that the use of $GaCl_3$ leads to reactions that are more finicky than the corresponding indium reactions.

4.4 Experimental:

The experimental procedure for the reaction of $CuCl_2$ and $InCl_3$ with Na_2S is given below. All other reactions, including those involving Na_2Se and Na_2Te, followed a similar procedure with similar amounts and ratios of reactants. Reactions were for the most part based on 0.100-0.200 g amounts of the sodium chalcogenide and the metal halide amount was calculated accordingly. The order of addition of the reactants and the reaction conditions were also similar for all the reactions presented.

$CuCl_2$ (1.19 mmol) and $InCl_3$ (1.04 mmol) were ground together with a mortar and pestle inside an inert atmosphere glovebox. Na_2S (2.56 mmol) was ground separately. The Na_2S was placed in a schlenk flask to which was added 20 ml of dried degassed toluene using Schlenk line techniques to avoid exposure to either air or moisture. The halide mixture was added with stirring, and the reaction mixture was heated to *ca.* 110°C under nitrogen flow. Once the temperature had stabilised, the flask was sealed and allowed to reflux and stir for 48 hours. The resulting slurry was allowed to settle and the toluene was taken off by cannula. The solid was washed with 2 x 20 ml ethanol or methanol, followed by 2 x 20 ml deionized water, and finally by 2 x 20 ml ethanol or methanol. The powder was then pumped to dryness under vacuum. The powder was then collected and stored in air. The resulting ethanol, methanol and water washings were evaporated to identify any sodium halide species.

5. *Conclusions:*

This thesis has dealt with the family of reactions that is called metathesis reactions. More specifically, this thesis has, for the most part, looked at liquid-mediated solid-state metathesis reactions. This is meant to describe the reactions as fully yet as succinctly as possible. Two, or more, solids are placed in a liquid in which neither dissolve and are allowed to react. There is some similarity to pure solid-state reactions but with the diluting effect of the liquid becoming the dominant factor in terms of heat limitation, particle separation and redistribution.

Various aspects of these reactions have been uncovered. Firstly, and perhaps surprisingly, most of the reactions do go to completion. Based on most of the previous literature in this area, solubility of one or more of the reactants has been seen as crucial to the success of these reactions. As has been discovered, there must be an alternative mechanism which allows the reaction to proceed. Whether this is due to partial solubility of the reactants or some other mechanism which acts through the fleeting impact and friction of the particles as they swirl in suspension, is not known.

Compared to pure solid-state reactions, liquid-mediated reactions proceed at a much slower rate and a much lower temperature. This contributes to the differences seen in the products found in these reactions. Low-temperature phases and metastable phases can become accessible because they do not decompose at the temperatures employed. Conversely, the lower temperatures may not allow certain reactions to go to completion and lead to mixed or incomplete products, particularly in transition metal reactions.

Reaction duration and temperature were found to be crucial to these reactions. The example of ternary $CuInS_2$ illustrates this particularly: At lower temperatures only CuS is obtained and at higher temperatures only $CuInS_2$ is obtained. The proper durations is also required even at the right temperature. Reaction times longer than 24 hours were required to obtain pure $CuInS_2$. Many of these reactions must be operating on the threshold of being exothermic or endothermic. For example CuS can form from

$CuCl_2$ and Na_2S with stirring alone at room temperature, while $CuInS_2$ requires a temperature of at least 80-90°C to proceed. Likewise, AgF and Na_2S will form Ag_2S in less than 8 hours while $CuInS_2$ needed at least 24 hours.

Most of the products are X-ray amorphous in the as-synthesised state and there have been shown interesting possibilities for the systematic and deliberate crystallisation of the product to any desired crystal size. Annealing can also be used to selectively convert a low-temperature phase into a higher-temperature phase as was seen with HgS converting from the black metacinnabar to the red cinnabar. Likewise, the product agglomerate size is significantly reduced both before and after annealing. This could have important implications for any further uses of the product, in such applications as powder metallurgy, ceramic sintering or any other applications where smaller particle sizes are desired, for physical or electronic reasons.

Liquid-mediated metathesis reactions are also easier to perform on a larger scale than solid-state metathesis reactions. They are also, arguably, safer than either solid-state metathesis reactions, which entail the risk of explosion and very high heats, or of reactions using the volatile and dangerous chalcogenide or pnictide gases.

In conclusion, these reactions have offered, and will continue to offer, a very interesting field of research and study. The little that is known about this family of reactions has proven fascinating and fruitful. Either further study into the variety of reactions possible or deeper study into a particular reaction, would be fruitful endeavours.

6. *References:*

[1] P. B. Avakyan, M. D. Nersesyan, A. G. Merzhanov, *Am. Ceram. Soc. Bull.*, 1996, **75**, 50.

[2] M. D. Aguas, L. Affleck, I. P. Parkin, M. V. Kuznetsov, W. A. Steer, Q. A. Pankhurst and L. F. Barquin, *J. Mater. Chem.*, 2000, **10**, 235.

[3] E. G. Gillian and R. B. Kaner, *Chem. Mater.*, 1996, **8**, 333.

[4] D. W. Richerson, Modern Ceramic Engineering, 2nd ed., (New York, NY: Marcel Dekker, 1992).

[5] P. R. Bonneau, R. F. Jarvis and R. B. Kaner, *Nature*, 1991, **349**, 510.

[6] R. E. Treece, G. S. Macala, L. Rao, D. Franke, H. Ekert and R. B. Kaner, *Inorg. Chem.*, 1993, **32**, 2745.

[7] P. R. Bonneau, R. F. Jarvis and R. B. Kaner, *Inorg. Chem.*, 1992, **31**, 2127.

[8] I. P. Parkin, *Chem. Soc. Rev.*, 1996, **25**, 199.

[9] Artur Nartovski, Personal Communication.

[10] D. Franke, H. Eckert, R. B. Kaner and R. E. Treece, *Anal. Chim. Acta*, 1993, **283**, 987.

[11] R. R. Chianelli and M. B. Dines, *Inorg. Chem.*, 1978, **17**, 2758.

[12] M. Müllenborn, R. F. Jarvis, B. G. Yacobi, R. B. Kaner, C. C. Coleman and N. M. Haegel, *Appl. Phys. A*, 1993, **56**, 317.

[13] S. S. Kher and R. L. Wells, *Chem. Mater.*, 1994, **6**, 2056.

[14] R. L. Wells and J. F. Janik, *Eur. J. Solid State and Inorg. Chem.*, 1996, **33**, 1079.

[15] L. I. Halaoui, S. S. Kher, M. S. Lube, S. R. Aubuchon, C. R. S. Hagan, R. L. Wells and L. A. Coury, *Nanotech.*, 1996, **622**, 178.

[16] X. F. Qian, X. M. Zhang, C. Wang, W. Z. Wang, Y. Xie and Y. T. Qian, *J. Phys. Chem. Solids*, 1999, **60**, 415.

[17] X. F. Qian, X. M. Zhang, C. Wang, K. B. Tang, Y. Xie and Y. T. Qian, *J. Alloys Comp.*, 1998, **278**, 110.

[18] X. F. Qian, X. M. Zhang, C. Wang, Y. Xie and Y. T. Qian, *Inorg. Chem.*, 1999, **38**, 2621.

[19] X. F. Qian, Y. Xie, Y. T. Qian, X. M. Zhang, W. Z. Wang and L. Yang, *Mat. Sci. Eng. B*, 1997, **49**, 135.

[20] X. F. Qian, X. M. Zhang, C. Wang, W. Z. Wang and Y. T. Qian, *Mat. Res. Bull.*, 1998, **33**, 669.

[21] S. H. Yu, J. Yang, Y. S. Wu, Z. H. Han, J. Lu, Y. Xie, Y. T. Qian, *Mat. Res. Bull.*, 1998, **33**, 1207.

[22] X. M. Zhang, X. F. Qian, C. Wang, Y. Xie and Y. T. Qian, *Mat. Sci. Eng. B*, 1999, **57**, 170.

[23] S. H. Yu, J. Yang, Y. S. Wu, Z. H. Han, Y. Xie and Y. T. Qian, *Mat. Res. Bull.*, 1998, **33**, 1661.

[24] S. H. Yu, L. Shu, J. Yang, K. B. Tang, Y. Xie, Y. T. Qian and Y. H. Zhang, *Nanostr. Mat.*, 1998, **10**, 1307.

[25] W. Z. Wang, Y. Geng, P. Yan, F. Y. Liu, Y. Xie and Y. T Qian, *Inorg. Chem. Commun.*, 1999, **2**, 83.

[26] W. Z. Wang, Y. Geng, Y. T. Qian, C. Wang and X. M. Liu, *Mat. Res. Bull.*, 1999, **34**, 403.

[27] Y. D. Li, H. W. Liao, L. Q. Li and Y. T. Qian, *Mat. Chem. Phys.*, 1999, **58**, 87.

[28] R. A. Bley and S. M. Kauzlarich, *J. Am. Chem. Soc.*, 1996, **118**, 12461.

[29] C. S. Yang, R. A. Bley, S. M. Kauzlarich, H. W. H. Lee and G. R. Delgado, *J. Am. Chem. Soc.*, 1999, **121**, 5191.

[30] G. A. Shaw, Personal Communication.

[31] G. A. Shaw, Ph. D. Thesis, University College, University of London, Aug. 2000.

[32] A. Hector and I. P. Parkin, *J. Chem. Soc., Chem. Commun.*, 1993, **13**, 1095.

[33] A. L. Hector and I. P. Parkin, *Inorg. Chem.*, 1994, **33**, 1727.

[34] L. S. Price, I. P. Parkin, A. M. E. Hardy, R. J. H. Clark, T. G. Hibbert and K. C. Molloy, *Chem. Mater.*, 1999, **11**, 1792.

[35] R. Kobayashi, Y. Jin, F. Hasegawa, A. Koukitu and H.Seki, *J. Cryst. Growth*, 1991, **113**, 491.

[36] A. C. Jones, *Chem. Soc. Rev.*, 1997, **26**, 101.

[37] L. Butler, G. Redmond and D. Fitzmaurice, *J. Phys. Chem.*, 1993, **97**, 10750.

[38] R. A. Baldwin, E. E. Foos and R. L. Wells, *Mat. Res. Bull.*, 1997, **32**, 159.

[39] H. Weller, *Adv. Mater.*, 1993, **5**, 88.

[40] M. Brandebyge, J. Schiøtz, M. R. Sørensen, P. Stolze. K. W. Jacobsen, J. K. Nørskov, L. Olesen, E. Lægsgaard, I. Stensgaard and F. Besenbacher, *Phys. Rev. B*, 1995, **52**, 8499.

[41] P. Buffat, J.-P. Borel and R. L. Whetten, *Phys. Rev. A*, 1976, **13**, 2287.

[42] A. N. Goldstein, C. M. Echer and A. P. Alivisatos, *Science*, 1992, **256**, 1425.

[43] R. W. Siegel, *Phys. Today*, 1993, **Oct.**, 64.

[44] M. J. Mayo, R. W. Siegel, Y. X. Liao and W. D. Nix, *J. Mater. Res.*, 1992, **7**, 973.

[45] K. L. Lewis, J. A. Savage, K. J. Marsh and A. P. C. Jones, "New Optical Materials", *Proc. SPIE-Int. Soc. Opt. Eng.*, 1983, **400**, 21.

[46] C. Y. Yeh and C. Sarini, U.S. Patent 4,560,804.

[47] B. T. Kilbourne, A Lanthanide Lanthology - Part 1, (White Plains, NY: Molycorp Inc., 1993).

[48] A. Bornstein and R. Reisfeld, *J. Non-Cryst. Solids*, 1982, **50**, 23.

[49] B. R. Pamplin, J. L. Shay and J. H Wernick, Eds., Science of the Solid State, Vol. 7: Ternary Chalcopyrite Semiconductors: Growth, Electronic Properties and Applications, (Oxford: Pergamon Press, 1975).

[50] Y. F. Nicolau, M. Dupuy and M. Brunel, *J. Electrochem. Soc.*, 1990, **137**, 2915.

[51] P. O'Brien and A. Ryoki, *J. Mater. Chem.*, 1995, **5**, 1761.

[52] N. N. Greenwood and A. Earnshaw, Chemistry of the Elements, (New York, NY: Pergamon, 1984).

[53] M. A. Hasse, J. Qiu, J. M. DePuydt and H. Cheng, *Appl. Phys. Lett.*, 1991, **59**, 1272.

[54] A. G. Stanley, "Cadmium Sulphide Solar Cells", in Applied Solid State Science 15, R. Wolfe, Ed., (New York, NY: Academic Press, 1975).

[55] A. Yoshikawa, S. Yamaga, K. Takanaka and H. Kasai, *J. Cryst. Growth*, 1985, **72**, 13.

[56] J. P. Singh and R. K. Bedi, *Thin Solid Films*, 1991, **199**, 9.

[57] A. Ortiz, J. C. Alonso, M. Garcia and J. Toriz, *Semicond. Sci. Tech.*, 1990, **137**, 2915.

[58] I. Fielder and M. Bayard, Artist's Pigments, a Handbook of their History and Characteristics, Vol. 1, R. L. Feller, ed., (Cambridge: Cambridge University Press, 1986).

[59] Inger Ekvall, Personal Comunication.

[60] PDF-2 Database, 1990, International Centre for Diffraction Data, Swarthmore, PA 19081.

[61] M. G. Bawendi, A. R. Kortan, M. L. Steigerwald and L. E. Brus, *J. Chem. Phys.*, 1989, **91**, 7282.

[62] A. R. West, Solid State Chemistry and its Applications, (Chichester: J. Wiley and Sons, 1992).

[63] J. C. Fitzmaurice and I. P. Parkin, *Main Group Met. Chem.*, 1994, **17**, 481.

[64] N. N. Greenwood and E. A. Earnshaw, Chemistry of the Elements, (Oxford: Pergamon Press, 1990).

[65] N. P. Novilov, I. P. Borovinskaya and A. G. Merzhanov, Combustion Processes in Chemical technology and Metallurgy, A. G. Merzhanov, ed., (Chernoglovka, 1975)

[66] R. J. Errington, Advanced Practical Inorganic Chemistry and Metalorganic Chemistry, (London: Chapman & Hall, 1997).

[67] J. B. Goodenough, *Prog. Solid State Chem.*, 1971, **5**, 149.

[68] C. N. R. Rao, *Annu. Rev. Phys. Chem.*, 1989, **40**, 291.

[69] (a) F. Hulliger, *Struct. Bonding*, 1968, **4**, 83. (b) J. B. Goodenough, *J. Solid State Chem.*, 1972, **5**, 144. (c) F. Hulliger, in Structure and Bonding in Crystals, M. O'Keefe and A. Navrotsky, Eds., (New York, NY: Academic Press, 1981).

[70] (a) N. E. Brese and M. O'Keeffe, *Struct. Bonding*, 1992, **97**, 307. (b) F. J. DiSalvo and S. J. Clarke, *Curr. Opinion Solid State Mater. Sci.*, 1996, **1**, 241.

[71] A. F. Wells, Structural Inorganic Chemistry, 5th ed., (Oxford: Clarendon Press, 1986).

[72] W. Jeitschko and D. J. Brown, *Acta Crystallogr.*, 1977, **B33**, 3401.

[73] (a) G. P. Meisner, *Physica B*, 1981, **108**, 763. (b) L. F. DeLong and G. P. Meisner, *Solid State Commun.*, 1985, **53**, 119.

[74] G. P. Meisner, M. S. Torikachvili, K. N. Yang, M. B. Maple and R. P. Guertin, *J. Appl. Phys.*, 1985, **57**, 3073.

[75] B. C. Seles, D. Mandrus and R. K. Williams, *Science*, 1996, **272**, 1325.

[76] Z. Dziewiecki and M. Jagiello, *Przem. Chem.*, 1989, **68**, 401.

[77] M. Yamamoto, K. Shirai and K. Hiramatsu, *Jap. J. Appl. Phys.*, 1991, **30**, L1036.

[78] R. Ranjan and S. Kaja, *J. Magn. Magn. Mater.*, 1989, **79**, 242.

[79] K. Lida, *J. Magn. Magn. Mater.*, 1983, **35**, 226.

[80] P. Trespaillebarrau and M. Suery, *Mater. Sci. Tech.*, 1994, **10**, 497.

[81] (a) H. G. von Schnering, in Encyclopedia of Inorganic Chemistry, R. B. King, Ed., (Chichester: John Wiley & Sons, 1994). (b) A. Kjekshus, *Acta Chem. Scand.*, 1971, **25**, 411. (c) A. Kjekshus, T. Rakke and A. F. Andersen, *Acta Chem. Scand.*, 1974, **28**, 996. (d) J. D. Smith, in Comprehensive Inorganic Chemistry, J. C. Bailar Jr., H. J. Emeléus, R. Nyholm and A. F. Trotman-Dickenson, Eds., (Oxford: Pergamon Press, 1973).

[82] H. C. Yi and J. J. Moore, *J. Mater. Sci.*, 1990, **25**, 1159

[83] A. L. Hector and I. P. Parkin, *Z. Naturforsch.*, 1994, **49b**, 477.

[84] H. G. von Schnering and W. Hönle, *Chem. Rev.*, 1988, **88**, 243.

[85] J. Gopalakrishnan, S. Pandey and K. K. Rangan, *Chem. Mater.*, 1997, **9**, 2113.

[86] A. Wold and D. Bellavance, in Preparative Methods in Solid State Chemistry, P. Hagenmuller, Ed., (New York, NY: Academic Press, 1972).

[87] W. M. Macdonald, C. L. Reynolds and A. C. Anderson, *Scripta Metall.*, 1981, **15**, 891.

[88] L. Thome, H. Bernas, P. Heubes, M. Diecher and E. Recknagel, *Nucl. Instrum. Methods, Phys. Res.*, 1982, **199**, 431.

[89] J. H. Hamlyn-Harris, D. H. St. John and D. K. Sood, *Mater. Sci. Eng. A*, 1991, **147**, 201.

[90] C. A. Ross, L. M. Goldman and F. Spaepen, *J. Electrochem. Soc.*, 1993, **140**, 91.

[91] U. Pitterman and S. Ripper, *Phys. Status Solidi A*, 1986, **93**, 131.

[92] M. Robbins, J. J. Hauser and J. T. Plewes, *J. Electrochem. Soc.*, 1986, **133**, C323.

[93] Y. Senzaki and W. L. Gladfelter, *Abstr. Papers Am. Chem. Soc.*, 1993, **133**, 27-INOR.

[94] F. R. Klingan, A. Miehr, R. A. Fischer and W. A. Hermann, *Appl. Phys. Lett.*, 1995, **67**, 822.

[95] P. S. Kumar and J. P. Nair, *J. Mater. Proc. Tech.*, 1996, **156**, 511.

[96] H. X. Li, H. Y. Chen, S. H. Dong, J. S. Yang and J. F. Deng, *Appl. Surf. Sci.*, 1998, **125**, 115.

[97] J. L. Shay and J. H. Wernik, Eds., Ternary Chalcopyrite Semiconductors: Growth, Electronics, Properties and Applications, (Oxford: Pergamon, 1976).

[98] J. Hedström, H. Ohlsen, M. Bodegård, A. Kylner, L. Stolt, D. Hariskos, M. Ruckh and H. W. Schock, in Proc. 23rd IEEE Photovoltaics Conf., (New York: IEEE, 1993).

[99] V. Nadenau, D. Braunger, D. Hariskos, M. Kaiser, C. Köble, A. Oberacker, M. Ruckh, U. Rühle, R. Schäffler, D. Schmid, T. Walter, S. Zweigart and H. W. Schock, *Prog. Photovolt.*, 1995, **3**, 363.

[100] J. R. Tuttle, M. A. Contreras, A. M. Gabor, K. R. Ramanathan, A. L. Tennant, D. S. Albin, J. Keane, R. Noufi, *Prog. Photovolt.*, 1995, **3**, 383.

[101] N. Kohara, T. Negami, M. Nishitani and T. Wada, *Jpn. J. Appl. Phys.*, 1995, **34**, L1141.

[102] Y. Yamaguchi, *J. Appl. Phys.*, 1995, **78**, 1476.

[103] A. Rockett and R. W. Birkmire, *J. Appl. Phys.*, 1991, **70**, R81.

[104] L. C. Yang, H. Z. Xiao, W. N. Shafarman and R. W. Birkmire, *Sol. Energy Mater. Sol. Cells*, 1995, **36**, 445.

[105] C. Guillen and J. Herrero, *Sol. Energy Mater.*, 1992, **23**, 31.

[106] K. Zwiebel, *Prog. Photovolt.*, 1995, **3**, 279.

[107] D. Cahen, G. Dagan, Y. Mirovsky, G. Hodes, W. Giriat and M. Lubke, *J. Electrochem. Soc.*, 1985, **132**, 1062.

[108] D. Suri, K. Napgal and G. Chadha, *J. Appl. Crystallogr.*, 1989, **22**, 578.

[109] L. Stolt, J. Hedström, J. Kessler, M. Ruckh, K. Velthaus and H. W. Schock, *Appl. Phys. Lett.*, 1993, **62**, 597; Y. Yamamoto, T. Yamaguchi, T. Tanaka, N. Tanahashi and A. Yoshida, *Sol. Energy Mater. Sol. Cells*, 1997, **49**, 399; Y. L. Wu, H. Y. Lin, C. Y. Sun, M. H. Yang and H. L. Hwang, *Thin Solid Films*, 1989, **168**, 113.

[110] C. C. Landry, J. Lockwood and A. R. Barron, *Chem. Mater.*, 1995, **7**, 699; S. P. Grindle, C. W. Smith and S. D. Mittleman, *Appl. Phys. Lett.*, 1979, **35**, 24; S. V. Krishnaswamy, A. S. Manocha and J. R. Szedon, *J. Vac. Sci. Tech., Part A*, 1983, **1**, 510; J. A. Thornton, T. C. Lommasson, H. Talieh and B. H. Tseng, *Sol. Cells*, 1988, **12**, 1.

[111] T. Isomura, T. Kariya and S. Shirakata, *Cryst. Res. Technol.*, 1996, **31**, 523; Y. D. Temburkhar, *Bull. Mater. Sci.*, 1997, **20**, 1011; R. Nomura, K. Kanaya and H. Matsuda, *Chem. Lett.*, 1988, 1849; A. N. Tiwari, D. K. Pandya and K. L. Chopra, *Thin Solid Films*, 1985, **130**, 217.

[112] C. D. Lokhande and S. H. Pawar, *Phys. Status Solidi A*, 1989, **111**, 11; J. F. Guillenmole, P. Cowache, L. Robbiola, R. Diaz, H. Hallak, D. Lincot and J. Vedel, *Cryst. Res. Technol.*, 1996, **3**, 509.

[113] J. W. Park, G. Y. Chung, B. T. Ahn, H. B. Im and J. S. Song, *Thin Solid Films*, 1994, **245**, 174.

[114] M. Gossla, T. Hahn, H. Metzzner, J. Conrad and U. Geyer, *Thin Solid Films*, 1995, **268**, 39; H. L. Wang, C. Y. Sun, C. S. Fang, C. H. Chang, M. H. Cheng, H. H. Yang, H. H. Liu and H. Tunan-Mu, *J. Cryst. Growth*, 1981, **55**, 116.

[115] R. Nomura, Y. Sekl and H. Matsuda, *J. Mater. Chem.*, 1992, **2**, 765; R. Nomura, Y. Sekl, K. Konoshi and H. Matsuda, *Appl. Organomet. Chem.*, 1992, **6**, 685; J. McAleese, P. O'Brien and D. J. Otway, *Chem. Vap. Deposition*, 1998, **4**, 94.

[116] H. Hahn, *Z. Anorg. Chem.*, 1953, **271**, 153.

[117] B. Li, J. Huang and Y. Qian, *Adv. Mater.*, 1999, **11**, 1456.